

Proceedings of the

**7th INTERNATIONAL SYMPOSIUM ON
VIBRATIONS OF CONTINUOUS SYSTEMS**

Zakopane, Poland
July 19-24, 2009



PREFACE

The International Symposium on Vibrations of Continuous Systems is a forum for leading researchers from across the globe to meet with their colleagues and present both old and new ideas on the field. Each participant has been encouraged to either present results of recent, significant research or to reflect on some aspect of the vibrations of continuous systems which is particularly interesting, unexpected, or unusual. This latter type of presentation was proposed to encourage participants to draw on understanding obtained through - in many cases - decades of research. In addition to the technical sessions, there is ample opportunity for the participants to meet in a very informal manner during excursions and hikes. Both technical and non-technical intensive discussions take place at these occasions. Past experience shows that all participants greatly benefit from getting to know their colleagues from around the world at a level not accomplished during normal conference settings.

The Seventh ISVCS takes place July 19-25, 2009 at the Hotel Litwor in Zakopane. Zakopane and its surrounding is considered the most attractive tourist region in Poland. The town of Zakopane is situated in southern Poland about 90 km to the south of Krakow, the historic city with a population of about 800 000 that was the capital of Poland until the 16th century. It lies in a valley at the foot of the Tatra Mountains on the border between Poland and Slovakia. The Tatra Mountains are the highest mountains in Poland with the highest peak Mount Rysy at 2499 m above sea level.

These Proceedings contain 26 summaries of the presentations to be made at the Symposium and short biographical sketches submitted by the participants.

Editorial Chairman
Stuart M. Dickinson

General Chairman
Peter Hagedorn

Registration Chairman
Ali H. Nayfeh

Honorary Chairman
Arthur Leissa

Local Arrangements Chairman
Piotr Cupial

CONTENTS

Summaries

High-Frequency Self-Excitation in Paper Calendars -----	1
E. W. Brommundt	
Vibrations of Plates and Shells in the Case of Thermo-Mechanical Coupling -----	4
E. Carrera and S. Brischetto	
Natural Frequencies and Critical Speeds of In-Plane Moving Rectangular Plates-----	7
L-Q. Chen and Y-Q. Tang	
Much Ado about Shear Correction Factors in Timoshenko Beam Theory-----	10
S. B. Dong , E. Taciroglu, and C. Alpdogan	
Dynamic Stiffness Analysis of Axially Loaded Timoshenko Beam with Cracks -----	13
M. Eisenberger	
Structural Elements with Engineered Damping -----	15
M. S. Ewing	
Trapped Mode, Pass-Band and Gap-Band Effects in Elastic Waveguide Structures -----	18
E. Glushkov and N. Glushkova	
On Self-Excited Vibrations due to Sliding Friction Between Moving Bodies -----	21
H. Hetzler	
Vibration of Cantilevered Rectangular Plates with Edge V-Notches or Slits -----	24
C. S. Huang , S. C. Liao, and I. C. Lee	
Vibration of a Solid Cylinder Fixed on One End-----	27
J. R. Hutchinson	
Embedding Negative Structures to Model Holes and Cut-Outs-----	30
S. Ilanko	
Implementation and Evaluation of Exact Dynamic Stiffness Method-----	33
for Free Vibration of Non-Uniform Beams	
S. Yuan, K. Ye, C. Xiao, F. W. Williams, and D. Kennedy	
Vibrations of Twisted Cantilever Plates -----	36
A. Leissa	
A Generalized Fourier Series Method for the Vibrations of Continuous Systems -----	39
W. L. Li	

A Discussion on the Physics and Truth of Nanoscales for Vibration of Nanobeams ----- Based Nonlocal Elastic Stress Field Theory C. W. Lim	42
Influence of Different Curvature on Chaotic Vibrations of Cylindrical Shell-Panels ----- with Clamped Edges K. Nagai , S. Maruyama, K. Hasegawa, N. Onozato, and T. Yamaguchi	45
Analysis and Design for Vibration of Laminated Composites by ----- Using the Three-Dimensional Theory Y. Narita	48
Dynamics of Circular Cylindrical Shells under Seismic Loads ----- F. Pellicano	51
Forced Vibration of Compressor and Turbine Blades ----- R. Rzadkowski	54
Tracking of Resonance Frequencies of Vibrating Beams by Phase-Locked Loops (PLL) ----- W. Seemann	57
Two Classical Problems on Stabilization of Statically Unstable Systems by Vibration ----- A. P. Seyranian	60
On the Vibrations of Single – and Multi – Walled Carbon Nanotubes ----- A. V. Singh and S. Arghavan	63
Stability of Shells in Frictional Contact ----- G. Spelsberg-Korspeter	66
Simulation of Pyroshocks ----- U. von Wagner , N. J ü ngel, and Alexander Lacher	69
Dynamics of a 1-Dimensional Wave Guide with Point-Wise Defects ----- J. Wauer , N. Glushkova, and E. Glushkov	72
Accurate Free Flexural Analysis of a Cantilever Piezoelectric Plate Carrying a Rigid Mass ----- S. D. Yu	75

Biographical Sketches of Participants

Eberhard W. Brommundt -----	79	Alexander Lacher -----	95
Erasmus Carrera -----	80	Arthur W. Leissa -----	96
Li-Qun Chen -----	81	Wenlong Li-----	97
Piotr Cupiał-----	82	Chee W. Lim -----	98
Stuart M. Dickinson -----	83	Ken-ichi Nagai -----	99
Stanley B. Dong -----	84	Yoshihiro Narita -----	100
Moshe Eisenberger-----	85	Francesco Pellicano -----	101
Mark S. Ewing -----	86	Romulad Rzadkowski -----	102
Evgeny Glushkov -----	87	Wolfgang Seemann-----	103
Peter Hagedorn -----	88	Alexander P. Seyranian -----	104
Hartmut Hetzler -----	89	Anand V. Singh-----	105
Daniel Hochlenert -----	90	Gottfried Spelsberg-Korspeter -----	106
Chiung-Shiann Huang-----	91	Utz von Wagner-----	107
James. R. Hutchinson -----	92	Jörg Wauer -----	108
Sinniah Ilanko-----	93	Shudong Yu-----	109
David Kennedy-----	94		

High-Frequency Self-Excitation in Paper Calenders

Eberhard W. Brommundt

Institut für Dynamik und Schwingungen, Technische Universität Braunschweig,
PF 3329, D-38023 Braunschweig, Germany, Eberhard@Brommundt.de

For printability, the surface of paper is finished by calendering: the paper sheet passes through the nip between two rolls where the web is compressed and its surface smoothed, cf. Figure 1. Often, after an operating period of one or two weeks, barring occurs: waves develop on the surfaces of the rolls producing wavy patterns on the paper, the bars, and the machine must be shut down.

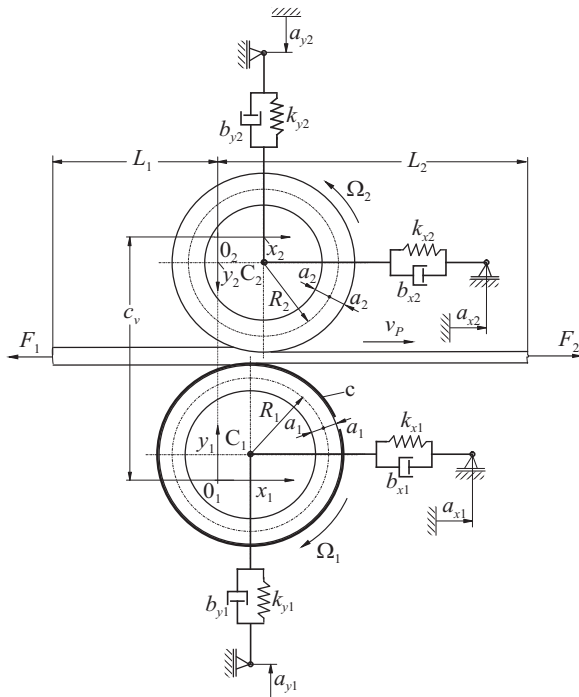


Figure 1: The system. Dimensions of the rolls and displacements of their centers

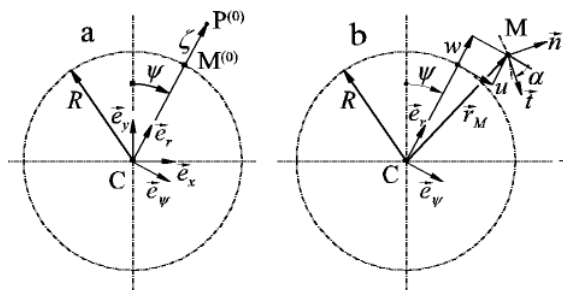


Figure 2: Deformations at the midline of a ring: a) initial shape, b) azimuthal displacement $u(\psi, t)$, and bending $w(\psi, t)$

variables $q_k(t)$, $k = 1, \dots, 48$, are introduced which are governed by the Lagrange equations

Self-excitation due to various time delays, contained in the roll system, in combination with regenerative wear seem to feed the deteriorating process, see Hader [1] and the literature quoted there. We believe that wear need not be the triggering effect. Maybe, there exists the combination of two processes: The first one is a friction induced self-excitation which can emerge even in a mill with ideally cylindrical rolls, to be discussed below. That being the case, the self-excited oscillation will produce corrugation by wear which, secondly, amplified by regeneration, may eventually govern the process.

The model contains two elastic rolls 1, 2, their hubs suspended as shown in Figure 1; the quantities a_{x1}, \dots, a_{y2} serve to adjust the nominal positions. Roll 1, its cover disregarded, is driven by a motor with $\Omega_M = \text{constant}$ via a flexible clutch. The paper and roll 2 are driven from below by friction at the contact. In the nip, the paper exhibits a nonlinear hysteretic characteristic, cf. Figure 4; the compression depends locally on the motions and deformations of the rolls. The slip between rolls and the paper are governed by the dynamic equilibrium conditions in the nip, taking Coulomb friction into account.

The rings deform like a curved thick beam and undergo the displacements $u(\psi, t)$, $w(\psi, t)$, see Figure 2, as well as the shear $v(\psi, t)$, not shown there. All three are measured with respect to the non-rotating Eulerian frame of polar coordinates of Figure 2. After establishing the kinetic energy T and the elastic potential U the system is discretized: Generalized

$$\frac{d}{dt} \left(\frac{\partial T}{\partial \dot{q}_k} \right) - \frac{\partial T}{\partial q_k} + \frac{\partial U}{\partial \dot{q}_k} = Q_k, \quad k = 1, \dots, 48, \quad \dim(q_k) = \text{length}, \quad (1)$$

where the generalized forces Q_k follow from $\delta W = \sum Q_k \delta q_k$, and δW is the virtual work of the forces not contained in the potential U , i.e. the dampings and the forces at the nip.

After the discretization, we have for roll 1, cf. Figures 1,2,3, mounted on a three point support which does not rotate, the 23 generalized variables q_1, \dots, q_{23} , cf. (2), and $\Omega_1 = \Omega_M + \dot{q}_3(t)/R_1$:

$$x_1(t) = q_1, \quad y_1(t) = q_2, \quad (2)$$

$$u_1(\psi_1, t) = q_3 + q_4 \cos(\psi_1) + q_5 \sin(\psi_1) + q_6 \cos(2\psi_1) + q_7 \sin(2\psi_1) + q_8 \cos(3\psi_1) + q_9 \sin(3\psi_1),$$

$$v_1(\psi_1, t) = q_{10} + q_{11} \cos(\psi_1) + q_{12} \sin(\psi_1) + q_{13} \cos(2\psi_1) + q_{14} \sin(2\psi_1) + q_{15} \cos(3\psi_1) + q_{16} \sin(3\psi_1),$$

$$w_1(\psi_1, t) = q_{17} + q_{18} \cos(\psi_1) + q_{19} \sin(\psi_1) + q_{20} \cos(2\psi_1) + q_{21} \sin(2\psi_1) + q_{22} \cos(3\psi_1) + q_{23} \sin(3\psi_1).$$

Similarly, the motion and deformation of roll 2 is described by the 24 variables q_{24}, \dots, q_{47} , $\Omega_2 = \dot{q}_{24}(t)/R_2$, and $\dot{q}_{48}(t)$ is the velocity of the longitudinally inextensible sheet of paper of the mass m_P .

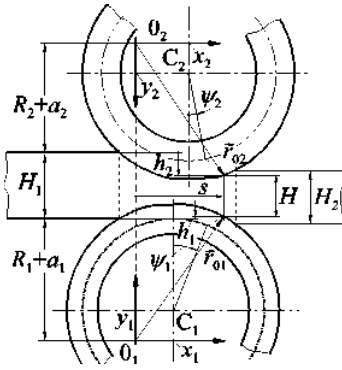


Figure 3: Geometric relations at the nip of the rolls

Figure 3 shows the instantaneous geometrical situation at the nip: the paper is compressed by the deformed rolls 1 and 2 (enlarged, not to scale); s = common Eulerian location along the nip. The transitions from the Eulerian polar coordinates of Figure 2 to s etc. follow from geometrical relations, read from Figure 3, by series expansions with respect to ψ_1 , and ψ_2 and algebraic manipulation. The vertical paper compression $H_1 - H(s, t) = h_1(s, t) + h_2(s, t) := h(s, t)$, see Figure 3, leads to the strain $\varepsilon_p(s, t) = h(s, t)/H_1$; compression positive!

Correspondingly, the instantaneous relative velocities between the paper and the roll surfaces are formulated as functions of (s, t) .

The normal stresses in the paper (pressure positive) have a hysteretic character. For loading, σ_{pl} , and unloading, σ_{pul} , the following hold

$$\sigma_{pl}(\varepsilon_p) = E_l \varepsilon_l \cdot (\exp(\varepsilon_p/\varepsilon_l) - 1), \quad (3)$$

$$\sigma_{pul}(\varepsilon_p) = E_{ul} \varepsilon_{ul} \cdot (\exp((\varepsilon_p - \varepsilon_r)/\varepsilon_{ul}) - 1);$$

where E_l , E_{ul} , ε_l , ε_{ul} are given parameters and the residual strain σ_r follows for a known local material maximum ε_m from $\sigma_{pl}(\varepsilon_m) = \sigma_{ul}(\varepsilon_m)$.

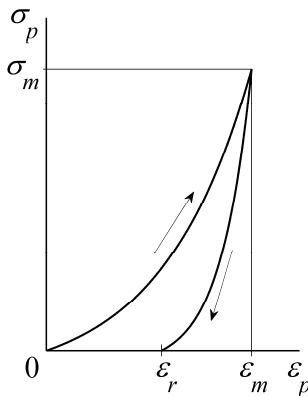


Figure 4: Stress-strain relation for the paper

After several further assumptions, the contributions of the contact and friction forces along the nip to the virtual work δW are established. Then the Lagrangian procedure (1) leads to the equations of motion

$$\mathbf{M} \ddot{\mathbf{q}} + \mathbf{\Omega G} \dot{\mathbf{q}} + \mathbf{\Omega}^2 \mathbf{C} \mathbf{q} + \mathbf{B} \dot{\mathbf{q}} + \mathbf{\Omega B}_l \mathbf{q} + \mathbf{K} \mathbf{q} = \mathbf{f}(\mathbf{q}, \dot{\mathbf{q}}), \quad \mathbf{q} := (q_1, \dots, q_{48})^T. \quad (4)$$

The 48×48 matrices \mathbf{M} , \mathbf{G} , \mathbf{C} , \mathbf{B} , \mathbf{B}_i , \mathbf{K} contain the inertia, gyroscopic, centrifugal, damping, internal damping, and stiffness coefficients, respectively; the right-hand side $\mathbf{f}(\mathbf{q}, \dot{\mathbf{q}})$ contains the nonlinearities. Diagonal are the matrices $\mathbf{\Omega}_1 := \Omega_1 \mathbf{I}_{23}$, $\mathbf{\Omega}_2 := \Omega_2 \mathbf{I}_{24}$, and $\mathbf{\Omega} = \text{diag}(\mathbf{\Omega}_1, \mathbf{\Omega}_2, 0)$; $\mathbf{I}_n := n \times n$ -identity.

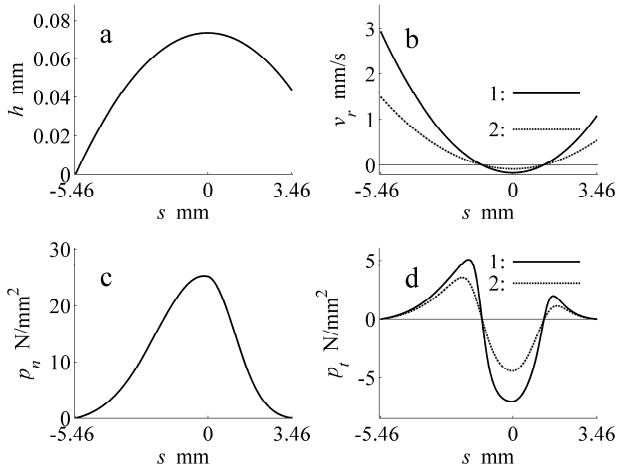


Figure 5: a) Paper impression, b) relative velocities paper \leftrightarrow rolls 1,2, c) normal pressure, d) tangential stresses paper \leftrightarrow rolls 1,2

To solve the set of 48 nonlinear ordinary differential equations (4) numerically, about 60 basic parameters are required. For example (cf. Figure 1): $R_1 = 0.31$ m, $R_2 = 0.42$ m, $a_1 = 36$ mm, $a_2 = 66$ mm, $H_1 = 0.15$ mm, $(F_1 - F_2) = 600$ N, $v_P \approx 25$ m/s, $\mu_{01} = 0.30$, $\mu_{02} = 0.25$ (friction), etc.

For the case of *stationary* displacements \mathbf{q}_0 with constant paper and angular velocities the nip length of $(3.46 + 5.46)$ mm = 8.92 mm results, cf. Figure 5, and the contact quantities shown there. (In spite of the small length of the nip the relative velocities between paper and rolls change their signs twice along the transit!) The stability of the stationary solution is studied by the (linear) *variational equation* about \mathbf{q}_0 obtained from (4) by numerical differentiation.

The following Table shows for the variational equation the 12 smallest of the 48 eigenvalues $\lambda_k/2\pi$, ordered by decreasing magnitude. Counted from below, the 9th, i.e. λ_{40} , has a positive real part: The stationary solution \mathbf{q}_0 is unstable.

Table: Eigenvalues $\tilde{\lambda}_k = \tilde{\delta}_k + f_k j$ Hz (i.e.: real and imaginary parts of λ are divided by 2π), $k = 37, \dots, 48$

$\tilde{\lambda}_{37 \dots 40}$	$-9.7934 + 664.78 j$	$-5.3461 + 545.95 j$	$-0.1775 + 212.31 j$	$0.0024664 + 149.37 j$
$\tilde{\lambda}_{41 \dots 44}$	$-0.053657 + 88.456 j$	$-0.078737 + 83.293 j$	$-0.013371 + 46.693 j$	$-0.0060862 + 40.40 j$
$\tilde{\lambda}_{45 \dots 48}$	$-0.008636 + 28.673 j$	$-0.007034 + 24.243 j$	$-0.003016 + 16.522 j$	$-0.006305 + 7.0342 j$

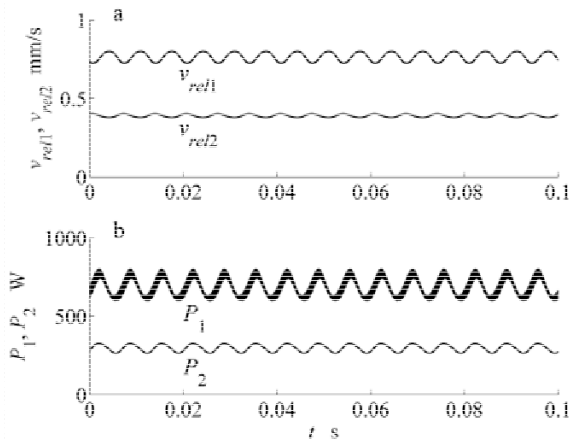


Figure 6: Self-excited oscillations. a) Relative velocities $v_{rel1,2}$ between rolls and paper at $s = -3$ mm, b) frictional powers $P_{1,2}$ between rolls and paper

The numerical solution of the nonlinear equation (4) leads, after transients, to a periodic self-excited oscillation $\mathbf{q}_s(t)$, vibrating with the frequency $f_s \approx 150$ Hz $\approx f_{40}$. Figure 6a shows for that motion the oscillations of the relative velocities in the nip at $s = -3$ mm, and Figure 6b shows the powers of the friction forces between paper and roll surfaces. They have considerable oscillating parts which, after synchronization by unbalances, will initiate roll corrugations.

The model offers some hints how to stabilize the operation of such a machine. For better technical relevance the model should include the soft cover of the lower roll and take longitudinal and shear deformation of the paper into account.

[1] Hader, P.: Selbsterregte Schwingungen von Papierkalandern. Dissertation, Duisburg-Essen. Shaker Verlag, Aachen (2005).

Vibrations of plates and shells in the case of thermo-mechanical coupling

E. Carrera, S. Brischetto

Aeronautics and Space Engineering Department, Politecnico di Torino, Italy
e.mail: erasmo.carrera@polito.it

Temperature variations are one of the most important causes of failure mechanisms in typical aerospace structures, such as plates and shells. These structures are subjected to severe thermal environments: high temperatures, high gradients and cyclic temperature changes. Due to these implications, the effects of both high-temperature and mechanical loadings have to be considered in the design process of such structures. A great deal of work has recently been devoted to the development of computational models to study the behavior of high-temperature plates and shells [1]. Among the various topics, the present work focuses on vibration analysis.

The analysis is accomplished considering full coupling between the mechanical and thermal field. An exhaustive comparison between the vibration frequencies of the pure mechanical case and the vibration frequencies of the full coupled thermo-mechanical case is made. Nowinski [2] wrote that the differences given by the effect of the thermo-mechanical coupling are about 0.3%-1.3%. There is no benchmark within the framework of a fully coupled theory available. This work aims to cover this gap. This dynamic analysis has been accomplished using several higher-order two-dimensional models obtained in the framework of Carrera's Unified Formulation (CUF) [3]. In the case of multi-layered structures, these models can be equivalent single layer or layer wise and the order of expansion in the thickness direction is taken as a free parameter ($N=1$ to $N=4$). The governing equations are obtained by extending the Principle of Virtual Displacements (PVD) to the thermo-mechanical coupling by simply adding the internal thermal work [4]: consistent constitutive equations must be considered in this case. The governing equations are solved in closed form using Navier's solution. Imposing the in-plane vibration mode, by means of the wave number, a certain number of vibration modes through the thickness, which depend on the degrees of freedom of the employed two-dimensional model, can be obtained.

Constitutive Equations. The constitutive equations for the thermo-mechanical coupling in the case of a general layer k are:

$$\begin{aligned}\sigma_p^k &= Q_{pp}^k \epsilon_p^k + Q_{pn}^k \epsilon_n^k - \lambda_p^k \theta^k, \\ \sigma_n^k &= Q_{np}^k \epsilon_p^k + Q_{nn}^k \epsilon_n^k - \lambda_n^k \theta^k, \\ \eta^k &= \lambda_p^{kT} \epsilon_p^k + \lambda_n^{kT} \epsilon_n^k + \chi^k \theta^k,\end{aligned}\tag{1}$$

where σ and ϵ are the stresses and strains, split into in-plane (p) and out-plane (n) components. η is the entropy and θ the temperature referring to a reference value. Matrices Q and λ contain the elastic coefficients and the coefficients of thermo-mechanical coupling, respectively. Scalar χ is equal to $\frac{\rho C_v}{T_r}$ where ρ is the mass density, C_v is the specific heat and T_r is the reference temperature.

Governing equations. The variational statement is obtained from the PVD for the pure mechanical case by simply adding the internal thermal work:

$$\int_V \left(\delta \epsilon_p^T \sigma_p + \delta \epsilon_n^T \sigma_n - \delta \theta \eta \right) dV = -\delta L_{in} , \quad (2)$$

where V stands for the volume of the considered multilayered structure and $\delta L_{in} = \int_V \rho \delta \mathbf{u}^T \ddot{\mathbf{u}} dV$ is the external virtual work made by the inertial forces. \mathbf{u} is the displacement vector, $\ddot{\mathbf{u}}$ is the second temporal derivative and ρ is the mass density. The governing equations are obtained by substitution of the constitutive equations, geometrical relations and CUF; this latter permits several two-dimensional models to be obtained.

In the case of thermo-mechanical coupling, the vibration problem is investigated using the governing equations (a thermostatic approximation is used):

$$\begin{aligned} \mathbf{K}_{uu}^{k\tau s} \mathbf{u}_\tau + \mathbf{K}_{u\theta}^{k\tau s} \theta_\tau &= M \ddot{\mathbf{u}}_\tau \\ \mathbf{K}_{\theta u}^{k\tau s} \mathbf{u}_\tau + \mathbf{K}_{\theta\theta}^{k\tau s} \theta_\tau &= 0 . \end{aligned} \quad (3)$$

If the effect of the thermal field is not considered, the system is simplified as:

$$\mathbf{K}_{uu}^{k\tau s} \mathbf{u}_\tau = M \ddot{\mathbf{u}}_\tau . \quad (4)$$

The matrices $\mathbf{K}_{uu}^{k\tau s}$, $\mathbf{K}_{u\theta}^{k\tau s}$, $\mathbf{K}_{\theta u}^{k\tau s}$ and $\mathbf{K}_{\theta\theta}^{k\tau s}$ are the so-called fundamental nuclei: expanding and assembling them in an opportune way, several two-dimensional theories can be obtained. Classical theories, such as CLT (Classical Lamination Theory) and FSDT (First order Shear Deformation Theory) are obtained as particular cases of the refined models based on CUF. The refined theories are called LD1-LD4, where the last digit indicates the order of expansion in the thickness direction for the three displacement components and for the temperature. The thermo-mechanical coupling is indicated with (TM).

Results. Some preliminary results are here presented to outline the effect of the thermo-mechanical coupling for the vibration problem. A simply supported one-layered isotropic plate is considered. In Table 1, having assumed the wave number in the plane ($m = n = 1$), the fundamental frequency f in Hz is reported for the CLT, FSDT, LD2 and LD4 theories. The comparison is made between the pure mechanical case, the thermo-mechanical coupling (TM) and the thermo-mechanical coupling with the imposed temperature at the top and bottom of the structure equal to the external room temperature (TM)*. The importance of refined models for thick plates is confirmed and a difference of about 1%, independently of the considered thickness ratio and the employed two-dimensional model, can be noticed in the case of the coupling effect. For the imposed temperature case, the CLT and FSDT do not give any frequency because their degrees of freedom are not sufficient to impose such temperature conditions. Once the in-plane vibration mode (m, n) has been chosen, several thickness vibration modes are obtained which depend on the number of degrees of freedom. For a thick plate, the modes through the thickness, in terms of displacement and temperature, are given for the free and imposed cases (LD4 model), see Figure [1]. Further results will be presented at the symposium: multilayered plate and shell geometries, vibration modes for higher values of wave number and different frequencies from the fundamental one which represents the other thickness vibration modes.

References

- [1] Noor A.K., Burton W.S., 1992, Computational models for high-temperature multilayered composite plates and shells, *Applied Mechanics Reviews*, vol.45, pp.419-446.
- [2] Nowinski J.L., *Theory of Thermoelasticity with Applications*, Sijthoff & Noordhoff, 1978, The Netherlands.
- [3] Carrera E., 2002, Temperature profile influence on layered plates response considering classical and advanced theories, *AIAA Journal*, vol.40, pp.1885-1896.
- [4] Carrera E., Boscolo M., Robaldo A., Hierarchic multilayered plate elements for coupled multified problems of piezoelectric adaptive structures: formulation and numerical assessment, *Archives of Computational Methods in Engineering*, vol.14, pp.383-430.

a/h	5	10	50	100
LD4(TM)	173.10	47.158	1.9481	0.4875
LD4(TM)*	172.88	47.094	1.9454	0.4869
LD4	172.40	46.946	1.9390	0.4852
LD2(TM)	174.86	47.306	1.9484	0.4876
LD2(TM)*	174.15	47.093	1.9392	0.4853
LD2	174.15	47.093	1.9392	0.4853
FSDT(TM)	175.52	47.517	1.9577	0.4899
FSDT(TM)*	-	-	-	-
FSDT	174.10	47.088	1.9392	0.4853
CLT(TM)	189.87	48.607	1.9596	0.4900
CLT(TM)*	-	-	-	-
CLT	188.08	48.148	1.9411	0.4854

Table 1: Vibration problem for an isotropic plate. Fundamental frequency f in Hz for several 2D theories and thickness ratios. Wave number $m = n = 1$.

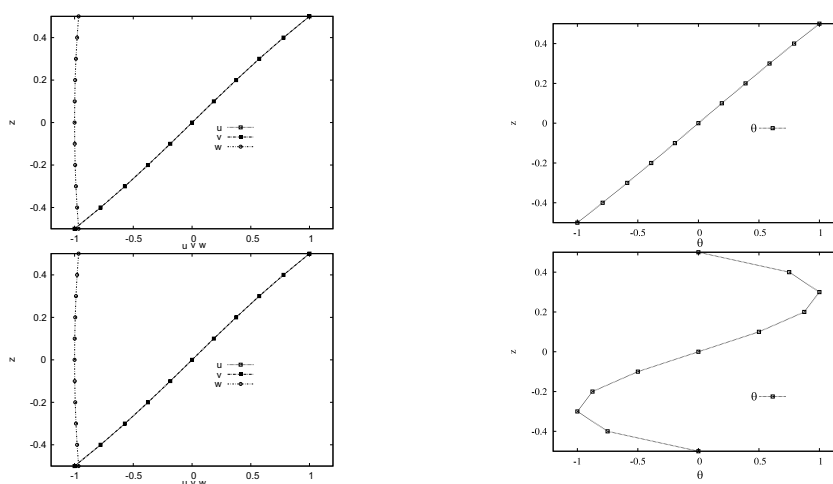


Figure 1: Free (top) and imposed (bottom) configurations for an isotropic one-layered plate. Thickness vibration modes in terms of displacements and temperature amplitudes for a thick plate ($a/h=5$). Fundamental frequency for $m = n = 1$.

Natural Frequencies and Critical Speeds of in-Plane Moving Rectangular Plates

Li-Qun Chen, You-Qi Tang

Department of Mechanics, Shanghai University, Shanghai 200444, China

Transverse vibration of an in-plane tensioned plate moving in its plane is a significant problem that was first studied by Ulsoy and Mote. Lin investigated natural frequencies and critical speeds for the plate with pinned-pinned-free-free boundaries [2]. Some sophisticated numerical approaches, such as the modal spectral element method [3], the finite strip method method [4], and the differential quadrature method [5] were developed. The present paper demonstrates that the modal functions of axially moving beams can be used to simplify the solution procedure. Natural frequencies and critical speeds are calculated for the boundaries different from those in [2].

A thin rectangular plate, with mass per area ρ , Young's modulus E , Poisson's ratio μ , initial tension N_{x0} in the x direction only, and length a , width b , and thickness h in the x , y , and z directions respectively, lie in plane xy and moves with speed Γ in direction x . The out-plane free vibration is governed by [1,2]

$$v_{,tt} + 2\gamma v_{,xt} + (\gamma^2 - 1)v_{,xx} + \zeta(v_{,xxxx} + 2\xi^2 v_{,xxyy} + \xi^4 v_{,yyyy}) = 0 \quad (1)$$

Dimensionless transverse displacement v , coordinates (x, y) , time t and other parameters are defined by

$$v \leftrightarrow \frac{v}{h}, \quad t \leftrightarrow \frac{t}{a} \sqrt{\frac{N_{x0}}{\rho}}, \quad x \leftrightarrow \frac{x}{a}, \quad y \leftrightarrow \frac{y}{b}, \quad \zeta = \frac{Eh^3}{12N_{x0}a^2(1-\mu^2)}, \quad \gamma = \Gamma \sqrt{\frac{\rho}{N_{x0}}}, \quad \xi = \frac{a}{b} \quad (2)$$

Separation of variables in Eq. (1) leads to

$$v(x, y, t) = \psi(x, y)e^{i\omega t} + \bar{\psi}(x, y)e^{-i\omega t} \quad (3)$$

where $\psi(x, y)$ is the mode function and ω is the natural frequency. Substitution of Eq. (3) into Eq. (1) yields

$$-\omega^2 \psi + 2i\omega\gamma\psi_{,x} + (\gamma^2 - 1)\psi_{,xx} + \zeta(\psi_{,xxxx} + 2\xi^2\psi_{,xxyy} + \xi^4\psi_{,yyyy}) = 0 \quad (4)$$

Assume the solution to Eq. (4) as

$$\psi(x, y) = \sum_{m=1}^{\infty} \sum_{n=1}^{\infty} \phi_n(x) \varphi_m(y) \quad (5)$$

For the plate with pinned edges at $y=0$ and $y=1$, choose $\varphi_m(y)$ satisfying the boundary conditions as $\varphi_m(y) = \sin(m\pi y)$. For the plate with clamped edges at $y=0$ and $y=1$, choose $\varphi_m(y)$ as

$$\varphi_m(y) = \cos \mathcal{G}_m x - \cosh \mathcal{G}_m x - \frac{\cos \mathcal{G}_m - \cosh \mathcal{G}_m}{\sin \mathcal{G}_m - \sinh \mathcal{G}_m} (\sin \mathcal{G}_m x - \sinh \mathcal{G}_m x) \quad (6)$$

where $\cos \mathcal{G}_m \cosh \mathcal{G}_m - 1 = 0$. Substituting Eq. (5) into Eq. (4), multiplying $\varphi_m(y)$ on both hands, integrating the resulting equation from $y=0$ to $y=1$ and applying the orthogonal condition yield

$$\zeta \phi_n'''' + (\gamma^2 + 2B_2 \zeta \xi^2 - 1) \phi_n'' + 2i\omega\gamma \phi_n' + (B_4 \zeta \xi^4 - \omega^2) \phi_n = 0 \quad (7)$$

where $B_2 = \int_0^1 \varphi_m'' \varphi_m \, dy / \int_0^1 \varphi_m^2 \, dy$, $B_4 = \int_0^1 \varphi_m'''' \varphi_m \, dy / \int_0^1 \varphi_m^2 \, dy$. The characteristic equation of Eq. (7) is

$$\zeta \beta_n^4 - (\gamma^2 + 2B_2 \zeta \xi^2 - 1) \beta_n^2 - 2\omega\gamma \beta_n + (B_4 \zeta \xi^4 - \omega^2) = 0 \quad (8)$$

Denote the 4 roots of Eq. (8) as β_{nj} ($j=1,2,3,4$). Then the modal function is

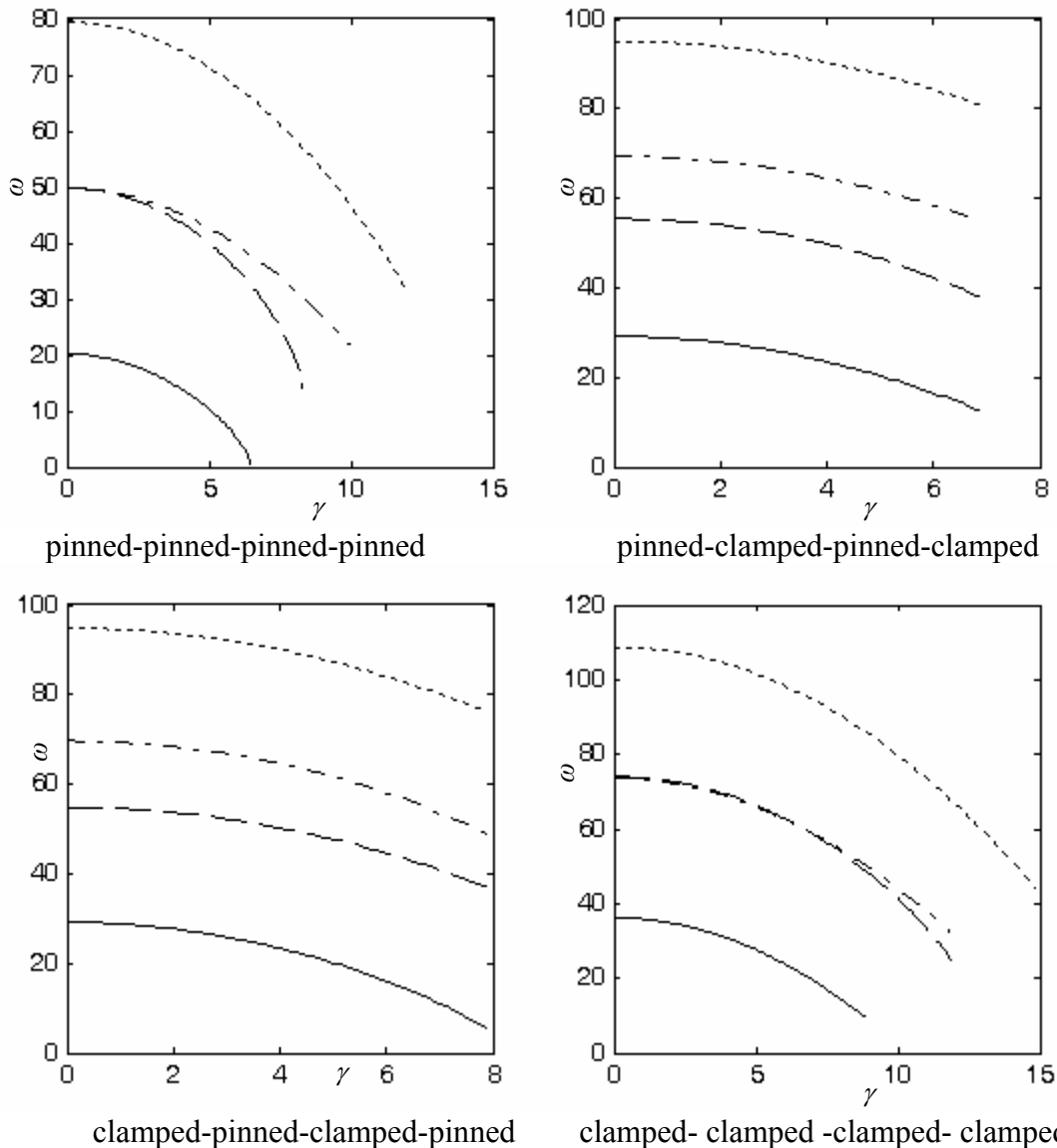
$$\begin{aligned} \phi_n(x) = & e^{i\beta_{n1}x} - \frac{(\lambda_{n4} - \lambda_{n1})(e^{i\beta_{n3}} - e^{i\beta_{n1}})}{(\lambda_{n4} - \lambda_{n2})(e^{i\beta_{n3}} - e^{i\beta_{n2}})} e^{i\beta_{n2}x} - \frac{(\lambda_{n4} - \lambda_{n1})(e^{i\beta_{n2}} - e^{i\beta_{n1}})}{(\lambda_{n4} - \lambda_{n3})(e^{i\beta_{n2}} - e^{i\beta_{n3}})} e^{i\beta_{n3}x} \\ & - \left[1 - \frac{(\lambda_{n4} - \lambda_{n1})(e^{i\beta_{n3}} - e^{i\beta_{n1}})}{(\lambda_{n4} - \lambda_{n2})(e^{i\beta_{n3}} - e^{i\beta_{n2}})} + \frac{(\lambda_{n4} - \lambda_{n1})(e^{i\beta_{n2}} - e^{i\beta_{n1}})}{(\lambda_{n4} - \lambda_{n3})(e^{i\beta_{n2}} - e^{i\beta_{n3}})} \right] e^{i\beta_{n4}x} \end{aligned} \quad (9)$$

and the auxiliary equation is

$$\begin{aligned} & \left[e^{i(\beta_{n1}+\beta_{n2})} + e^{i(\beta_{n3}+\beta_{n4})} \right] (\lambda_{n1} - \lambda_{n2})(\lambda_{n3} - \lambda_{n4}) + \left[e^{i(\beta_{n1}+\beta_{n3})} + e^{i(\beta_{n2}+\beta_{n4})} \right] (\lambda_{n3} \\ & - \lambda_{n1})(\lambda_{n2} - \lambda_{n4}) + \left[e^{i(\beta_{n2}+\beta_{n3})} + e^{i(\beta_{n1}+\beta_{n4})} \right] (\lambda_{n2} - \lambda_{n3})(\lambda_{n1} - \lambda_{n4}) = 0 \end{aligned} \quad (10)$$

For the plate with pinned or clamped edges at $x=0$ and $x=1$, $\lambda_{nj} = \beta_{nj}^2$ or $\lambda_{nj} = \beta_{nj}$ respectively.

Based on Eqs. (8) and (10), the natural frequencies can be calculated numerically. Figure 1 presents the first 4 natural frequencies under different boundary conditions for the changing dimensionless axially moving speed and fixed $\zeta=1$, $\xi=1$. The solid, dashed, dash-dot and dotted lines denotes the natural frequency ω_{11} , ω_{12} , ω_{21} , and ω_{22} . The natural frequencies decrease with the increasing axially moving speeds. The exact values at which the first natural frequency vanishes are the critical speeds and afterwards the system is unstable about the straight equilibrium.



clamped-pinned-clamped-pinned clamped-clamped-clamped-clamped

Figure1. the first 4 natural frequencies changing with the axial speed

If Eq. (1) has an equilibrium solution, the time-independent equilibrium of the linear equation is

$$(\gamma^2 - 1)v_{,xx} + \zeta(v_{,xxxx} + 2\xi^2 v_{,xxyy} + \xi^4 v_{,yyyy}) = 0 \quad (11)$$

with the solution

$$v = C_1 \cos \alpha_1 x + C_2 \sin \alpha_1 x + C_3 \cos \alpha_2 x + C_4 \sin \alpha_2 x \quad (12)$$

where

$$\alpha_{1,2} = \sqrt{\left(\frac{\gamma^2 - 1}{2\zeta} + B_2 \xi^2\right) \mp \sqrt{\left(\frac{\gamma^2 - 1}{2\zeta} + B_2 \xi^2\right)^2 - B_4 \xi^4}} \quad (13)$$

Substitution of Eq. (12) into the boundary conditions at $x=0$ and $x=1$ leads to a set of homogeneous linear equations, whose non-trivial solution condition can be used to calculate the critical speeds numerically. Figure 2 shows the first critical speeds changing with the flexural rigidity under different boundary conditions for $\zeta=0.5$ (dashed), 1 (solid) and 2 (dotted). The critical speed increases with the increasing flexural rigidity ζ and the decreasing slenderness ratio ζ^{-1} , which is the same as the conclusions in [2]

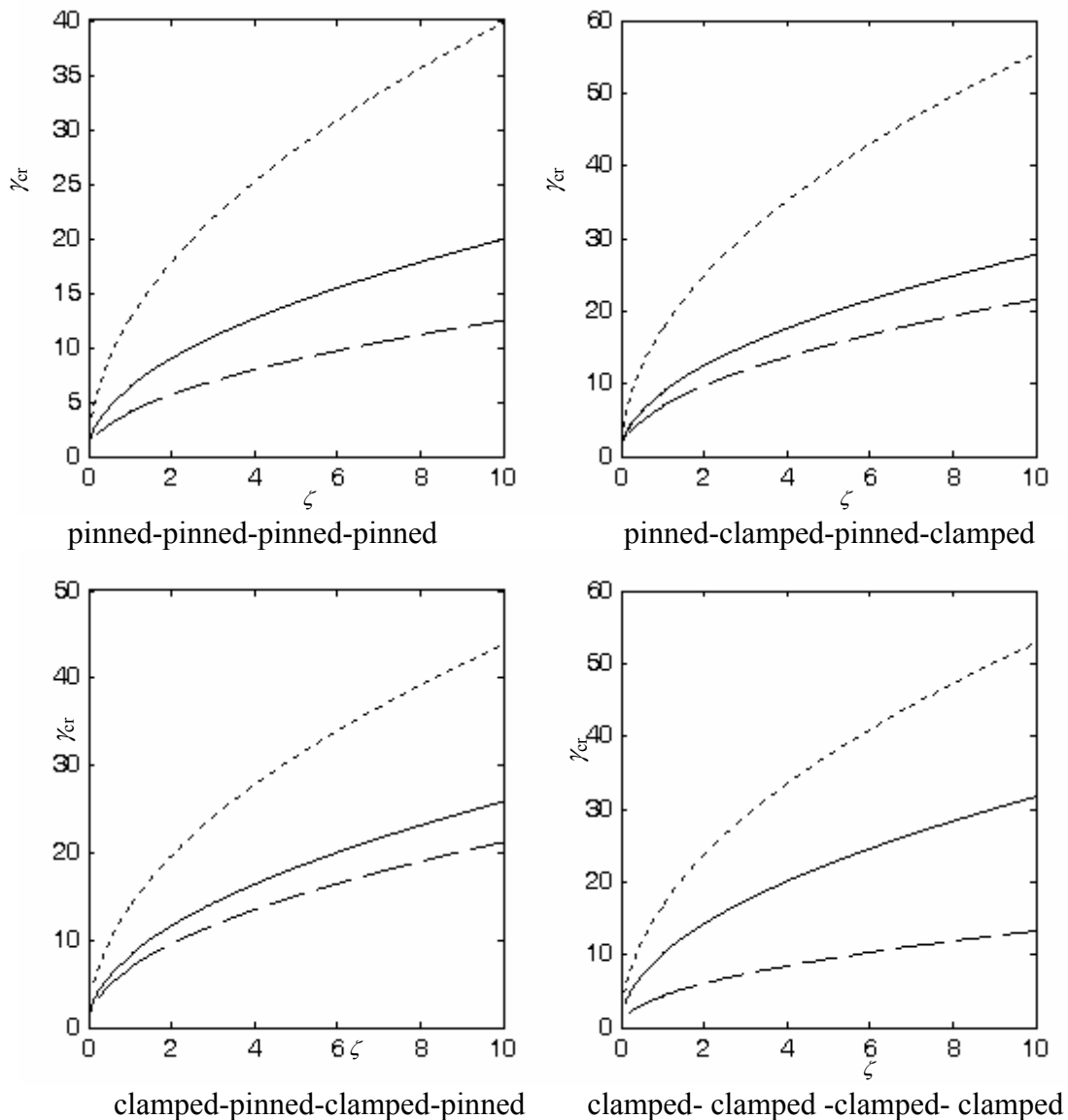


Figure 2. the first critical speeds changing with the stiffness ratio

- [1] AG Ulsoy, Jr CD Mote. *ASME Journal of Engineering for Industry* 1982; 104(1): 71-78.
 - [2] CC Lin. *International Journal of Solids Structures* 1997; 34(24): 3179-3190.
 - [3] J Kim, J Cho, U Lee, S Park. *Computers and Structures* 2003; 81: 2011-2020.
 - [4] YF Zhou, ZM Wang. *Journal of Sound and Vibration*, 2008; 316(1-5): 198-210.
 - [5] Hatami S, Ronagh HR, Azhari M. *Computers and Structures* 2008; 86(17-18): 1738-1746.
- This work was supported by the National Natural Science Foundation of China (Project No 90816001).

Much Ado about Shear Correction Factors in Timoshenko Beam Theory

S. B. Dong, E. Taciroglu and C. Alpdogan

Civil and Environmental Engineering Department
University of California
Los Angeles, California, 90095-1593, USA

Abstract

Shear correction factors in Timoshenko beam theory have received much attention as evidenced by a substantial body of technical literature. Most of the recent contributions have emphasized the use of three-dimensional data to define suitable correction factors. While all correction factor values put forth to date have some rational basis, there still remains a lack of unanimity on the "best" method for affixing the values. In this presentation, we offer some definitive comments that will clarify various issues relating to shear correction factors.

Our approach relies on having three-dimensional solutions for a prismatic beam for both static and dynamic problems, and critically examining the results. The solution technique herein is based on a version of semi-analytical finite elements (SAFE), where only the cross-section of the prismatic beam undergoes finite element modeling, i.e., in the (x, y) plane. In our code, both six-node triangles and eight-node are used in which the element matrices are determined by standard isoparametric formulation. The kinematic degrees of freedom at the nodes are dependent upon the axial coordinate z and time t . The governing equations of motion are of the form

$$\mathbf{K}_1 \mathbf{U}_{,zz} + \mathbf{K}_2 \mathbf{U}_{,z} + \mathbf{K}_3 \mathbf{U} + \mathbf{M} \ddot{\mathbf{U}} = \mathbf{0} \quad (1)$$

where \mathbf{U} of length $3M$ is the assemblage of the nodal displacements for the M nodes of the finite element mesh, i.e.,

$$\mathbf{U}^T(z, t) = \left[\cup \mathbf{u}(z, t) \quad \cup \mathbf{v}(z, t) \quad \cup \mathbf{w}(z, t) \right] \quad (2)$$

System matrices \mathbf{K}_1 , \mathbf{K}_2 , \mathbf{K}_3 , and \mathbf{M} , as well as the details of this SAFE formulation, are given in Taweel et al (2000). We note that \mathbf{K}_1 and \mathbf{K}_3 are symmetric and \mathbf{K}_2 is antisymmetric. While this approach will accommodate inhomogeneous, anisotropic cross-sections, our attention is concentrated on homogeneous, isotropic beams with an arbitrarily shaped cross-section.

In the past last half century, three-dimensional data from elastostatic analyses of Saint-Venant flexure have been used to define suitable correction factors. Cowper (1966) and Mason and Herrmann (1967) defined their correction factors by distilling a Timoshenko beam theory through integration of the three-dimensional equations of elasticity. In their transverse shear force-shear angle relation, they integrated the warpage data of Saint-Venant flexure to define the shear correction factors. Renton (1991) used the energy/length due to transverse shearing stresses (a constant) to arrive at the shear correction factors. In his examples, available Saint-Venant solutions for cross-sections with one plane of structural symmetry, were used. A number of subsequent investigators have followed this methodology using finite elements for other cross-sectional shapes. We will show by detailed examination of the displacement field of Saint-Venant flexure, that Cowper (1966) and Mason and Herrmann (1967) approach, in fact, leads to a compelling explanation as to how the effect of transverse shear is taken into account and its direct connection to the shear correction factors. Also, Schramm et al (1994), in using Renton's approach for unsymmetric cross-sections, introduced the notion of principal shear axes that do not coincide with the principal bending axes. We will argue that this concept is not viable.

We will also consider shear correction factors from elastodynamic data. For plates, Mindlin (1951) is well known for this basis in his shear deformation plate theory (the elastostatics analogue is due to Reissner (1945)). In this approach, the lowest frequency of infinitely long straight-crested thickness-shear motions is equated to that by his first order shear deformation plate theory. For beams, however, the dynamic approach has received considerably less attention than that based on flexure data. Hutchinson (2001) has determined correction factors for beams of rectangular and circular cross-sections. One obvious reason for considerably less activity by this approach is an unavailability of elastodynamic data for cross-sections of arbitrary shapes. With the SAFE approach, this is not an issue. Using solution form $\mathbf{U}(z, t) = \mathbf{U}_o e^{i(kz - \omega t)}$ in Eq. (1), where k is an axial wave number and ω denotes the frequency, the following algebraic eigenproblem is obtained.

$$\left(-k^2 \mathbf{K}_1 + ik \mathbf{K}_2 + \mathbf{K}_3\right) \mathbf{U}_o = \omega^2 \mathbf{M} \mathbf{U}_o \quad (3)$$

As \mathbf{K}_1 and \mathbf{K}_3 are symmetric and \mathbf{K}_2 is antisymmetric, the left-hand side of Eq. (3) is Hermitian. Therefore, real natural frequencies will emerge from this system. From the data for the appropriate lowest thickness-shear branch, the shear correction factor can be established. Also with the lowest branch of the flexural spectrum, the accuracy and range of application of the correction factors in a Timoshenko beam theory can be assessed.

References

- (1) Cowper, G.R. (1966). The Shear Coefficient in Timoshenko's Beam Theory. *J. Applied Mech.*, ASME, **33**:2, 335-340.
- (2) Hutchinson, J.R. (2001). Shear Coefficients for Timoshenko Beam Theory, ASME, **68**:(1), 87-92.
- (3) Mason Jr., W.E., and Herrmann, L.R. (1968) Elastic Shear Analysis of General Prismatic Beams, *J. Engr Mech. Div*, ASCE, **94**:EM4, 965-983.
- (4) Mindlin, R.D. (1951). Influence of Rotatory Inertia and Shear on Flexural Motions of Isotropic, Elastic Plates, *J. Applied Mech.*, ASME, **18**, 31-38.
- (5) Reissner, E. (1945). The Effect of Transverse Shear Deformation on Bending of Elastic Plates, *J. Applied Mech.*, ASME, **67**, A69-A77.
- (6) Renton, J.D. (1991). Generalized Beam Theory Applied to Shear Stiffness, *Int. J. Solids Structures*, **27**:15, 1955-1967.
- (7) Schramm, U., Kitis, L., Kang, W. and Pilkey, W.D., (1994). On the Shear Deformation Coefficient in Beam Theory. *Finite Elements in Analysis and Design*, **16**, 141-162.
- (8) Taweel, H., Dong, S.B., and Kazic, M. (2000). Wave Reflection from the Free End of a Cylinder with an Arbitrary Cross-Section, *Int. J. Solids Structures*, **37**, 1701-1726.

Dynamic Stiffness Analysis of Axially Loaded Timoshenko Beam with Cracks

Moshe Eisenberger

Faculty of Civil and Environmental Engineering

Technion – Israel Institute of Technology

Technion City, 32000, Israel

e-mail: cvrmosh@technion.ac.il

The structural vibratory characteristics of structural elements are affected by cracks which are found in several locations and depth along the elements. This subject was addressed extensively and presented in a state of the art review by Dimarogonas [1].

Cracks are commonly modeled as mass-less rotational springs that are characterized by their depth. This paper addresses the title problem using the dynamic stiffness method [2]. Using the dynamic stiffness method it is possible to obtain a condensed reduced order system of equations without any loss of accuracy due to the size reduction. The reduced system is derived symbolically using four types of building blocks that include a rotational spring representing a crack at the left, right, and both ends of the element, and a regular element without cracks. The problem at hand is divided to several elements where the boundaries between elements are located just next to the crack on one of its sides. There are several possibilities for such division and for all of the models the same results are obtained.

The dynamic stiffness matrices for the three cases that have cracks are derived from the differential equations of motion analytically, including the discontinuities introduced by the presence of the cracks. The differential equations of Timoshenko beam segment loaded by an axial load are solved. The four constants are calculated by applying the boundary values of the shapes that represent the equilibrium state of each column in the dynamic stiffness matrix. The

values are frequency dependent. The assembly of the structural dynamic stiffness is performed in this paper by steps, i.e. after the addition of each element using the appropriate building blocks representing the particular model, a condensation procedure that eliminates the common degrees of freedom for the elements is carried out in order to reduce the problem size. The condensation is performed analytically and the resulting matrix is maintained at the size of 4 by 4 matrix. After all cracked sub-elements were assembled the four end boundary restraints and releases, two at each end, are introduced for the completion of the derivation. Using the Wittrick-Williams algorithm all the natural frequencies are found.

The advantages of the proposed procedure are demonstrated in several examples. In these the exact characteristics of the procedure are demonstrated, and the results are compared to existing results in the open literature. Using the dynamic stiffness approach, including the effect of the axial loading, also the exact buckling loads of Timoshenko beams with multiple cracks are found.

The proposed derivation will be used in the future for the identification of cracks in beams. The reduced size of the resulting eigenvalue problem with the unknowns limited to the number of cracks, their location, and depth will result in relatively small problem of identification. The sensitivities of the natural frequencies to changes in these parameters will be derived analytically and thus reduce the computational cost significantly.

REFERENCES

- [1] A.D. Dimarogonas, "Vibration of cracked structures: A state of the art review", *Eng. Frac. Mech.*, Vol. 55, pp. 831-857, (1996).
- [2] A.Y.T. Leung, *Dynamic Stiffness Method and Substructures*, Springer, New York (1993).

Structural Elements with Engineered Damping

Mark S. Ewing, Associate Professor and Chair
University of Kansas Aerospace Engineering
1530 West 15th Street, Lawrence, Kansas 66045

Structural damping has the important role of limiting response to excitation, avoiding excessive deflection as well as the associated strain and velocity which cause fatigue and noise, respectively. Real structures—and the damping treatments often applied to them to reduce vibration—have damping which is proportional to both strain (a displacement), strain rate (a velocity) and even relative displacement in the case of mechanically-joined structures. With both displacement- and velocity-related damping, then, any accounting for damping must be frequency-dependent. A common and useful way to model proportional damping is to prescribe a “complex” stiffness, \mathbf{E} to materials of the form: $\mathbf{E}(\omega) = E[1 + i\eta(\omega)]$, where E is the elastic modulus, η is the damping loss factor and ω is the circular frequency.

Methods for predicting damping in sandwich beams

One of the most common damping treatments used in the transportation industry is constrained-layer damping, which is based on the application of a thin visco-elastic material (VEM) to a beam or plate, and subsequently adding a “cover sheet”, thereby forming a “sandwich” structure. For sandwich beams with a VEM core, Ross, Unger and Kerwin [1] developed a kinematically-consistent way to model this configuration. Their method allows the user to prescribe different damping loss factors for the top and bottom sheet and, more importantly, to the VEM. Then, the overall damping loss factor is simply the imaginary component of the resulting composite elastic modulus:

$$\eta = \frac{\text{Im}(E)}{\text{Re}(E)}$$

General methods for estimating and predicting damping in structures

A more general method of accounting for damping in structural components was suggested by Johnson, Kienholz and Rogers [2] in 1981, the so-called modal strain energy method (MSEM). All material properties are modeled in a finite element analysis as real and constant so a standard normal modes analysis may be used. Then,

$$\eta^{(r)} = \sum_{i=1}^N \eta_i \cdot \frac{E_{Si}^{(r)}}{E_S^{(r)}}$$

where $\eta^{(r)}$ is the system’s modal loss factor at the r^{th} mode, η_i is the material loss factor for material i , $E_{Si}^{(r)}$ is the strain energy in material i when the structure deforms in natural vibration mode r , and $E_S^{(r)}$ is the total strain energy in natural vibration mode r . They also proposed a way to account for a frequency-dependent loss factor.

More recently, Liu and Ewing [3] proposed a method based on the loss factor definition used in the experimental power input method (EPIM), which was described by Carfagni and Pierini in 1999 [4]. That is, the loss factor is defined as the power input per radian divided by the total mechanical energy, namely:

$$\eta = \frac{P_D}{\omega \cdot E_{Tot}} = \frac{E_D}{2 \cdot \pi \cdot E_{Tot}}$$

where P_D is the dissipated power; E_{Tot} is the total mechanical (reversible, vibrational) energy, which is the summation of strain energy and kinetic energy, $E_{Tot} = E_S + E_K$; E_D is the energy dissipated per cycle during period T ;

$P_D = \frac{1}{T} \cdot E_D = \frac{\omega}{2 \cdot \pi} \cdot E_D$; and ω is the circular frequency. Note that, for a steady-state condition, the energy dissipated **is** the energy input since it sustains the average vibration energy at a uniform level. In the case of a velocity-based measurement process during which the structure is mechanically excited by a shaker at a **single point**, the loss factor can be shown [4] to be equal to:

$$\eta(\omega) = \frac{\text{Re}[Y_{ff}(\omega)]}{\sum_{i=1}^N m_i \cdot \omega \cdot |Y_{if}(\omega)|^2}$$

where Y_{ff} is the velocity-to-force driving point frequency response function (FRF), Y_{if} is the FRF relating the velocity at point i to the driving point force, and m_i is the mass representing the i^{th} measurement point. The analytical power input method (APIM) is based on the EPIM, with the difference that the computations of the FRFs are done analytically in a finite element analysis [3].

Beams with constrained layer damping

A beam with constrained layer damping has been studied, resulting in a comparison of the Ross-Unger-Kerwin (RUK) technique to the APIM and the MSEM. The results, shown below, reveal a number of discrepancies. At low frequency, the RUK technique over-predicts damping. Across the frequency range, the MSEM has numerous apparent problems. These are all understandable by one with a grasp of the vibration of continuous systems, and will be discussed in the conference presentation.

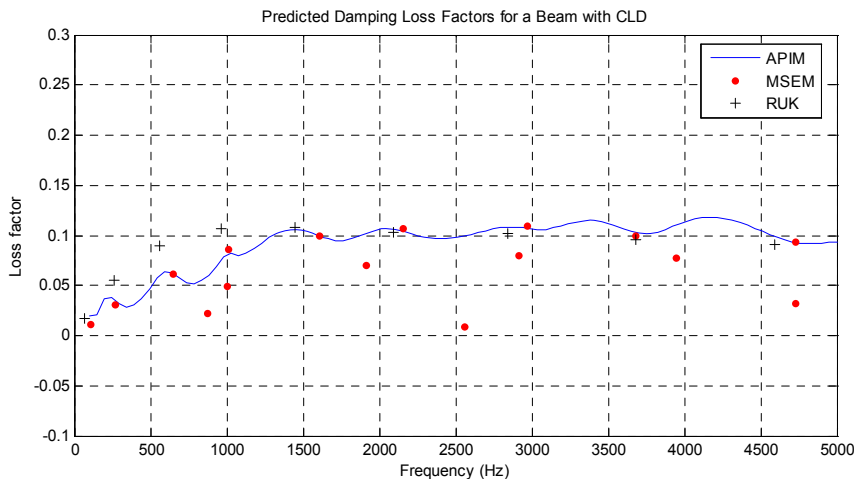


Figure 1. Predicted, frequency-dependent damping loss factor for a sandwich beam.

Uniform Plates with constrained layer damping

A uniform plate with a uniform constrained layer damping treatment was analyzed and tested to determine the damping loss factor. The comparison between the experimental power input method, the modal strain energy method, the analytical power input method and the free decay method is

shown in Figure 2. [The free decay method is a method in which a harmonic force is terminated and the decay is noted.] The “undulations” in the loss factors from APIM and EPIM are, at first, troubling. In fact, many researchers have reported this effect, and have remarked on this phenomenon. In particular it will be shown that the failure of the PIM techniques to correctly evaluate damping in beams and plates is *an artifact of the choice of excitation point*. In particular, for techniques which use only a single excitation point, the excitation point is almost always on or near a node line for a large number of frequencies—a fact which can be seen by looking at the mode shapes for the structure. In fact, many experimentalists have given up on the PIM, when all they needed to do was to use a handful of (even randomly-selected) excitation points. Alternative techniques for damping estimation will also be presented, namely the Impulse Response Decay Method and the Random Decrement Method, which have recently been studied by Ewing, Dande and Vatti [5].

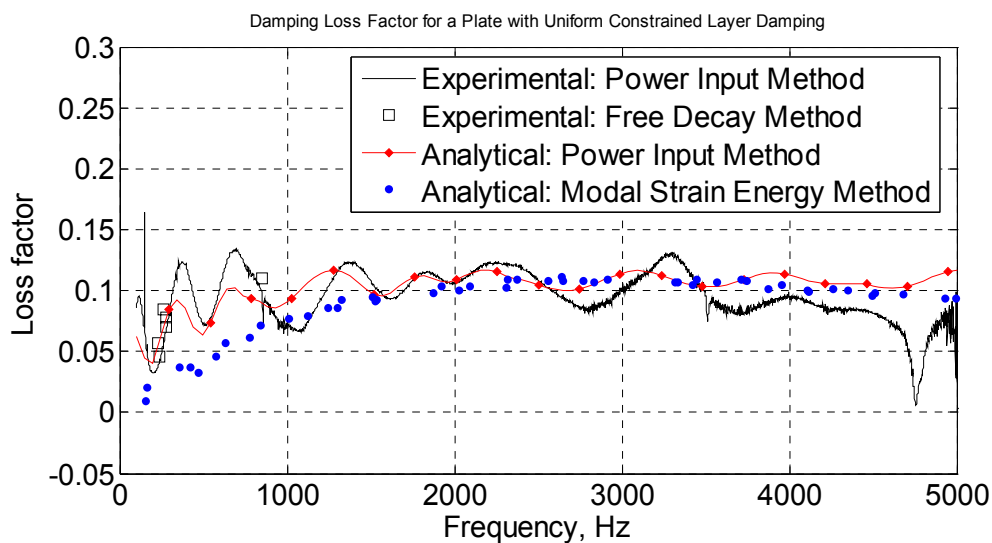


Figure 2. Predicted, frequency-dependent damping loss factor for a sandwich beam.

References

- [1] Ross, D., Ungar, E. E. and Kerwin, E.M., Damping of Plate Flexural Vibrations by Means of Viscoelastic Laminae, Structural Damping, American Society of Mechanical Engineers, edited by Jerome E. Ruzicka, 1959, pp 49-87.
- [2] Johnson, C. D., Kienholz, D. A. and Rogers, L. C., Finite element prediction of damping in beams with constrained viscoelastic layers, Shock and Vibration Bulletin, No. 50, 1981, Part 1, pp. 71-82.
- [3] Liu, W.B. and Ewing, M.S., Experimental and Analytical Estimation of Loss Factors by the Power Input Method, AIAA Journal, Vol 45, No 2, Feb 2007, pp 477-484.
- [4] Carfagni, M. and Pierini, M., Determining the Loss Factor by the power input method (PIM), Part 1: Numerical Investigation, Journal of Vibration and Acoustics, July 1999, Vol. 121, pp. 417-421.
- [5] Ewing, M., Dande, H., and Vatti, K., Validation of Panel Damping Loss Factor Estimation Algorithms Using a Computational Model, Proceedings, 50th AIAA Structures, Structural Dynamics and Materials Conference, 4-7 May, 2009.

Trapped Mode, Pass-band and Gap-band Effects in Elastic Waveguide Structures with Single and Multiple Obstacles

Evgeny Glushkov and Natalia Glushkova

Institute for Mathematics, Mechanics and Informatics, Kuban State University
35040 Krasnodar, Russia, evg@math.kubsu.ru

The field of our interests includes elastodynamics, wave propagation and diffraction phenomena in structures with obstacles (defects) of different nature (cracks, inclusions, cavities, surface irregularities and massive objects, etc.). The study is carried out using analytically-based computer models relying on solutions in terms of path Fourier integrals, Green's matrices for the structures and asymptotics for body and traveling waves derived from those integrals. For obstacles with sharp edges or corner points the singularities at those points are explicitly derived and used then for regularization of the numerical schemes developed.

In our presentation we focus at the resonance phenomena of a time-averaged oscillation $\mathbf{u}e^{-i\omega t}$ featured by the time-harmonic wave energy localization near the obstacles in the form of energy vortices. These phenomena, which are also known as trapped-mode effects, are usually accompanied by a sharp stopping of the wave energy flow along the waveguide and, consequently, in deep and narrow gaps in the frequency plots of transmission coefficients. The trapped modes are tightly connected with the distribution of natural frequencies (resonance poles) ω_n in the complex frequency plane ω : the closer ω_n locates to the real axis, the sounder this effect is. At that, specific forms of energy localization are governed by the eigen-solutions \mathbf{u}_n associated with the resonance poles ω_n , which are actually the spectral points of the related boundary-value problems. In ideally-elastic structures certain combinations of obstacles may result in totally real poles yielding very narrow gaps.

On the other hand, recent studies of structures with multiple defects, carried out with our PhD students M. Golub (cracks) and A. Eremin (rigid inclusions), have shown that the eddies of wave energy may work not only as blockers but as energy pumps, as well. It has been demonstrated that accounting for the mutual influence among the obstacles leads to realignment of the streamline structure in such a way that the energy circulation in the vortex zones formed around the obstacles becomes coordinated, providing so strong energy sucking that the reflected field becomes unnoticeable. In other words, the obstacles are invisible for the guided-wave detection at such frequencies. On the transmission coefficient plots such pass modes appear as narrow peaks centered at frequencies ω_p located closely to the resonance pole ω_n : $\omega_p \approx \text{Re}\omega_n$. The number of such pass-frequencies ω_p (and correspondingly of the transmission peaks) is proportional to the number of obstacles N . As N increases the peaks fill in a small vicinity of $\text{Re}\omega_n$ forming a narrow pass band inside a wider gap band.

Historically our interest in these effects goes back to the 1980s when the wave energy vortices and inverse fluxes were revealed in layered elastic waveguides practically simultaneously with the eddies in acoustic harmonic fields [?]. The first seminar presentations of those results gave rise to hot discussions, so that we were able to publish it properly just in the 1990s [?, ?]. Hence, it was a pleasure to learn about the recent works by the Optics Group, University of Glasgow (<http://www.physics.gla.ac.uk/kevin/research2.html>) having provided the experimental evidence of the existence of energy vortex zones in harmonic fields.

First, it was found that the vortex zones could occur in wave energy fluxes emitted by harmonic sources into elastic layered structures that were even without obstacles. They appeared just due to the interference of excited guided waves, but at certain resonance frequencies the vortices developed in a near-source field were able to accumulate a large amount of wave energy with much higher energy density than in the streams flowing around them from the source to infinity. Then we considered energy vortices developed near massive rigid objects (slabs) oscillating on an elastic layered base. As it proved, they play a key role in the controlling of energy outflow from under the contact zone up to the forming of so-called high-frequency slab-base resonance.

This effect is of the same nature as the resonance oscillation of a point mass on spring. Since the traveling waves carry energy away from the contact zone, it causes a non-zero damping component of the contact stiffness. Therefore, the unlimited resonance was considered to be impossible at $\omega > \omega_0$, where ω_0 is the first cut-off frequency. However, with contact areas of certain size the energy vortices developed under the slab edges shut down completely the waveguide's cross-section reducing the damping component to zero. In this case, the base works as an ideal spring with possible unlimited resonance oscillation for a certain slab mass. If a system of massive objects is subject to incident surface waves, only the first slab exhibits a high-amplitude oscillation at the resonance frequency while the objects behind it remain at rest. Hence, high-frequency resonances could be used for vibroprotection.

Mathematically the high-frequency resonance indicates the existence of a discrete spectral point ω_n lying on the continuous spectrum $\omega > \omega_0$ of the wave problem considered. It was expected that with massless crack-like obstacles such resonance was impossible because the mass-spring mechanism did not work in this case. Nevertheless, the tracing of trajectories of spectral poles ω_n in the lower complex half-plane $\text{Im } \omega \leq 0$ in the course of crack size and location varying, the facts of poles' touching to the real axis $\text{Im } \omega = 0$ have been revealed [?]. The eigenforms \mathbf{u}_n associated with the real poles ω_n display strong localization of oscillation near the crack. Similar effects have been obtained for a single cavity or inclusion.

With a system of several obstacles the main question was how the resonance properties inherent to each of them were transformed due to the mutual wave interaction. At first glance, one can expect that with sufficiently large spacing between neighboring obstacles the spectrum ω_n should be a combination of spectral points of every object taken alone. On the other hand, in 2D models the amplitudes of traveling waves that ensure the wave interaction between the obstacles are independent of distance. Finally, from the physical point of view, if the first obstacle has blocked the signal propagation, the presence of the following ones is of no importance because the disturbance does not arrive at them. That is, additional obstacles should not change the frequency of resonance blocking and, consequently, the near-real spectral poles ω_n .

Even the first calculations showed that wave interaction between obstacles realizes both seemingly alternative possibilities. The positions of the poles ω_n significantly vary with varying horizontal distance between the cracks; however, this occurs in such a way that resonance blocking frequencies conditioned by each individual crack remain intact [?]. With increasing distance between the obstacles, the values of $\text{Re } \omega_n$ monotonically decrease and the negative imaginary parts $\text{Im } \omega_n$ alternatively decrease and increase within certain limits with the upper boundary $\text{Im } \omega_n = 0$. Thus, the poles ω_n move in the lower half-plane of the complex plane ω

from right to left alternatively deviating from and approaching the real axis up to the points of touching it at certain discrete values of the distance. The most interesting feature is that the poles approach the real axis only near the aforementioned frequency bands of blocking by a single defect and, when a pole leaves the axis, it gives place to the next one that approaches the axis. As a result, nearly real-valued poles ω_n ensuring resonance blocking are always present in these frequency bands irrespective of the distance between the obstacles. The poles moving downwards rapidly cease affecting the blocking. The invariance of resonance stopping frequencies of single obstacles assembled in a group allows one to form a sufficiently wide band gap by combining individual gaps of several obstacles instead of the use of large quantity of periodic obstacles.

Those resonance effects may be of interest for the development of wave methods for defects' location and identification (NDE and structural health monitoring) as well as for the assessment of dynamic strength and failure properties of new laminate composite materials with micro and macro defects. In the latter case, along with infinite waveguide structures, the dynamic response and behavior of finite-size samples (beams, plates) have also been considered using the models developed. Furthermore, the phenomenon of abrupt signal screening by a system of obstacles (interdigital contacts, grooves, etc.) is used in solid electronics and photonics for designing frequency filters. Similar gap bands are characteristic of acoustic wave propagation (phonons) in periodic composite and crystal structures (atomic phonon lattice), and so on.

Together with comparatively complex for simulation 2D and 3D elastic layered structures, simplified 1D models such as a springly-supported defected string or beam, have been considered. They were suggested by Prof. Wauer for making clear the resonance effects as well as the forming of gap bands and pass bands in multidefected structures. This work was started in 2008 during our visit to ITM, KIT, Karlsruhe supported by the DFG Mercator Visiting Professorship Programme and continued then in KubSU, Krasnodar thanks to the support from the Russian Ministry of Science and Education, project No 2.1.1/1231.

References

- [1] R.V. Waterhouse, D.G. Crighton, and J.E. Ffowcs-Williams, A criterion for an energy vortex in a sound field // *J. Acoust. Soc. Am.*, 1987, 81. 1323-1326.
- [2] V.A.Babeshko, E.V.Glushkov and N.V.Glushkova, Energy vortices and backward fluxes in elastic waveguides. *Wave Motion*, 1992, 16, 183-192.
- [3] E.V. Glushkov and N.V. Glushkova, Blocking property of energy vortices in elastic waveguides // *J. Acoust. Soc. Am.*, 1997, 102(3), 1356-1360.
- [4] E. Glushkov, N. Glushkova, M. Golub, A. Boström, Natural resonance frequencies, wave blocking, and energy localization in an elastic half-space and waveguide with a crack // *J. Acoust. Soc. Am.*, 2006, 119(6), 3589-3598.
- [5] E. V. Glushkov, N. V. Glushkova, M. V. Golub and Ch. Zhang, Resonance blocking of traveling waves by a system of cracks in an elastic layer // *Acoustical Physics*, 2009, 55(1), 8-16.

On self-excited vibrations due to sliding friction between moving bodies

Hartmut Hetzler (hetzler@itm.uni-karlsruhe.de)

Universität Karlsruhe (TH), Institut für Technische Mechanik, Germany

1 Introduction

Self-excited vibrations in systems of moving visko-elastic bodies are a common phenomenon in engineering applications. Popular examples reach from squealing vehicle brakes or clutches to insufficiently lubricated bearings. In the case of brake squeal, for instance, considerable effort has been expended during the last years on the basic mechanisms and appropriate modelling approaches. Today, it is commonly accepted that one of the main causes of brake squeal is a flutter type instability of the steady sliding state. This instability mainly arises from non-conservative contributions of the friction, which – after linearization and discretization – yield a non-symmetric stiffness matrix. While this mechanism has been known since the 1970s [1], it was not before the beginning of this century that the influence of the friction on the system's damping had been revealed [2]. Furthermore, the gyroscopic terms due to the transport motion give rise to gyroscopic-circulatory perturbation equations, which are known to exhibit a complicated stability behaviour ([3] for instance). Thus, one may ask whether there might be further frictional contributions to steady state stability.

2 Modeling

It is assumed that the stationary motion of an elastic body i may be decomposed into a prescribed rigid body motion \vec{r}_{Ti} and small motions \vec{w}_i about this transport motion, i.e. $\vec{r}_i = \vec{r}_{Ti} + \vec{w}_i$. For a linearized description, the contact zone Γ_C often may be described with respect to the intermediate configuration \vec{r}_{Ti} after the transport motion. Thus, from the identity $\vec{r}_{Ti}(\mathbf{x}, t) = \vec{r}_{Ti}(\mathbf{X}(\mathbf{x}, t), t)$ follows $\mathbf{x} = \mathbf{X}(\mathbf{x}, t)$, which relates the spatial coordinates $\mathbf{x} = (x, y, z)^\top$ of the intermediate configuration to the corresponding material coordinates $\mathbf{X} = (X, Y, Z)^\top$. If the intermediate configuration and the material reference coincide at $t = 0$, spatial and material are usually related by $\mathbf{x} = \mathbf{X} + \int_0^t \mathbf{v}_T dt$, thus $\dot{\mathbf{x}} = \dot{\mathbf{X}} + \mathbf{v}_T$. Please note that $\vec{r}_\alpha = \vec{r}_\alpha(\mathbf{x}, t)$ are spatial vector fields and material time derivatives must account for the transport motion, $\vec{v}_\alpha = \dot{\vec{r}} + \mathbf{v}_T^\top \frac{\partial}{\partial \mathbf{x}} \vec{r}_\alpha$ ($\alpha = i, j$). For a system of N bodies, evaluation of an analytical principle, like Hamilton's Principle for instance, and subtraction of the steady state yields a weak formulation of the perturbation equations

$$0 = \sum_{i=1}^N \int_{\Omega_i} \delta \vec{w}_i \cdot \left(\mathcal{M}_i[\ddot{\vec{w}}_i] + \mathcal{P}_i[\dot{\vec{w}}_i] + \mathcal{Q}_i[\vec{w}_i] \right) dv + \Delta \{ \delta \Pi_C \} - \Delta \{ \delta W_C \} - \Delta \{ \delta W_{np} \}, \quad (1)$$

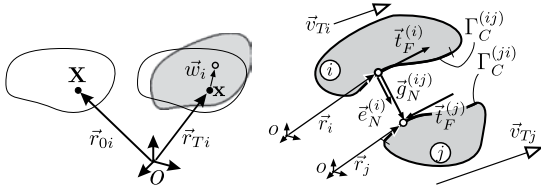


Figure 1.

where $\Delta\{\}$ denotes linearization, $\mathcal{M}_i = \mathcal{M}_i^\top$ is the mass operator of the i th body and $\mathcal{P}_i = \mathcal{D}_i + v_T \mathcal{G}_i$ contains the symmetric damping operator $\mathcal{D}_i = \mathcal{D}_i^\top$ as well as the skew-symmetric gyroscopic contributions $\mathcal{G}_i = -\mathcal{G}_i^\top$. Moreover, $\mathcal{Q}_i = \mathcal{K}_i + v_T \mathcal{N}_i + v_T^2 \mathcal{K}_i^*$ consists of the symmetric stiffness operator $\mathcal{K}_i = \mathcal{K}_i^\top$, the symmetric centrifugal effects $\mathcal{K}_i^* = \mathcal{K}_i^{*\top}$ and may exhibit skew-symmetric influences $\mathcal{N}_i = -\mathcal{N}_i^\top$ from internal damping. δW_{np} collects the virtual work of non-potential forces, that are not considered otherwise. In order to express the contributions of the contact $\Gamma_C^{(ij)}$ between body i and j , the gap vector $\vec{g}^{(ij)} = \vec{r}_j - \vec{r}_i$ is introduced, which connects a surface point on i to its mating contact partner on j . Using the decomposition of the positional field, the gap vector reads $\vec{g}^{(ij)} = (\vec{r}_j - \vec{r}_i) + (\vec{w}_j - \vec{w}_i) = \vec{g}_0 + \Delta \vec{g}$. On each contact partner, a tangential coordinate frame may be given by the outward surface normal $\vec{e}_N^{i/j}$. Using this, the normal gap g_N is given by $g_N^{(ij)} = \vec{g}^{(ij)} \cdot \vec{e}_N^{(i)}$. With $\vec{v}_{rel}^{(ij)} = \vec{v}_j - \vec{v}_i$, the direction of the sliding friction traction reads $\vec{e}_F^{(i)} = -\vec{e}_F^{(j)} = \vec{v}_{rel} / |\vec{v}_{rel}|$. For the sake of brevity, the superscript (ij) is dropped in the following and $\vec{e}_N = \vec{e}_N^{(i)}$.

Using a penalty approach, the linearized variation of the normal contact potential between body i and j reads $\Delta\{\delta \Pi_C^{(ij)}\} = \int_{\Gamma_C} \delta g_N k_C \Delta g_N da$, where $\delta(\Delta g_N) = \delta g_N$ has been used, $p = p(\Delta g_N) \approx p_0 + k_C(-\Delta g_N)$ is the linearized contact pressure and $k_C = \frac{\partial p}{\partial \Delta g_N} \Big|_0$ is the linear contact stiffness. Thus,

$$\Delta\{\delta \Pi_C\} = \sum_{(ij) \Gamma_C^{(ij)}} \int \delta \vec{g} \cdot \left[k_C (\vec{e}_N \otimes \vec{e}_N) \right]_0 \Delta \vec{g} da = \sum_{(ij) \Gamma_C^{(ij)}} \int \delta \vec{g} \cdot \mathcal{C}[\Delta \vec{g}] da, \quad (2)$$

where $\Delta\vec{g} = \vec{w}_j - \vec{w}_i$ and the contact stiffness $\mathcal{C} = \mathcal{C}^\top$ is symmetric and positive semi-definite. The subscript $[\dots]_0$ stresses that the bracketed terms refer to the linearization point.

The sliding friction stress vectors on the contacting bodies read $\vec{t}_F^{(\alpha)} = \mu p \vec{e}_F^{(\alpha)}$ ($\alpha = i, j$), where $\vec{t}_F^{(j)} = -\vec{t}_F^{(i)}$. Thus, the virtual work of the sliding friction between i - j reads $\delta W_C^{(ij)} = \int_{\Gamma_C^{(ij)}} \delta(\vec{r}_j - \vec{r}_i) \cdot [-\vec{t}_F^{(i)}] da = - \int_{\Gamma_C^{(ij)}} \delta\vec{g} \cdot \vec{e}_F^{(i)} \mu p(g_N) da$ from which Taylor expansion yields $\Delta\{\delta W_C^{(ij)}\} = - \int_{\Gamma_C^{(ij)}} \delta\vec{g} \cdot [\mu p_0 \Delta\vec{e}_F^{(i)} + \vec{e}_F^{(i)} \mu \Delta p] da$. Furthermore, with $v_{rel,0}^{(ij)} = \|\mathbf{v}_{Tj}^\top \frac{\partial}{\partial \mathbf{x}} \vec{r}_{0j} - \mathbf{v}_{Ti}^\top \frac{\partial}{\partial \mathbf{x}} \vec{r}_{0i}\|$ being the relative velocity in the linearization point, Taylor expansion of $\vec{e}_F^{(i)}$ yields $\Delta\vec{e}_F^{(i)} = \frac{1}{v_{rel,0}^{(ij)}} [\Delta\dot{\vec{g}} + \mathbf{v}_{Tj}^\top \frac{\partial}{\partial \mathbf{x}} \vec{w}_j - \mathbf{v}_{Ti}^\top \frac{\partial}{\partial \mathbf{x}} \vec{w}_i]$ and with $\Delta p = -k_C \Delta g_N = -k_C (\vec{e}_N \cdot \Delta\vec{g})$ one finally obtains

$$\begin{aligned} \Delta\{-\delta W_C\} &= \sum_{(ij)}^{n_C} \int_{\Gamma_C^{(ij)}} \delta\vec{g} \cdot \left(\left[\frac{\mu p_0}{v_{rel}^{(ij)}} \right]_0 \Delta\dot{\vec{g}} + \left[\frac{\mu p_0}{v_{rel}^{(ij)}} \right]_0 \left(\mathbf{v}_{Tj}^\top \frac{\partial}{\partial \mathbf{x}} \vec{w}_j - \mathbf{v}_{Ti}^\top \frac{\partial}{\partial \mathbf{x}} \vec{w}_i \right) - \left[\mu k_C (\vec{e}_F \otimes \vec{e}_N) \right]_0 \Delta\vec{g} \right) da \\ &= \sum_{(ij)}^{n_C} \int_{\Gamma_C^{(ij)}} \delta\vec{g} \cdot \left(\mathcal{R}_1[\Delta\dot{\vec{g}}] + \mathcal{R}_2[\vec{w}_i, \vec{w}_j] + \mathcal{R}_3[\Delta\vec{g}] \right) da, \end{aligned} \quad (3)$$

where $\mathcal{R}_1 = \mathcal{R}_1^\top$ is symmetric and positive semi-definite, while $\mathcal{R}_2 \neq \mathcal{R}_2^\top$, $\mathcal{R}_3 \neq \mathcal{R}_3^\top$ are nonsymmetric differential operators. The operators \mathcal{R}_1 and \mathcal{R}_2 stem from the changing direction of the friction stresses, while \mathcal{R}_3 arises from the change of contact pressure as the bodies deform. For small values of $v_{rel,0}^{(ij)} \ll 0$ the operator \mathcal{R}_1 will become very large. However, the limit $v_{rel,0}^{(ij)} = 0$ is not valid since it would involve stiction, which was precluded. For the second operator \mathcal{R}_2 this may not be observed: since nominator and denominator are of the order of magnitude of the velocity parameters, it will not become singular. In general it is found that \mathcal{R}_2 has rather small influence on the system.

3 Example: moving beam sliding through Winkler-type bedding

Above results are exemplified with the classical example of a moving Euler-Bernoulli-beam in frictional guides, cf. fig. 2 a), which is widely examined in literature (e.g. [6]). The example comprises a Euler-Bernoulli beam (body 2: length L ,

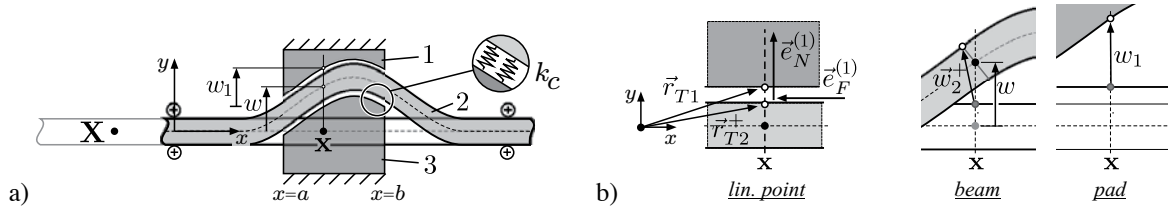


Figure 2.

height h , width b , density ρ , bending stiffness EI) which slides with the transport velocity v through two frictional pads (friction coefficient $\mu = \text{const}$), that are modelled as Winkler beddings (bodies 1 and 3, height h_p , width b , density ρ_p , bedding number k , spatial extent $a \leq x \leq b$). The transport motion is given by $x = X + vt$. The contact contributions are derived for the contact between the upper pad (body 1) and the beam (body 2) using the theory stated above. In this context, the superscript $()^+$ refers to the upper surface of the beam. The second contact follows analogously. The displacement of the beam's neutral fibre is denoted by $w(x, t)$ and $w_1(x, t)$ refers to the displacement of the friction pad's surface. Displacements are measured from the static solution. Thus, a point on the friction pad has the position $\vec{r}_1 = (x, w_1)_{xy}^\top + (0, w_1)_{xy}^\top = \vec{r}_{T1} + \vec{w}_1$, a point on the neutral fibre has $\vec{r}_2 = (x, 0)_{xy}^\top + (0, w)_{xy}^\top = \vec{r}_{T2} + \vec{w}_2$ and a point on the upper surface of the beam reads $\vec{r}_2^+ = (x, h/2)_{xy}^\top + (-h/2 w', w)_{xy}^\top = \vec{r}_{T2}^+ + \vec{w}_2^+$ (cf. fig. 2 b). The stiffness of the contact layer is given by k_C . If the displacement fields within the friction pads are assumed to be linear, the dynamics is described by

$$\int_0^L \delta w \left(\rho b h (\ddot{w} + 2v\dot{w}' + v^2 w'') + EI w'''' \right) dx + \sum_{i=1,3} \int_a^b \delta w_i \left(\frac{\rho_p b h_p}{6} \ddot{w}_i + k w_i \right) dx + \Delta\{\delta \Pi_C - \delta W_C\} = 0. \quad (4)$$

The upper tangential system in the reference configuration is given by $\vec{e}_F^{(2)} = (-1, 0)_{xy}^\top$ and $\vec{e}_N^{(2)} = (0, 1)_{xy}^\top$. The linearized gap vector reads $\Delta\vec{g}^{(21)} = \vec{w}_1 - \vec{w}_2^+ = (h/2 w', w_1 - w)_{xy}^\top$ and thus $\delta\vec{g}^{(21)} = \delta(\Delta\vec{g}^{(21)}) = (h/2 \delta w', \delta w_1 - \delta w)_{xy}^\top$.

Hence, the contact contributions read

$$\Delta \left\{ \delta \Pi_C^{(21)} \right\} = \int_a^b b k_C \left[\frac{h/2 \delta w'}{\delta w_1 - \delta w} \right]^\top \left[\begin{pmatrix} 0 \\ 1 \end{pmatrix} \otimes \begin{pmatrix} 0 \\ 1 \end{pmatrix} \right] \left[\frac{h/2 w'}{w_1 - w} \right] dx = \int_a^b b k_C (\delta w_1 - \delta w) (w_1 - w) dx \quad \text{and} \quad (5)$$

$$\begin{aligned} \Delta \left\{ \delta W_C^{(21)} \right\} &= \int_a^b \left[\frac{h/2 \delta w'}{\delta w_1 - \delta w} \right]^\top \left(\frac{\mu p_0}{v} \left[\frac{h/2 \dot{w}'}{\dot{w}_1 - \dot{w}} \right] - \frac{\mu p_0}{v} v \frac{\partial}{\partial x} \left[\frac{h/2 w'}{w} \right] + \mu k_C \left[\begin{pmatrix} -1 \\ 0 \end{pmatrix} \otimes \begin{pmatrix} 0 \\ 1 \end{pmatrix} \right] \left[\frac{h/2 w'}{w_1 - w} \right] \right) b dx \\ &= \int_a^b \delta w' \frac{h}{2} \left[\underbrace{\mu p_0 \left(\frac{h}{2v} \dot{w}' - \frac{h}{2} w'' \right)}_{\Delta \vec{e}_F \cdot \vec{e}_x} - \underbrace{\mu k_C (w_1 - w)}_{\Delta p} \right] + (\delta w_1 - \delta w) \mu p_0 \left[\underbrace{\frac{1}{v} (\dot{w}_1 - \dot{w}) - w'}_{\Delta \vec{e}_F \cdot \vec{e}_y} \right] b dx. \quad (6) \end{aligned}$$

The terms arising from the second contact on the lower surface are derived analogously. With the linearized upper friction traction $\Delta \vec{t}^+ = \mu p_0 \Delta \vec{e}_F + \vec{e}_{F0} \mu \Delta p = \Delta t_x \vec{e}_x + \Delta t_y \vec{e}_y$, the first addend in (6) is readily found to express the virtual work of the torque $h/2 \Delta t_x$, while the second is the virt. work of the Δt_y . Moreover, the first and the last underbraced term are components of $\Delta \vec{e}_F$, consisting of the local derivative together with the convective part. Equations (5) and (6) correspond to results from literature (e.g.[6]); however slight discrepancies arise due to the different types of normal contact formulation.

Finally, the spatial fields may be approximated by a Ritz-type ansatz of the form $w_k = \sum_i \varphi_{ki}(x) q_{ki}(t) = \Phi_k \mathbf{q}_k$. For $p_0 = const$ this yields the perturbation equations of the steady state in matrix form

$$\mathbf{M} \ddot{\mathbf{q}} + v \mathbf{G} \dot{\mathbf{q}} + \frac{\mu p_0}{v} \mathbf{D}_F \dot{\mathbf{q}} + [\mathbf{K} + k_C \mathbf{K}_N + \mu k_C \mathbf{C}_{F1} + \mu p_0 \mathbf{C}_{F2}] \mathbf{q} = \mathbf{0}. \quad (7)$$

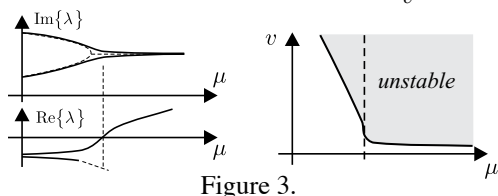


Figure 3.

As predicted above, $\mathbf{M} = \mathbf{M}^\top$, $\mathbf{D}_F = \mathbf{D}_F^\top$, $\mathbf{K} = \mathbf{K}^\top$, $\mathbf{K}_N = \mathbf{K}_N^\top$ are symmetric and positive definite, while $\mathbf{G} = -\mathbf{G}^\top$ is skew-symmetric and \mathbf{C}_{F1} , \mathbf{C}_{F2} are not symmetric. Usually, the entries of \mathbf{C}_{F1} are found to be much larger than those of \mathbf{C}_{F2} . Equation (7) is a gyroscopic-circulatory system, which may exhibit flutter instability

due to the non-symmetric positional forces (e.g. [7], [3]). Figure 3 schematically outlines the behaviour of the critical eigenvalues in case of flutter as well as a corresponding stability chart (e.g. [3]). Please note the influence of v on the stability border: for low v the influence of \mathbf{D}_F grows strongly and stabilizes the system, while for higher v the gyroscopic contributions further destabilize the system. The dashed line denotes the flutter border if damping and gyroscopic terms are absent. By consideration of tribological properties, the contact stiffness k_C may be expressed by a constitutive contact law, cf. [5].

4 Conclusion

Using an abstract approach, the frictional contributions to the linearized perturbation equations have been formulated generally without relying on specific structural models (like beams or plates). The arising terms have been discussed with respect to symmetry, definiteness and physical meaning. Thus, it is found that the structure of the perturbation equations as well as the influence of the contact parameters may be predicted to a great extent. Finally, the findings are demonstrated with a moving beam in frictional guides.

References

- [1] M. North, *Disc brake squeal*. In: MIRA Research Report 5, 1972.
- [2] H. Storck, F. Moser, *Two dimensional friction force in brake squeal*. In: Braking 2004 – Vehicle Braking & Chassis Control, 2004.
- [3] H. Hetzler, *Zur Stabilität von Systemen bewegter Kontinua mit Reibkontakt am Beispiel des Bremsenquietschens*, doctoral thesis, Universität Karlsruhe, 2008.
- [4] H. Hetzler, *On Moving Continua with Contacts and Sliding Friction: Modeling, General Properties and Examples*, International Journal of Solids and Structures, 2009, DOI: 10.1016/j.ijsolstr.2009.01.037
- [5] H. Hetzler, *On the influence of contact mechanics on friction induced flutter instability*, Proceedings in Applied Mathematics and Mechanics, 2009 (to appear)
- [6] D. Hochlenert, et.al., *Friction induced vibrations in moving continua and their application to brake squeal*, Journal of Applied Mechanics, 74:542-550, 2007
- [7] A.P. Seyranian, A.A. Mailybaev, *Multiparameter stability theory with mechanical applications*, World Scientific, 2003

Vibration of cantilevered rectangular plates with edge V-notches or slits

C. S. Huang, S. C. Liao, and I. C. Lee

Department of Civil Engineering, National Chiao Tung University, Hsinchu, Taiwan

INTRODUCTION

Plates in various geometric forms are commonly used in practical engineering. Among all the possible shapes of plates, the rectangular plate is of the greatest importance and interest in vibration analysis. There have been some vibration analyses of rectangular plates having V-notches or side cracks. Most of the works on vibrations of cracked rectangular plates considered simply supported boundary conditions along four edges or a pair of edges and used various integral equation techniques to find the natural vibration frequencies [1~3]. These solutions cannot be extended to solve problems with other boundary conditions because Levy's form of solution or Navier's form of solution was involved. Yuan and Dickinson [4] and Liew *et al.* [5] applied the Ritz method and different domain decomposition techniques to analyze the vibrations of cracked rectangular plates with various types of boundary conditions. Yuan and Dickinson [4] introduced artificial springs at the interconnecting boundaries between the sub-domains, while Liew *et al.* [5] imposed the continuity conditions in an integration sense, but not everywhere along the interconnecting boundaries. Huang *et al.* [6] investigated the vibrations of rectangular plates having V-notches by using the Ritz method with the admissible functions including corner functions to appropriately describe the stress singularities at the tip of V-notch. They showed numerical results for free rectangular plates.

The present contribution extends the work of Huang *et al.* [6] to consider cantilevered rectangular plates and further investigates the cases of V-notch angle equal to zero (slit). This work shows the corner functions established based on Williams' solution [7] do not give fast convergent solutions for cracked plates, especially for a plate with a large crack. A new set of admissible functions is introduced to remedy the shortcomings.

METHODOLOGY AND RESULTS

Consider a rectangular cantilever plate with a V-notch as shown in Fig. 1. When the V-notch angle α equals zero, it becomes side crack. Stress singularities exist at the tip of V-notch when α is less than 180° [7]. When the Ritz method is applied to find the natural frequencies and mode shapes for such plate, the admissible functions for transverse displacement are assumed as the sum of two sets of functions,

$$W(x, y) = x^2[W_p(x, y) + W_c(r, \theta)],$$

where the function before the brackets is inserted to satisfy the geometric boundary conditions along $x=0$; $W_p(x, y)$ consists of algebraic polynomials which forms a mathematically complete set of functions if an infinite number of terms are used; $W_c(r, \theta)$ is used to supplement $W_p(x, y)$ appropriately describing the important behaviors of the true solutions of $W(x, y)$. When V-notched plates are under consideration,

$W_c(r, \theta)$ must have the capability of appropriately describing the stress singularities around the tip of the V-notch. When a cracked plate is considered, $W_c(r, \theta)$ must not only be capable of appropriately describing the stress singularity behavior around the crack tip, but also to represent the discontinuities of displacement and slope across the crack.

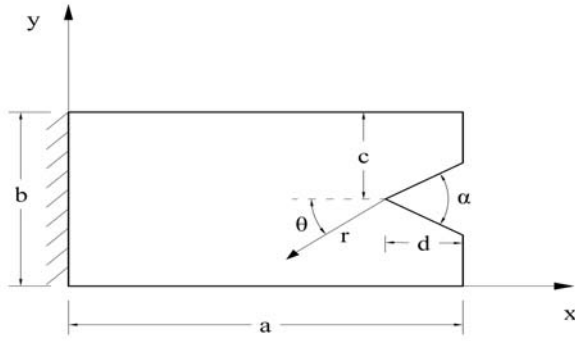


Fig. 1 Dimensions and coordinates for a V-notched plate

Following the solution procedure given in Williams [7], one can find the asymptotic solutions (i.e., corner functions) for a V-notch with free boundary conditions along its two sides. These corner functions are applied to construct $W_c(r, \theta)$,

$$W_{cn}^S(r, \theta) = r^{\lambda_n+1} \left[\frac{\gamma_2 \sin[(\lambda_n-1)\beta/2]}{\gamma_1 \sin[(\lambda_n+1)\beta/2]} \cos(\lambda_n+1)\theta + \cos(\lambda_n-1)\theta \right],$$

$$W_{cn}^A(r, \theta) = r^{\bar{\lambda}_n+1} \left[\frac{\bar{\gamma}_2 \cos[(\bar{\lambda}_n-1)\beta/2]}{\bar{\gamma}_1 \cos[(\bar{\lambda}_n+1)\beta/2]} \sin(\bar{\lambda}_n+1)\theta + \sin(\bar{\lambda}_n-1)\theta \right],$$

where superscripts “A” and “S” denote antisymmetric and symmetric corner functions, respectively, $\gamma_1 = (\lambda_n+1)(\nu-1)$, $\gamma_2 = -\lambda_n(\nu-1) + 3 + \nu$, $\bar{\gamma}_1 = (\bar{\lambda}_n+1)(\nu-1)$, $\bar{\gamma}_2 = -\bar{\lambda}_n(\nu-1) + 3 + \nu$, $\beta = 2\pi - \alpha$, and λ_n and $\bar{\lambda}_n$, respectively, are roots of the equations

$$\sin(\lambda_n\beta) = \frac{1-\nu}{3+\nu} \lambda_n \sin \beta \quad \text{and} \quad \sin(\bar{\lambda}_n\beta) = -\frac{1-\nu}{3+\nu} \bar{\lambda}_n \sin \beta.$$

Poisson’s ratio (ν) equal to 0.3 was used for all numerical results. The results with $\alpha \neq 0$ shown in Table 1 were obtained by using such $W_c(r, \theta)$ and regular polynomials for the admissible functions.

When applying these corner functions to analyze a side-cracked plate ($\alpha=0$), one finds that the convergence of numerical solutions is not fast enough to obtain accurate results before ill-conditioned matrixes occur. Consequently, the following set of functions is proposed for $W_c(r, \theta)$,

$$\left\{ r^{(2n+1)/2} \cos \frac{2l+1}{2} \theta \text{ and } r^{(2n+1)/2} \sin \frac{2l+1}{2} \theta \mid l = 0, 1, 2, \dots, n \text{ and } n = 1, 2, 3, \dots \right\}.$$

Using such set of functions considerably accelerates the convergence of the numerical solutions. The results with $\alpha = 0$ given in Table 1 were obtained using such set of functions and regular polynomials and are exact to at least three significant figures.

REFERENCES

1. B. Stahl, L. M. Keer, Vibration and stability of cracked rectangular plates, *International Journal of Solids and*

Structures 8(1) (1972) 69-91.

2. K. Neku, Free vibration of a simply-supported rectangular plate with a straight through-notch, *Bulletin of the Japan Society of Mechanical Engineers* 25(199) (1982) 16-23.
3. R. Solecki, Bending vibration of a simply supported rectangular plate with a crack parallel to one edge, *Engineering Fracture Mechanics*, 18(6) (1983) 1111-1118.
4. J. Yuan, S. M. Dickinson, The flexural vibration of rectangular plate systems approached by using artificial springs in the Rayleigh-Ritz method, *Journal of Sound and Vibration*, 159(1) (1992) 39-55.
5. K. M. Liew, K. C. Hung, M. K. Lim, A solution method for analysis of cracked plates under vibration, *Engineering Fracture Mechanics*, 48(3) (1994) 393-404.
6. C. S. Huang, A. W. Leissa, S. C. Liao, Vibration analysis of rectangular plates with edge V-notches, *International Journal of Mechanical Science*, 50 (2008) 1255-1262.
7. M. L. Williams, Surface stress singularities resulting from various boundary conditions in angular corners of plates under bending, *Proceedings of the First U.S. National Congress of Applied Mechanics*, 1952, pp.325-329.

Table 1 Frequency parameters for cantilevered square plates with a horizontal V-notch or slit

c/b	α	d/a	$\omega\alpha^2\sqrt{\rho h/D}$				
			1	2	3	4	5
		0	3.471	8.508	21.29	27.20	30.96
0.5	0°	0.1	3.471	8.440	21.23	26.50	30.34
		0.3	3.471	7.704	20.51	23.04	24.70
		0.5	3.471	6.026	17.75	19.00	21.72
	5°	0.1	3.474	8.439	21.26	26.51	30.34
		0.3	3.492	7.698	20.74	23.06	24.82
		0.5	3.519	6.044	18.30	19.56	21.75
	30°	0.1	3.489	8.437	21.37	26.54	30.32
		0.3	3.607	7.689	21.82	23.31	25.42
		0.5	3.800	6.172	20.85	22.30	22.41
0.75	0°	0.1	3.471	8.462	21.26	26.90	30.58
		0.3	3.471	7.952	20.26	22.29	28.35
		0.5	3.471	6.465	14.08	21.52	26.86
	5°	0.1	3.474	8.466	21.28	26.90	30.60
		0.3	3.492	7.990	20.33	22.36	28.51
		0.5	3.518	6.550	14.37	21.63	27.33
	30°	0.1	3.488	8.485	21.35	26.88	30.69
		0.3	3.604	8.176	20.73	22.75	29.25
		0.5	3.778	7.220	15.98	22.16	29.15

Vibration of a Solid Cylinder Fixed on One End

James R. Hutchinson

Civil and Environmental Engineering Department
University of California, Davis CA 95616

Introduction

The problem considered in this paper is that of a linearly elastic solid circular cylinder which is free along its sides and on one end but is fully fixed at the other end. The solution for the natural frequencies and mode shapes is accomplished by the series superposition method. This problem was treated by Leissa and So [1, 2] in 1995 using the Ritz Method. In those papers they considered both the free-free (both ends free) and the fixed-free cases. I wrote comments on those two papers [3, 4] in which I used the series superposition method of my 1980 paper [5] to find accurate frequencies for comparison with the free-free case. Most of frequency results from the two methods coincided completely. Where we had disagreements my frequencies were generally lower than those of Leissa and So, but usually only by one or two in the last significant figure. The fixed-free case is of particular interest because of the singularity that exists at the junction of the free and fixed surfaces.

Series Superposition Solution

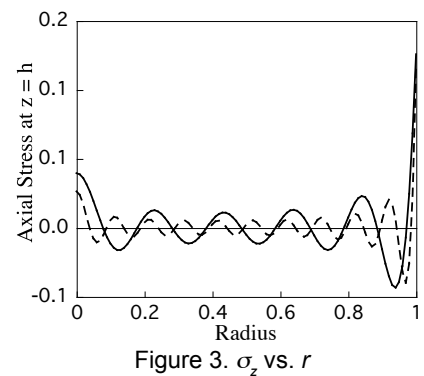
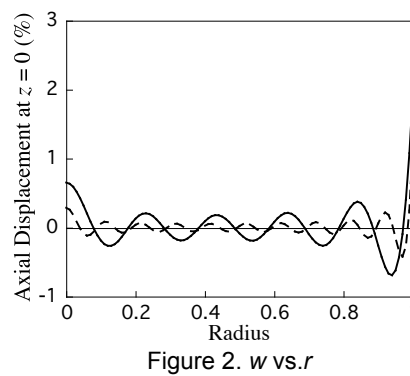
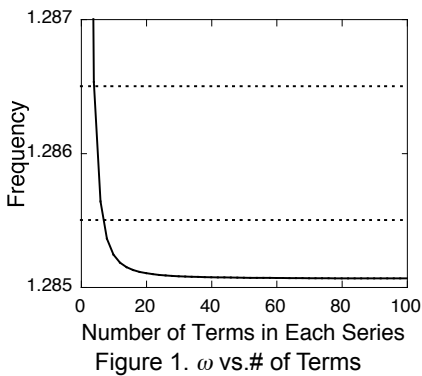
In this method, solution forms that are solutions of the governing differential equations are combined to satisfy identically some of the boundary conditions. The remaining boundary conditions are satisfied by orthogonalization. All symbols used in this paper are dimensionless. The radial displacement u , the tangential displacement v , and the axial displacement w are made dimensionless by dividing by the outer radius. All stress quantities are made dimensionless by dividing by the shear modulus G . The wave numbers α , β and δ are made dimensionless by multiplying by the outer radius. The time dependence is removed by assuming that all displacements and stresses vary sinusoidally in phase at the same frequency. The frequency ω is made dimensionless by multiplying by the radius and dividing by the shear wave velocity. The distance h is the height (or length) of the cylinder and is made dimensionless by dividing by the outer radius. The solution forms are shown in Table 1 of my 1980 paper. With the exception of the case when $n = 0$, where n is the circumferential wave number, these forms are combined in four series. Two of the series are Bessel series and two are trigonometric series. The four series are constructed to identically satisfy the following five boundary conditions, $u(r,0) = 0$, $v(r,0) = 0$, $\tau_{rz}(r,h) = 0$, $\tau_{\theta z}(r,h) = 0$ and $\tau_{rz}(1,z) = 0$. The remaining boundary conditions, $w(r,0) = 0$, $\sigma_z(r,h) = 0$, $\sigma_r(1,z) = 0$, $\tau_{r\theta}(1,z) = 0$ are satisfied by orthogonality. The series representing $w(r,0)$ and $\sigma_z(r,h)$ are multiplied by $rJ_n(\alpha_j r)$ where $\alpha_j = \text{zeroes of } J_n'(\alpha_j)$, integrated over the radius between zero and 1 and equated to zero. The series representing $\sigma_r(1,z)$ and $\tau_{r\theta}(1,z)$ are multiplied by $\sin(\alpha_j z)$ where $\alpha_j = (2j-1)\pi/2h$ with $j = 1, 2, 3 \dots$, integrated over z between zero and h and equated to zero. This leads to system of simultaneous equations, with a zero right hand side, of the order $2N_r + 2N_z$, where N_r and N_z are the number of terms in the radial and axial directions respectively. The unknowns in this system of equations are the coefficients of the four series A_i , B_i , C_i , and D_i . The only parameters in the equations are Poisson's Ratio ν the height h , the circumferential wavenumber n and the frequency ω . A value of Poisson's Ratio, height and circumferential wave number is chosen and the frequencies which make the determinant of the coefficients equal to zero is sought. On finding the frequencies the relative values of A_i , B_i , C_i , and D_i are determined and the series are summed to find the modal displacements and stresses. When $n = 0$ the problem has two solutions: one is the axisymmetric case, where v , $\tau_{r\theta}$ and $\tau_{\theta z}$ are zero, the other is the pure shear case, where only v , $\tau_{r\theta}$ and $\tau_{\theta z}$ are non-zero. The solution process for the axisymmetric case follows the same process as above except that the boundary condition on $\tau_{r\theta}(1,z)$ is no longer relevant so the order of the characteristic matrix reduces to $2N_r + N_z$. For the pure shear case there is an exact solution and the method of series superposition is not needed, and, hence, not treated in this paper.

Results

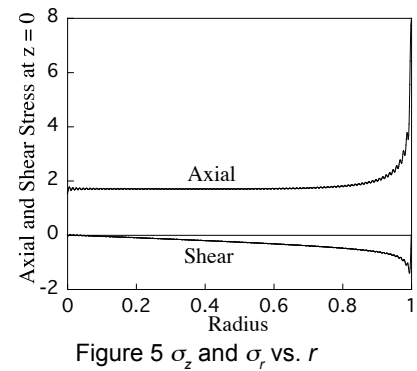
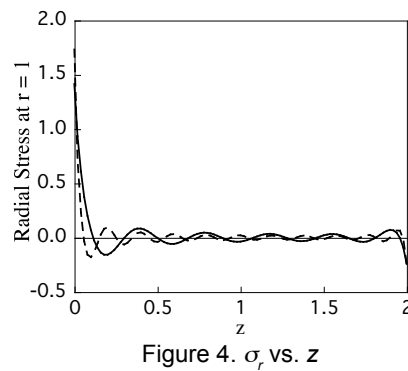
The first consideration is convergence of the solution as more terms are chosen. Figures 1, 2, 3, 4 and 5 are for the axisymmetric problem with a Length to Diameter ratio of 1 ($h = 2$) and Poisson's Ratio of 0.3. These Figures all use an equal number of terms in each series. Figure 1 shows the convergence of the fundamental frequency as more terms are chosen in the series. Figures 2, 3 and 4 show how well the boundary conditions on w at $z = 0$, σ_z at $z = h$ and σ_r at $r = 1$ are satisfied. Figure 5 shows the stress distribution on the fixed boundary. Both displacements and stresses in these Figures have been normalized to maximum displacement of 1 (i.e. $w(0,h) = 1$). In Figures 2, 3 and 4 the solid lines are for 10 terms in each series and the dashed lines are for 20 terms in each series. Figure 5 is the solution using 200 terms in each series.

Leissa and So (2) in their Table V give the axisymmetric frequency for $L/D = 1$ and $\nu = 0.3$ as 1.286. Their answer thus lies between the two horizontal dotted lines shown in Figure 1. Figure 1 shows that my answer to the same number of

significant figures is 1.285. My results agree completely with the results in Leissa and So's Table V for 39% of the data and are lower by 1 in the last significant figure for 38% of the data. With 8 terms in each series, 4 place accuracy is achieved. With 14 terms, 5 place accuracy is achieved, and with 90 terms, 6 places accuracy is achieved. The frequency to six

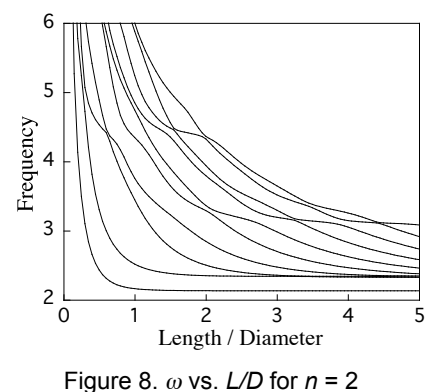
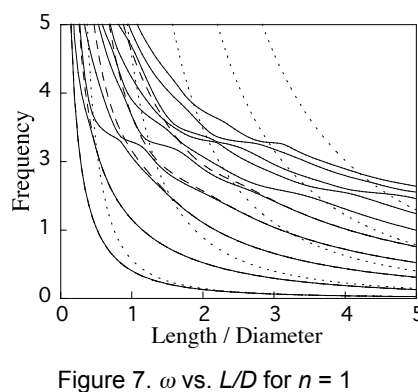
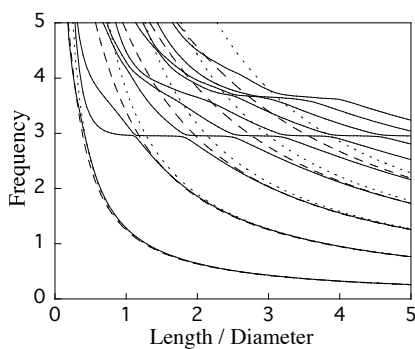


significant figures for this example is 1.28506. Figures 2, 3 and 4 show that the zero boundary conditions are reasonably approximated with this solution. They further show that over most of the boundary they converge to zero as more terms are chosen. The peaks at the end points do not converge to zero as fast as in the center portion; however, with one exception they all converge. The one exception is σ_r at $z = 0$ which grows as more terms are chosen. For example with 10 100 and 200 terms the radial stresses at $z = 0$ are 1.4, 2.8, and 3.4 respectively. As expected modal stresses do not converge as fast as modal displacements. Figure 5 shows both the axial and shear stress along the fixed boundary. The axial stress shows a peak at the singular point. This peak grows as the number of terms is increased. For example with 10, 100 and 200 terms the axial stresses at this point are 3.3, 6.4 and 7.9 respectively. The shear stress at the singular point was set identically to zero, but Figure 5 shows that it gets to zero as a step function. One can conclude that at the singular point (1,0) there is a line load with both horizontal and vertical force components, and that the shear stress has a finite value on the fixed face with a zero value on its adjacent free face.



As expected modal stresses do not converge as fast as modal displacements. Figure 5 shows both the axial and shear stress along the fixed boundary. The axial stress shows a peak at the singular point. This peak grows as the number of terms is increased. For example with 10, 100 and 200 terms the axial stresses at this point are 3.3, 6.4 and 7.9 respectively. The shear stress at the singular point was set identically to zero, but Figure 5 shows that it gets to zero as a step function. One can conclude that at the singular point (1,0) there is a line load with both horizontal and vertical force components, and that the shear stress has a finite value on the fixed face with a zero value on its adjacent free face.

Figures 6 through 11 show the frequencies as a function of the length to diameter ratio. These are for n equal to 0, 1, 2, 3, 4, and 5. All are for Poisson's Ratio equal to 0.3 and show the lowest ten frequencies. In addition to the series solutions Figure 6 shows the first five frequencies for the elementary rod (dotted lines) and the rod with Love's modification (dashed lines). It can be seen that for the first frequency the elementary solution is actually a better match to the series solution than Love's modification. This is not true for the higher frequencies. For $L/D = 5$, Love's modification matches the series solution for the four lowest frequencies, whereas the elementary rod solution only shows a match for the first two. In Figure 7 the Timoshenko beam solution is shown as dashed lines and the Euler-Bernoulli solution as dotted lines.



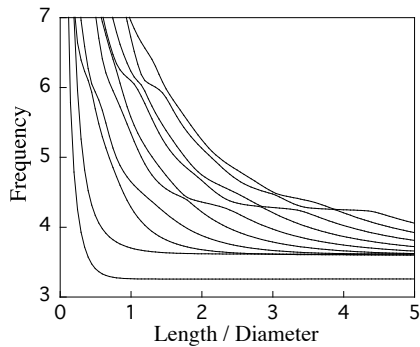


Figure 9. ω vs. L/D for $n = 3$

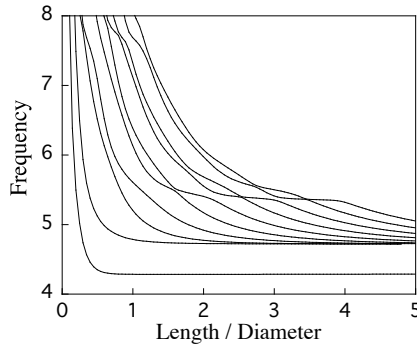


Figure 10. ω vs. L/D for $n = 4$

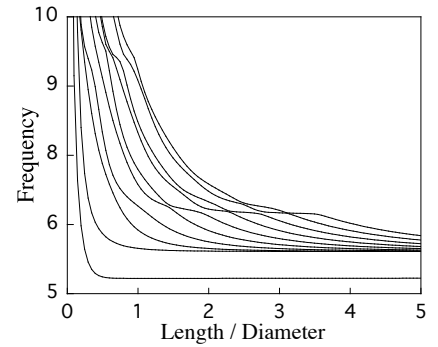
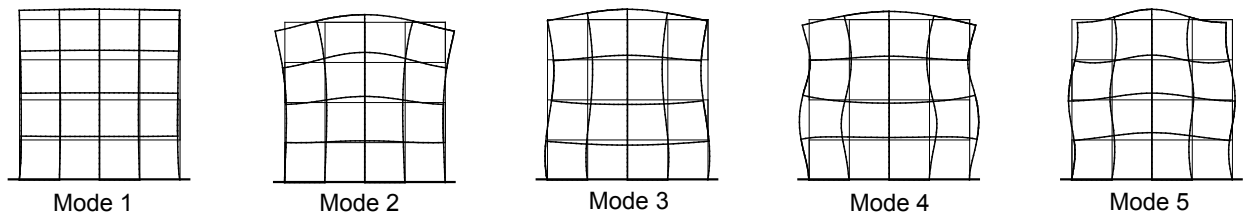


Figure 11. ω vs. L/D for $n = 5$

A Timoshenko shear coefficient of $(6 + 12\nu + 6\nu^2)/(7 + 12\nu + 4\nu^2)$ was used. Figure 7 shows that the Timoshenko beam gives a good match for the lowest frequency at L/D above 0.1, the second above 0.5, the third above 1.5, the fourth above 2.5 and the fifth above 3.2. The Euler-Bernoulli solution only matches the lowest frequency above an L/D of 3. In Figures 6 through 11 it can be seen that there are many places where the curves come very close together, however, close inspection shows that they never cross. The only way these curves can cross is if Poisson's Ratio is zero.

In this type of problem it is important to not only consider the frequencies but also the mode shapes. It lets one see how well the boundary conditions are met as in Figures 2, 3 and 4, but it also gives some insight into the physics of the problem. A sampling of the mode shapes is given below. These are for the axisymmetric modes with L/D equal to 1. It can be seen that the first mode greatly resembles the first rod mode, whereas the higher modes have no relationship to rod modes. This outcome is in agreement with Figure 5 where only the fundamental frequency matched the elementary solution



for L/D equal to 1. The first mode shape can also help explain why the Love modification is actually not as accurate as the elementary rod solution in this case. Both allow the radial displacement from the Poisson's ratio effect. The Love modification includes the radial inertia thereby lowering the frequency; however, the radial displacement is constrained at $z = 0$. This constraint will raise the frequency, thus for the very short rod the elementary solution represents a better compromise.

Conclusions

The series superposition method works very well for this type of problem. It produces highly accurate solutions for both the frequencies and mode shapes. The frequencies found using this method concur reasonably well with the frequencies found by Leissa and So [1, 2]. Comparisons with elementary solutions for both the rod and beam clearly show the range of applicability of these theories. The method also leads to a description of the singularity.

References

1. A. W. Leissa and J. So "Accurate vibration frequencies of circular cylinders from three-dimensional analysis." *J. Acoust. Soc. Am.* **98**, 2136-2141 (1995)
2. A. W. Leissa and J. So "Comparisons of vibration frequencies for rods and beams from one-dimensional and three-dimensional analyses." *J. Acoust. Soc. Am.* **98**, 2122-2135 (1995)
3. J. R. Hutchinson Comments on "Accurate vibration frequencies of circular cylinders from three-dimensional analysis." [*J. Acoust. Soc. Am.* **98**, 2136-2141 (1995)], *J. Acoust. Soc. Am.* **100**, 1894-1895 (1996)
4. J. R. Hutchinson Comments on "Comparisons of vibration frequencies for rods and beams from one-dimensional and three-dimensional analyses." [*J. Acoust. Soc. Am.* **98**, 2122-2135 (1995)], *J. Acoust. Soc. Am.* **100**, 1890-1891 (1996)
5. J. R. Hutchinson "Vibrations of solid cylinders" *J. Appl. Mech.*, 47 901-907 (1980)

Embedding negative structures to model holes and cut-outs

S. Ilanko

*Department of Engineering
The University of Waikato
Te Whare Wananga o Waikato
Gate 1 Knighton Road
Private Bag 3105, Hamilton 3240
New Zealand
ilanko@waikato.ac.nz*

It has now been established that geometric boundary conditions and continuity conditions can be modelled by using either positive or negative stiffness or inertia type penalty term [1-5]. The experience of working with negative stiffness and inertial parameters has led to the question: what if both stiffness and mass were to be taken as negative? Changing the sign of all stiffness and inertial terms of a structure is simply equivalent to multiplying both sides of an eigenvalue equation by minus one, which does not change its frequencies or modes. Basically, a negative structure in such a sense has the same vibratory properties as that of its positive counterpart, although the structure itself may not have a physical meaning.

However, an interesting question emerges about the behaviour of a structure formed by attaching such a negative structure to a larger positive structure: would it be possible to effect a hole or a cut-out in a plate by embedding a “negative plate” to a plate without the hole? The idea is that the negative plate to be attached must have the same shape as that of the hole and the same magnitude of stiffness and mass distribution but with opposite sign (see Figure 1). The negative plate unit would be bonded to the larger (uncut) plate by using distributed penalty stiffness over the area of bonding to prevent any relative motion between the negative part and the positive part.

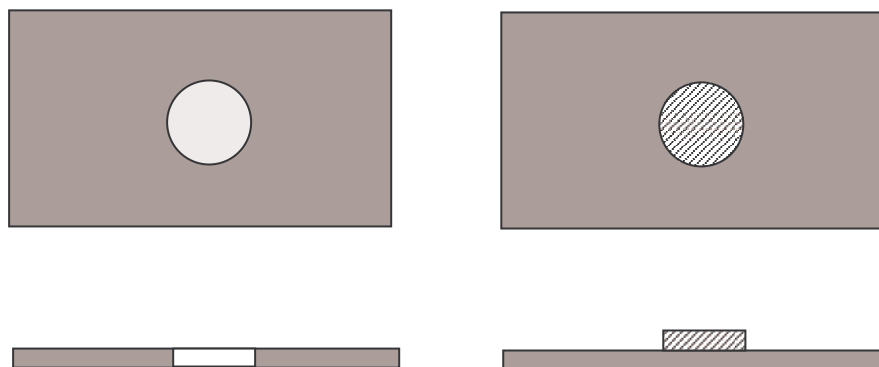


Figure 1

To see if this concept works, a cantilever beam of length L , flexural rigidity EI , and mass per unit length m was made into a free-free beam of length $L/2$, by attaching another cantilever beam of length $L/2$, flexural rigidity $-EI$ and mass per unit length $-m$. The two beams were connected by means of a uniform distribution of elastic springs of high stiffness k per unit

length along the entire length of the negative beam, and a Rayleigh-Ritz analysis was carried out to determine the natural frequencies and modes (see Figure 2). Positive and negative values were used for k , and the average of the two results was taken to minimise any error due to violation of the constraint condition along the bonded length.



Figure 2

The result was interesting. Using a series of 7 terms each for the two cantilever beams and a non-dimensional stiffness coefficient $\alpha = 10^{11}$, which may be regarded as a penalty parameter, the first three non-zero natural frequencies of the free-free beam were determined. These are given in Table 1 together with those calculated using a straight-forward Rayleigh-Ritz approach with simple polynomials. Interestingly, while the first natural frequency is slightly worse than that obtained using simple polynomials for a free-free beam, the second one is slightly better and the third is worse. It is not clear why the trend changes but, unlike in typical penalty applications where the penalty terms are used to enforce geometric boundary conditions, in this case, they are indirectly being used to relax the conditions at the centre of a clamped beam to make to the free end of a smaller beam. However, the results show that embedding a negative structure to model a cut-out may be possible. While this may seem encouraging, it has to be stated that the use of more terms for the displacement or the use of a negative beam of very short or very long length causes numerical problems. In addition, the first two natural frequencies are not exactly zero but are either small values or complex numbers. This may be due to the fact that the set of functions used are not from a complete set that would allow perfectly free conditions to be modelled. For the final free-free beam, all admissible functions used, when extended to the original clamped support point, have a zero displacement and a zero slope. Another potential contributing factor is that with penalty terms it is not possible to obtain a complete cancellation of the positive structure by the negative structure in practical applications because the penalty values must be finite. Further investigations are being conducted to identify the source(s) of the problem and to see if these could be addressed by using other types of admissible functions.

	7 terms per beam with $\alpha = \pm 10^{11}$	Simple polynomial 7 terms	Exact
ω_1	4.732	4.730	4.730
ω_2	7.874	7.971	7.853
ω_3	11.665	11.367	10.996

Table 1 First three non-zero natural frequencies of a free-free beam

References

1. Ilanko, S. & Dickinson, S.M. 1999 Asymptotic modelling of rigid boundaries and connections in the Rayleigh–Ritz Method. *Journal of Sound and Vibration* 219: 370–378.
2. Ilanko, S. 2002 Existence of natural frequencies of systems with imaginary Restraints and their convergence in asymptotic modelling. *Journal of Sound and Vibration*, 255, 5, 883-898.
3. Ilanko, S. 2005 Introducing the use of positive and negative inertial functions in asymptotic modelling. *Proc. R. Soc. A* 461, (2060), 2005: 2545–2562.
4. Williams, F.W. & Ilanko, S. 2006 The use of the reciprocals of positive and negative inertial functions in asymptotic modelling. *Proc. R. Soc. A*, 462 (2070):1909 –1915.
5. Ilanko, S. & Williams, F.W. 2008 Wittrick-Williams algorithm proof of bracketing and convergence theorems for eigenvalues of constrained structures with positive and negative penalty parameters, *International Journal for Numerical Methods in Engineering*, 75 (1), 83 – 102.

IMPLEMENTATION AND EVALUATION OF EXACT DYNAMIC STIFFNESS METHOD FOR FREE VIBRATION OF NON-UNIFORM BEAMS

Si Yuan, Kangsheng Ye, Cheng Xiao

Department of Civil Engineering, Tsinghua University, Beijing, 100084, China

F. W. Williams and D. Kennedy

Cardiff School of Engineering, Cardiff University, Cardiff CF24 3AA, UK

When exact dynamic stiffnesses are used for solving free vibration problems of skeletal structures, solution of the governing differential equations results in the transcendental eigenproblem

$$\mathbf{K}(\lambda)\mathbf{D} = \mathbf{0} \quad (1)$$

where $\lambda = \omega^2$, ω is the circular frequency, $\mathbf{K}(\lambda)$ is the global dynamic stiffness matrix and \mathbf{D} is the joint displacement amplitude vector, becoming the mode vector at the natural frequencies. The Wittrick-Williams (WW) algorithm [1] gives the total number of eigenvalues below a trial value λ^* as

$$J = J_0(\lambda^*) + s\{\mathbf{K}(\lambda^*)\} \quad (2)$$

Here $s\{\mathbf{K}\}$ is the sign count of \mathbf{K} , i.e. the number of negative leading diagonal elements of the upper triangular matrix \mathbf{K}^Δ obtained from \mathbf{K} by ordinary Gaussian elimination, and J_0 is the total number of member fixed-end eigenvalues lying below λ^* . A Newton-based recursive second order convergence method [2] combines the WW algorithm with inverse iteration, to compute isolated eigenvalues and the corresponding modes accurately and efficiently.

The axial and flexural vibrations of a non-uniform Bernoulli-Euler beam are governed, respectively, by the second- and fourth-order linear ordinary differential equations

$$\frac{d}{dx} \left(EA(x) \frac{du_j(x)}{dx} \right) + \lambda^* m(x) u_j(x) = 0 \quad \frac{d^2}{dx^2} \left(EI(x) \frac{d^2 v_j(x)}{dx^2} \right) - \lambda^* m(x) v_j(x) = 0 \quad (3)$$

Here, $EA(x)$ and $EI(x)$ are the axial and flexural rigidities, and $m(x)$ is the distributed mass per unit length. The collocation software COLSYS [3] is used to obtain the displacement amplitudes $u_j(x)$ ($j = 1, 2$) and $v_j(x)$ ($j = 1, 2, 3, 4$) for appropriate boundary conditions, from which the columns of the dynamic stiffness matrix \mathbf{K} can be formed. An analogous procedure yields the derivatives of \mathbf{K} needed in the convergence method [2].

A key requirement is to avoid the stiffness singularities that occur at fixed-end member eigenvalues. Here the beam is divided into sufficient elements to ensure that the lowest fixed-end eigenvalue of each exceeds a known upper bound λ_u on the eigenvalue being sought. Working from one end, the length l of each element is chosen such that

$$l \leq \pi \sqrt{\left(\min_{0 \leq x \leq l} EA(x) \right) / \left(\lambda_u \max_{0 \leq x \leq l} m(x) \right)} \quad \text{and} \quad l \leq 4.73004 \sqrt{\left(\min_{0 \leq x \leq l} EI(x) \right) / \left(\lambda_u \max_{0 \leq x \leq l} m(x) \right)} \quad (4)$$

i.e. so that λ_u is a lower bound on the lowest fixed-end eigenvalue of a *uniform* element of length l having the most extreme section properties occurring within the element.

The solution procedure is similar to that of [2], with the following extensions.

- (1) Axial and flexural natural frequencies are found separately.
- (2) The beam stiffness matrix and its derivative are computed by solving the governing equations using a numerical solver, rather than by using closed form formulae.
- (3) Different sets of mesh points are automatically and adaptively generated for each natural frequency, rather than using a fixed geometry with occasional mesh points.
- (4) J_0 is guaranteed to vanish.
- (5) The non-uniform beam has no coincident eigenvalues. (This can be deduced physically.)
- (6) The examples in this paper are specifically for the chain of collinear non-uniform elements required to assemble a single non-uniform beam. The theory is readily extended to frames of any topology and with any number of uniform and non-uniform beams.

Axial and flexural natural frequencies are compared with exact results ω_k obtained, respectively, using the Sturm-Liouville solvers SLEDGE [4] and SLEUTH [5] (with error tolerance 10^{-8}), and with analytical results where available [6]. Table 1 gives results for a beam of length L , clamped at $x = 0$ and free at $x = L$, with rectangular cross-section of constant breadth b and varying height $h(x)$, where

$$h(x) = h_0(1 - \beta \frac{x}{L}), \quad m(x) = \rho b h(x), \quad EA(x) = E b h(x), \quad EI(x) = \frac{E b h^3(x)}{12} \quad (0 \leq x \leq L) \quad (5)$$

for two values of the taper slope parameter β . The axial mode functions $u(x)$ were also compared with exact modes $u_k(x)$ at the points $x_i = i L/n_p$ ($i = 0, 1, \dots, n_p$). Figure 1 shows the relative errors

$$\varepsilon_\omega = \left| \frac{\omega - \omega_k}{\omega_k} \right|, \quad \varepsilon_u = \max_{i=0,1,\dots,n_p} \left| \frac{u_k(x_i)}{u_k(x_j)} - \frac{u(x_i)}{u(x_j)} \right| \quad \text{with} \quad |u_k(x_j)| = \max_{i=0,1,\dots,n_p} |u_k(x_i)| \quad (6)$$

Table 1. Selected natural frequencies of cantilevered linearly tapered beam.

	$\beta = 0.5$		$\beta = 0.9$	
	Axial	Flexural	Axial	Flexural
	$\omega_k \left(\div \sqrt{\frac{E}{\rho L^2}} \right)$	$\omega_k \left(\div \sqrt{\frac{E h_0^2}{12 \rho L^4}} \right)$	$\omega_k \left(\div \sqrt{\frac{E}{\rho L^2}} \right)$	$\omega_k \left(\div \sqrt{\frac{E h_0^2}{12 \rho L^4}} \right)$
1	1.794010905	3.823784848	2.203290325	4.630723862
2	4.802060761	18.31726091	5.153187899	14.93079267
3	7.908961712	47.26482701	8.185995112	32.83312114
4	11.03509458	90.45047766	11.25893456	58.91706749
5	14.16798651	148.0017449	14.35406566	93.38808978
10	29.85977557	651.3863523	29.95772393	393.1830235
20	61.26819673	2736.661945	61.31743639	1633.125164
30	92.68170352	6260.030017	92.71445167	3727.806332
40	124.0964352	11221.50150	124.1209456	6677.371650
50	155.5116496	17621.07843	155.5312279	10481.85021

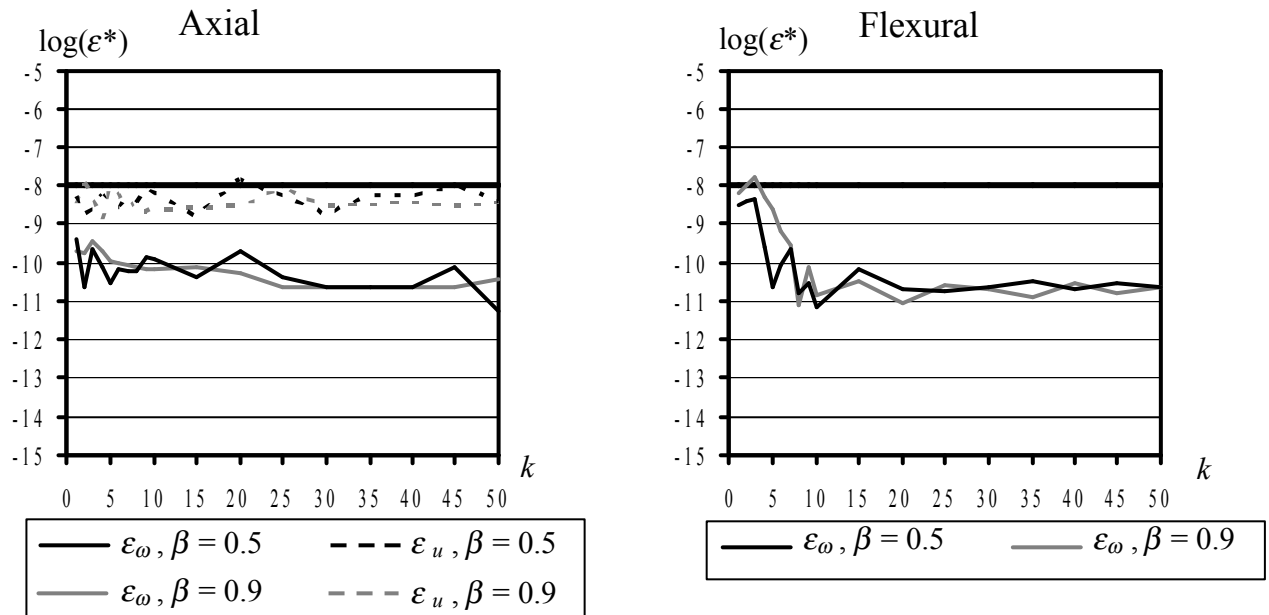


Figure 1. Relative errors for axial and flexural natural frequencies.

It is seen that the specified error tolerance of $\varepsilon = 10^{-8}$ was essentially achieved in all cases, and solution times were comparable to those of SLEDGE or SLEUTH. It is therefore concluded that the proposed method is a successful extension of the exact dynamic stiffness method to non-uniform Bernoulli-Euler beams with uncoupled axial and flexural behaviour. Exactness, efficiency and reliability are retained by the use of a state-of-the-art ODE solver. The method is readily extended to the vibration of Timoshenko beams, Euler buckling of non-uniform beams, as well as to analogous problems of shells of revolution and to more general Sturm-Liouville problems.

Acknowledgements

The authors gratefully acknowledge financial support from the National Natural Science Foundation of China, the Ministry of Education of China (No. 704003), the Engineering and Physical Sciences Research Council (grant number GR/R05406/01) and the Royal Academy of Engineering.

References

- [1] Williams FW, Wittrick WH. An automatic computational procedure for calculating natural frequencies of skeletal structures. **International Journal of Mechanical Sciences** 1970; 12(9): 781–791.
- [2] Yuan S, Ye KS, Williams FW, Kennedy D. Recursive second order convergence method for natural frequencies and modes when using dynamic stiffness matrices. **International Journal for Numerical Methods in Engineering** 2003; 56(12): 1795-1814.
- [3] Ascher U, Christiansen J, Russell RD. Algorithm 569, COLSYS: Collocation software for boundary value ODEs [D2]. **ACM Transactions on Mathematical Software** 1981; 7(2): 223-229.
- [4] Pruess S, Fulton CT. Mathematical software for Sturm-Liouville problems. **ACM Transactions on Mathematical Software** 1993; 19(3): 360–376.
- [5] Greenberg L, Marletta M. Algorithm 775: The code SLEUTH for solving fourth-order Sturm-Liouville problems. **ACM Transactions on Mathematical Software** 1997; 23(4): 453-493.
- [6] Banerjee JR, Williams FW. Exact Bernoulli-Euler dynamic stiffness matrix for a range of tapered beams. **International Journal for Numerical Methods in Engineering** 1985; 21(12): 2289-2302.

Vibrations of Twisted Cantilever Plates

Arthur Leissa
Fort Collins, Colorado, USA

Turbomachinery blades are used extensively in gas turbines and steam turbines. A typical blade with an attached shroud is shown in Fig. 1. The blade has considerable twist along its length. It has curvature (camber) in the direction transverse (chordwise) to its length, but negligible curvature in its longitudinal (spanwise) direction. Typical cross-sections are airfoil shapes, varying in thickness along the chord (Fig. 2). Free vibration frequencies and mode shapes of rotating blades are essential to analyze the behavior of turbine, compressor and fan blades in their operating environments.

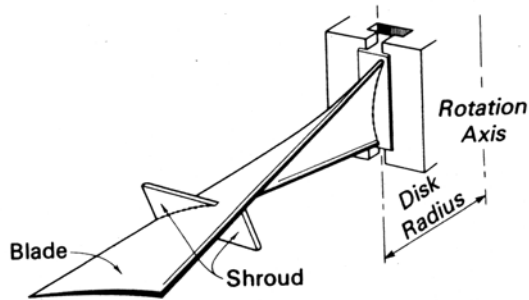


Fig. 1. Shrouded fan blade

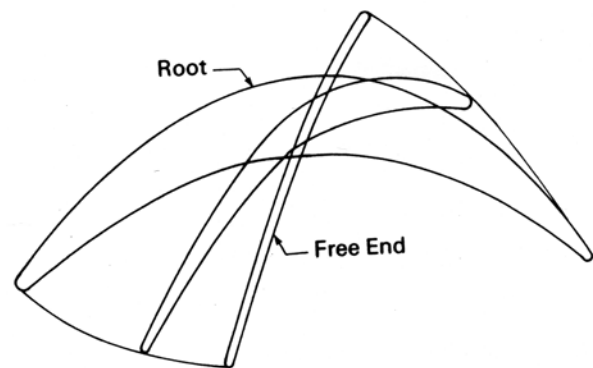


Fig. 2. Blade cross-sections

A review article [1] published 38 years ago summarized approximately 100 publications which dealt with the vibrations of turbomachinery blades. An update five years later [2] described 57 additional ones. The early analyses were based upon one-dimensional beam theories which, to various degrees, included the complications of variable thickness, pretwist, shear deformation, rotary inertia, Coriolis effects, thermal gradients, torsional warping, bending warping and elastic root supports. Numerous two-dimensional analyses were also carried out later [1, 2], mainly using finite elements, but also shallow shell theory. Ultimately, some three-dimensional investigations were made, almost entirely by finite elements. Published experimental data was minimal due to its proprietary nature.

However, where direct comparisons of computationally obtained frequencies were available, considerable differences were found. A relatively simple test model for the computational methods is a pretwisted rectangular plate (Fig. 3). The fundamental free vibration mode for this configuration is simple, spanwise bending. Some analysts determined an increase in its frequency with increasing pretwist angle (W). Others said it decreases. The second frequency is usually for a torsional mode; it definitely increases with increasing W . But some said it increased greatly, others said only slightly. If a computer program cannot solve this simple problem accurately, it cannot be relied upon to analyze complicated turbomachinery blades.

Because of this questionable reliability, a two-year study of this problem on available computer programs was undertaken jointly by NASA and the U.S. Air Force. A set of 20 precision-machined twisted plates were manufactured, with different aspect ratios, thickness ratios and pretwist angles. Experimental frequency and mode shape data were determined for each configuration at two separate, government laboratories. Simultaneous with this, industry, government and university researchers were asked to obtain computational results from some of the best available one-dimensional beam analyses and two- and three-dimensional finite element and shell analysis codes. All results were obtained under static, non-rotating conditions. Altogether, 16 laboratories were involved. Extensive numerical results were obtained by 19 different programs. Experimental and computational results were summarized and compared in three journal articles [3-5] and in a NASA report [6].

Considerably different results were obtained from the various computer programs. Figure 4 is a plot of the first bending mode frequencies for moderately thin ($b/h = 20$) twisted plates of square aspect ratio ($a/b = 1$) for five pretwist angles (0, 15, 30, 45, 60 degrees). Figure 5 shows the frequencies of the first torsion mode for the same twisted plates. In each plot the experimental results are shown as a dotted line. In the presentation, similar results for the other configurations and other modes will be shown. The various analytical methods used to generate the computer programs will be briefly described.

REFERENCES

1. Leissa, A.W., "Vibrational Aspects of Rotating Turbomachinery Blades", *Applied Mechanics Reviews*, Vol. 34, pp. 351-357, 1981.
2. Leissa A.W., "Update to Vibrational Aspects of Rotating Turbomachinery Blades", *Applied Mechanics Update*, pp. 359-362, 1986.
3. Leissa, A.W., MacBain, J.C. and Kielb, R.E., "Vibrations of Twisted Cantilevered Plates---- Summary of Previous and Current Studies", *Journal of Sound and Vibration*, Vol. 96, No.2, pp. 159-173, 1984.
4. Kielb, R.E., Leissa, A.W. and MacBain, J.C., "Vibrations of Twisted Cantilever Plates ---- A Comparison of Theoretical Results", *International Journal for Numerical Methods in Engineering*, Vol. 21, pp. 1365-1380, 1985.
5. MacBain, J.C., Kielb, R.E. and Leissa, A.W., "Vibrations of Twisted Cantilevered Plates---- Experimental Investigation", *ASME Journal of Engineering for Gas Turbines and Power*, Vol. 107, pp. 187-196, 1984.
6. Kielb, R.E., Leissa, A.W., MacBain, J.C. and Carney, K.S., "Joint Research Effort on Vibrations of Twisted Plates", NASA References Publication 1150, 99 pp., 1985.

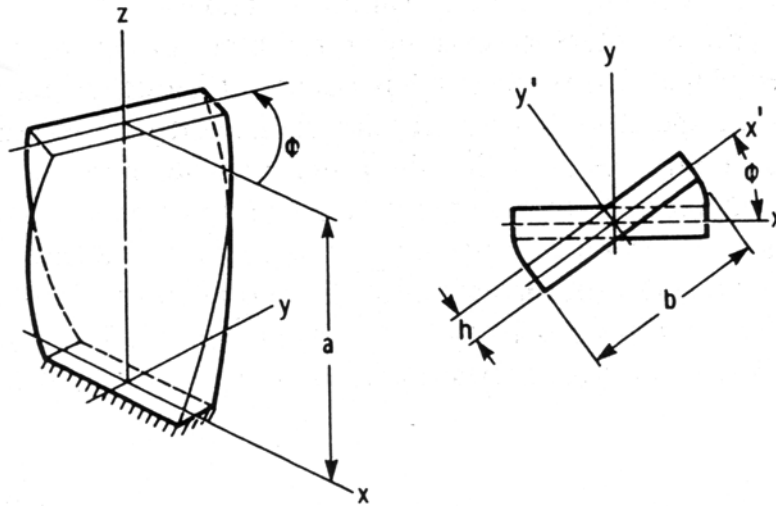


Fig. 3. Twisted cantilever plate

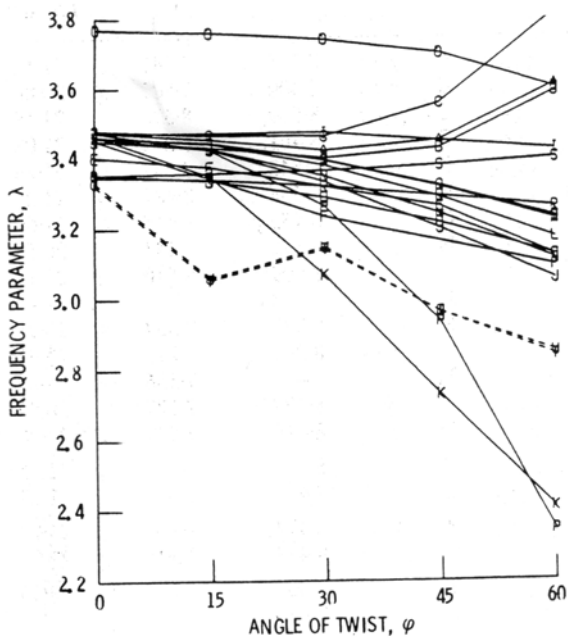


Fig. 4. Variation of first bending mode frequency with pretwist angle
 $a/b = 1$, $b/h = 20$

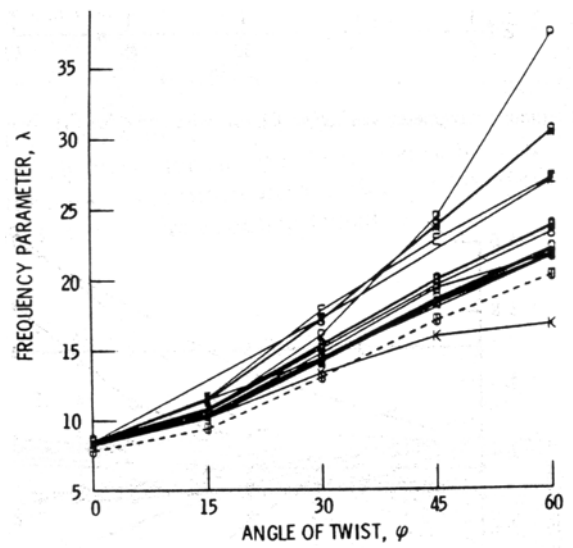


Fig. 5. Variation of first torsion mode frequency with pretwist angle.
 $a/b = 1$, $b/h = 20$

A generalized Fourier series method for the vibrations of continuous systems

Wen L. Li

Department of Mechanical Engineering, Wayne State University
5050 Anthony Wayne Drive, Detroit, Michigan 48202, U.S.A.

Email: wli@wayne.edu

Fourier series is perhaps the most desired form in expanding a continuous function or solution due to its completeness and excellent stability in numerical calculations. In structural dynamics, however, the solution in the form of Fourier series is traditionally only available for a few simple boundary conditions. It is widely accepted that the vibrations of continuous systems are generally not amenable to a Fourier series solution. In this presentation, a general and sophisticated Fourier series method is described for the vibration analysis of beams and plates with *arbitrary* boundary conditions. For simplicity, in what follows a beam problem will be used to elaborate essence of the generalized Fourier series solution.

For a beam with an arbitrary boundary support at each end, the beam function $w(x)$ has to be sufficiently smooth, that is, $w(x) \in C^3$ for $\forall(x) \in (0, L)$. It is well known that a continuous function defined over a domain can be expanded into a Fourier series *inside* the domain (i.e., boundary points are excluded). The word “inside” is highlighted because it often becomes a show stopper when the traditional Fourier method is employed to solve a boundary value problem. Mathematically, expanding $w(x)$ into a Fourier series simply implies that it is viewed as a periodic function (with period L) defined over the entire x axis. Consequently, as shown in Figure 1(a), if the beam is allowed to move at an end, the displacements will be generally different at the ends and the Fourier series of the displacement function will subsequently only converge to the mean value, $(w(0)+w(L))/2$, at $x=0, \pm L, \pm 2L, \dots$. This deems the unsuitability of the traditional Fourier series method since the solution fails to produce the correct boundary values at $x=0, \pm L$. This problem, however, can be easily avoided by viewing $w(x)$ as a part of an *even function* defined over $[-L, L]$. The Fourier expansion of this even function will then only contain the cosine terms, and be able to correctly converge to $w(x)$ at *any* point over $[0, L]$. This treatment alone still cannot revive the traditional Fourier series method because the satisfaction of boundary conditions means that *each of the first three derivatives* has to be correctly produced, at each end, by the series representation. Referring to Figure 1(b), the derivative $w'(x)$ is obviously an odd function over $[-L, L]$. Thus, its (sine) series expansion will invariantly converge to zero at $x=0$ and L , regardless of the actual slope values. To overcome this problem, we construct a new beam function

$$\bar{w}(x) = w(x) - \xi_1(x)\alpha_0 - \xi_2(x)\alpha_1 \quad (1)$$

where $\alpha_0 = dw(x)/dx|_{x=0}$, $\alpha_1 = dw(x)/dx|_{x=L}$ and $\xi_1(x)$ ($\xi_2(x)$) denotes a sufficiently smooth closed-form function whose derivative is equal to 1 and 0 (0 and 1) at $x=0$ and $x=L$, respectively [1]. In other words, $\bar{w}(x)$ represents a residual beam function which is continuous over $[0, L]$ and has zero-slopes at the both ends. It is clear that the cosine series representation of $\bar{w}(x)$ is now able to converge correctly to both the function itself and its derivative at every point on the beam. In seeking an exact solution, two similar terms must also be included in Eq. (1) to take care of the discontinuities potentially associated with the third-order derivative. Mathematically, what has been said can be finally expressed as [1]

$$w(x) = \sum_{m=0}^{\infty} a_m \cos \lambda_m \xi + \xi_1(x)\alpha_0 + \xi_2(x)\alpha_1 + \xi_3(x)\beta_0 + \xi_4(x)\beta_1. \quad (\lambda_m = m\pi/L) \quad (2)$$

The “physical” impact of these mathematical treatments is that the arbitrary boundary conditions for the original beam are reconfigured into a guided support at each end (that is, zero slope and zero restraining force in the transverse direction) for the new beam function $\bar{w}(x)$ which is almost automatically sought in the form of a cosine expansion or modal superposition (which may be a preferred term by a dynamist). The displacement can also be expanded into sine series. In that case, the supplementary terms are used to

remove the discontinuities potentially associated with the displacement and its second-order derivative at the ends. While the sine series is advantageous for beams which are restrained from any transverse motions at both ends, the cosine series is generally more suitable for all other boundary conditions [2].

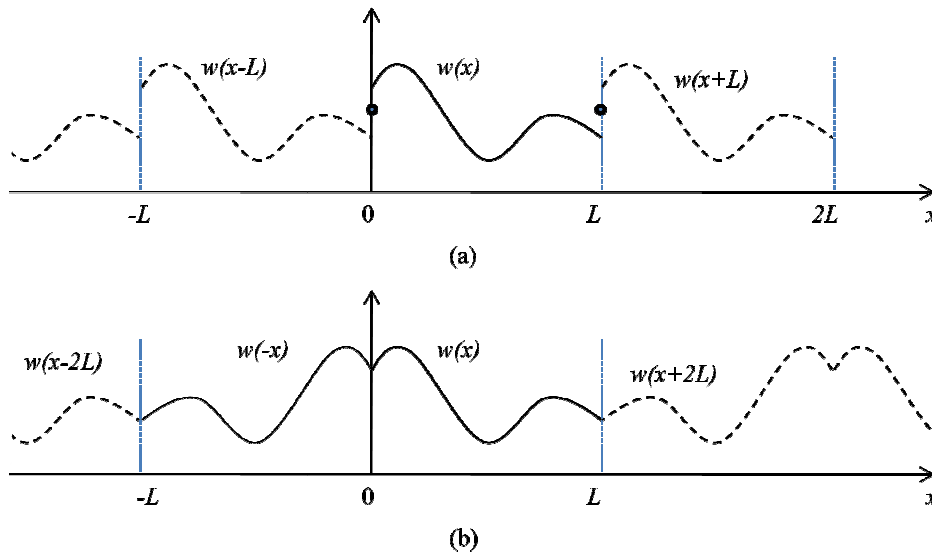


Figure 1. An illustration of the convergence of (a) the conventional Fourier series, and (b) the improved Fourier series.

Mathematically, an exact (or classical) solution for the beam problem is a *particular* function $w(x) \in C^3$ which simultaneously satisfies the governing equation at *every field point* and the boundary conditions at *every boundary point*. Thus, seeking the exact solution is simply turned into finding an appropriate set of Fourier coefficients so that both the governing equation and boundary conditions are satisfied *exactly on a point-wise basis*.

Although the beam problem is used to illustrate the essence of this generalized Fourier series method, it is important to point out that the series expansion given in Eq. (1) is actually able to represent and uniformly converge to *any function* $f(x) \in C^3$ for $\forall(x) \in [0, L]$, regardless whether it is used to describe a displacement field, a pressure field or a temperature distribution. Also, this series can be directly differentiated, term-by-term, to obtain the uniformly convergent series expansions for up to the fourth-order derivatives. As one of the most important outcomes, for any given function $f(x) \in C^4$, its series expansion given in Eq. (1) will converge at a remarkable rate of $\mathcal{O}(\lambda_m^5)$ according to a well-established convergence theorem in mathematics [1, 3].

For plate problems, the two dimensional version of Eq. (1) has to be used to express the displacement solution as [4]

$$w(x, y) = \sum_{m=0}^{\infty} \sum_{n=0}^{\infty} A_{mn} \cos \lambda_{am} x \cos \lambda_{bn} y + \sum_{l=1}^4 \left(\xi_b^l(y) \sum_{m=0}^{\infty} c_m^l \cos \lambda_{am} x + \xi_a^l(x) \sum_{n=0}^{\infty} d_n^l \cos \lambda_{bn} y \right) \quad (3)$$

In the above equation, the first and third derivatives along each boundary edge have been simply represented by their respective cosine series expansions.

Results: As example, consider a square plate with each of its edges elastically restrained in both transverse and rotational directions. The calculated frequency parameters are listed in Table 1 together with those obtained from a FEM model which consists of 300×300 elements with 543,606 DOF's. Two representative mode shapes are plotted in Figure 2.

Table 1. Frequency parameters, $\Omega = \omega a^2 \sqrt{\rho h / D}$, for a square plate with $ka^3 / D = 100$ and $Ka / D = 1000$ at each edge (k and K are respectively the stiffnesses of the transverse and rotational springs; a and b are the length and width of the plate, respectively).

$r=a/b$	$\Omega = \omega a^2 \sqrt{\rho h / D}$					
	1	2	3	4	5	6
1.0	17.509	25.292	25.292	33.893	46.285	46.856
	17.474 [†]	25.228	25.228	33.795	46.264	46.779
1.5	20.718	27.455	35.433	44.712	47.694	69.282
	20.664 [†]	27.362	35.357	44.595	47.623	69.194

[†]Results from FEM with 300×300 elements.

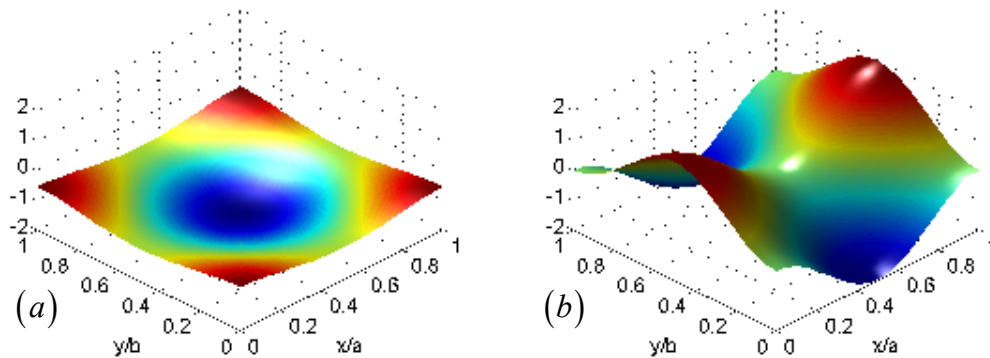


Figure 2. The mode shapes for square plate with $ka^3 / D = 100$, $Ka / D = 1000$ at all four edges. The (a) first, and (b) fifth mode shapes.

The accuracy and reliability of this method have been repeatedly demonstrated for the vibrations of beams [1, 2], plates [4, 5], multi-span beams [6, 7], 2- and 3-D frames, two coupled plates, and strong coupling of a plate and an acoustic volume. Of many important advantages, the proposed Fourier series method can be generally applied to beams, plates, shells and their assemblies even when other analytical methods fail to work due to, such as, the nonexistence of the closed-form expressions for the component modes or the inability of satisfying the boundary or coupling conditions under the actual system condition.

Acknowledgments: The author would like to thank Mrs. Hongan Xu, Xuefeng Zhang and Jingtao Du for their involvement and contributions. The author also gratefully acknowledges the financial support from NSF Grant: CMMI-0827233.

References:

1. Li, W. L. (2000). "Free vibration of beams with general boundary conditions," *Journal of Sound and Vibration*, 230, 521-539.
2. Li, W. L. (2002). "Comparison of Fourier sine and cosine series expansions for beams with arbitrary boundary conditions," *Journal of Sound and Vibration*, 255, 185-194.
3. Tolstov, G. P. (1965). *Fourier Series*. Englewood Cliffs NJ: Prentice-Hall.
4. Li, W.L., Zhang, X.F., Du, J.T., Liu, Z.G. (2009). "An exact series solution for the transverse vibration of rectangular plates with general elastic boundary supports," *Journal of Sound and Vibration*, 321, 254-269
5. Du, J. T., Li, W. L., Jin, G. Y., Yang, T. J., Liu, Z. G. (2007). "An analytical method for the in-plane vibration analysis of rectangular plates with elastically restrained edges," *Journal of Sound and Vibration* 306, 908-927
6. Li, W. L., Xu, H. A. "An exact Fourier series method for the vibration analysis of multi-span beam systems," *Computational and Nonlinear Dynamics*. (in print)
7. Xu, H. A., Li, W. L. (2008). "Dynamic behavior of multi-span bridges under moving loads, with focusing on the effect of the coupling conditions between spans," *Journal of Sound and Vibration*, 312, 736-753,

A Discussion on the Physics and Truth of Nanoscales for Vibration of Nanobeams based Nonlocal Elastic Stress Field Theory

C.W. Lim

Department of Building and Construction, City University of Hong Kong, Hong Kong, P.R. China

Abstract

Two critical but overlooked issues in the physics of nonlocal elastic stress field theory for nanobeams are discussed: (i) why does the presence of increasing nonlocal effects induce reduced nanostructural stiffness in many, but not consistently for all, cases of study, ie. increasing static deflection, decreasing natural frequency and decreasing buckling load, in virtually all previously published works in this subject (a total of 51 papers known since 2003) although intuition in physics tells otherwise? and (ii) the intriguing conclusion that nanoscale effects are missing in the solutions in many exemplary cases of study for bending of nanobeams. Applying the nonlocal elasticity field theory in nanomechanics and an exact variational principal approach, the exact equilibrium conditions, domain governing differential equation and boundary conditions for vibration of nanobeams are derived for the first time. These new equations and conditions involve essential higher-order terms which are missing in virtually all nonlocal models and analyses in previously published works in statics and dynamics of nonlocal nano-structures. Such negligence of higher-order terms in these works results in misleading nanoscale effects which predicts completely incorrect, reverse trends with respect to what the conclusion of this paper tells. Effectively, for the first time this paper not only discovers the truth of nanoscale, as far as nonlocal elastic stress modelling for nanostructures is concerned, on equilibrium conditions, governing differential equation and boundary conditions but also reveals further the true basic vibration responses for nanobeams with various boundary conditions. It also concludes that the widely accepted equilibrium conditions of nonlocal nanostructures currently are in fact not in equilibrium, but they can be made perfect should the nonlocal bending moment be replaced by an equivalent nonlocal bending moment. The conclusions above are illustrated by other approaches in nanostructural models such as strain gradient theory, modified couple stress models and experiments.

1. Introduction

Since the discovery of carbon nanotubes (CNTs) in the early 1990s, many continuum modelling approaches based on elastic, linear or nonlinear beam and shell models were developed for the analysis of static and dynamic responses and the stability and vibration of CNTs [1,2]. As size-dependent effects become significantly more prominent at the nano-scale, such classical continuum models becomes invalid because they do not exhibit intrinsic size-dependence features and do not allow inclusions and property inhomogeneities that are fundamental and significant in atomic modeling. Therefore, the nonlocal field theories first extensively developed by Eringen in the early 1970's were applied to study CNTs [3]. The nonlocal field theories indicate that the stress at a point in a domain is dependent on the strain at every other point in the domain. According to Eringen [4], the nonlocal constitutive equation with kernel function could be reduced to a second-order ordinary differential equation for convenient analysis of static and dynamic responses of CNTs, such as bending, vibration, buckling and wave propagation. Works applying this theory were published [5-8] by directly extending the classical models without rigorous verification. These models can be regarded as the partial nonlocal stress models that neglected the very important higher-order nonlocal effects and, hence, the nanobeams do not satisfy the very fundamental, static equilibrium condition. Consequently, these partial nonlocal models induced rather inexplicable solutions.

Applying the nonlocal theory and an exact variational principal approach, this paper derives the correct equilibrium conditions, domain governing differential equation and boundary conditions for vibration of nanobeams. Some vibration examples for nanobeams with various loading and boundary conditions are solved to illustrate the true effects of nanoscale based on this exact nonlocal elastic stress field theory.

2. Derivation of New Governing Differential Equations

In accordance with the nonlocal stress theory [4], the simplified nonlocal constitutive equation for a one-dimensional Euler-Bernoulli nanobeam is

$$\sigma_{xx} - \tau^2 L^2 \frac{d^2 \sigma_{xx}}{dx^2} = E \varepsilon_{xx} \quad (1)$$

which can be non-dimensionalized using the following dimensionless parameters

$$\bar{\sigma}_{xx} = \frac{\sigma_{xx}}{E}, \quad \tau = \frac{e_0 a}{L}, \quad \bar{x} = \frac{x}{L}, \quad \bar{z} = \frac{z}{L}, \quad \bar{w} = \frac{w}{L} \quad (2)$$

where σ_{xx} is the normal stress, ε_{xx} the normal strain, E Young's module, $e_0 a$ the nanoscale coefficient, L the length of nanobeam, w the deflection amplitude within a vibration cycle, and x and z the longitudinal and transverse coordinates.

Using an exact variational approach, the energy U stored in a deformed structure and the kinetic energy T during free vibration are

$$U = \int_V \int_0^{\varepsilon_{xx}} \sigma_{xx} d\varepsilon_{xx} dV \quad \text{and} \quad T = \frac{1}{2} \int_0^L \rho A \left(\frac{dw}{dt} \right)^2 dx \quad (3,4)$$

where ρ is the density per unit length. The variational principal requires that

$$\delta I = \delta(U - T) = 0 \quad (5)$$

which yields a higher-order governing differential equation as

$$\sum_{n=1}^{\infty} (2n-3) \tau^{2(n-1)} \bar{w}^{(2(n+1))} - \frac{\rho A L^4}{E I T^2} \left(\frac{d\bar{w}}{d\bar{t}} \right)^2 = 0 \quad \text{or} \quad \bar{M}_{eq}^{(2)} - \frac{\rho A L^4}{E I T^2} \left(\frac{d\bar{w}}{d\bar{t}} \right)^2 = 0 \quad (6a,b)$$

where $\langle n \rangle$ indicates n -order differentiation with respect to \bar{x} and \bar{M}_{eq} is defined as an dimensionless equivalent nonlocal bending moment. For simply harmonic motion, let

$$\bar{w}(\bar{x}, t) = \bar{W}(\bar{x}) e^{i\omega t} \quad (7)$$

Substituting this equation into the higher-order governing differential equation (6a) yields

$$\sum_{n=1}^{\infty} (2n-3) \tau^{2(n-1)} \bar{W}^{(2(n+1))} + \bar{\omega}^2 \bar{W} = 0 \quad \text{and} \quad \bar{\omega} = \omega L^2 \sqrt{\frac{\rho A}{E I}} \quad (8,9)$$

which is an eigenvalue equation where $\bar{\omega}$ the dimensionless angular frequency.

3. Example

For a nanobeam simply supported at $\bar{x} = 0, 1$, the boundary conditions are

$$\bar{W}(0) = 0, \quad \bar{M}(0) = 0, \quad \bar{W}(1) = 0, \quad \bar{M}(1) = 0 \quad (10)$$

For nontrivial solution of the eigenvalue equation (8), we may set

$$\bar{W}(\bar{x}) = c_k \sin(k\pi\bar{x}) \quad (k = 1, 2, 3, \dots) \quad (11)$$

where c_k is the k -mode amplitude of vibration. Substituting Eq. (11) into Eq. (8) yields

$$\bar{\omega} = (k\pi)^2 \sqrt{\sum_{n=1}^{\infty} (-1)^n (k\pi)^{2(n-1)} (2n-3) \tau^{2(n-1)}} \quad (12)$$

Denoting $\bar{\omega}_c = \omega_c L^2 \sqrt{\rho A / E I} = (k\pi)^2$ as the classical k -mode dimensionless natural frequency where ω_c is the dimensional natural frequency for a classical Euler-Bernoulli beam simply supported at both ends, the ratio of dimensionless frequency of a nanobeam to that of a classical thin beam is

$$R_{\omega} = \frac{\bar{\omega}}{\bar{\omega}_c} = \sqrt{\sum_{n=1}^{\infty} (-1)^n (2n-3) \tau^{2(n-1)} (k\pi)^{2(n-1)}} = \sqrt{1 + \tau^2 (k\pi)^2 - 3\tau^4 (k\pi)^4 + \dots} \quad (13)$$

where τ defined in Eq. (2) is a dimensionless nanoscale parameter indicating the strength of nanoscale effect. In Eq. (13), the classical natural frequency can be recovered when $\tau = 0$ which indicates vanishing nanoscale influence. It also shows that the nonlocal effect increases the natural frequency of nanobeam and

the result is in complete contradiction to virtually all previous published works [5,6,8]. As an example, Reddy [8] presented the ratio of natural frequency as

$$R_{\omega[8]} = \frac{\bar{\omega}_{[8]}}{\bar{\omega}_c} = \sqrt{\frac{1}{1 + (k\pi)^2 \tau^2}} \quad (14)$$

in which equivalent notations have been standardized and the expression rearranged. For example, $n = 2$ is used in Eq. (13) and the result is shown in Fig. 1 to demonstrate the relationship between R_{ω} and τ for various modes k . It is obvious that $R_{\omega} \geq 1$ for increasing τ is contradictory to $R_{\omega[8]} \leq 1$ for increasing τ . In addition, the nonlocal effect for higher vibration modes is more significant.

4. Conclusions

Through an exact nonlocal stress field approach and a rigorous variational principle formulation, this paper has successfully derived new equilibrium conditions which include higher-order nonlocal terms. The domain governing higher-order differential equations and higher-order boundary conditions have also been established. An example of a simply supported nanobeam is presented. It concludes that increasing nanoscale results in higher nanobeam stiffness and consequently higher natural frequency. The conclusion contradicts all previous published results. It is also shown that the nonlocal effect for higher vibration modes is more significant. In addition, the classical natural frequency is recovered in the limit of vanishing nonlocal nanoscale.

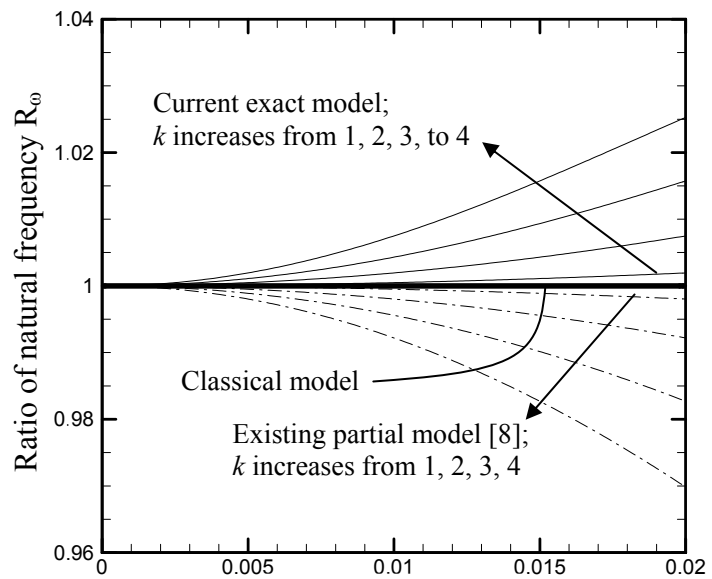


Fig.1. Nonlocal effect of the ratio of natural frequency for different modes

References

- [1] B.I. Yakobson, C.J. Brabec and J. Bernholc, Nanomechanics of carbon tubes: instabilities beyond linear range, *Physical Review Letters*, **76**, 2511–2514, 1996.
- [2] C.Q. Ru, Effective bending stiffness of carbon nanotubes, *Phys. Rev. B*, **62**, 9973–9976, 2000.
- [3] A.C. Eringen, Nonlocal polar elastic continua, *International Journal of Engineering Science*, **10**(1), 1-16, 1972.
- [4] A.C. Eringen, On differential equations of nonlocal elasticity and solutions of screw dislocation and surface waves, *Journal of Applied Physics*, **54**(9), 4703-4710, 1983.
- [5] J. Peddieson, G.R. Buchanan and R.P. McNitt. Application of nonlocal continuum models to nanotechnology. *International Journal of Engineering Science*, **41**(3-5), 305-312, 2003.
- [6] Q. Wang and K.M. Liew, Application of nonlocal continuum mechanics to static analysis of micro- and nano-structures. *Physics Letter A*, **363**, 3, 236-242, 2007.
- [7] C.W. Lim and C.M. Wang, Exact variational nonlocal stress modeling with asymptotic higher-order strain gradients for nanobeams, *Journal of Applied Physics*, **101**, 054312, 2007.
- [8] J.N. Reddy and S.D. Pang, Nonlocal continuum theories of beams for the analysis of carbon nanotubes. *Journal of Applied Physics*, **103**, 023511, 2008.
- [9] C.W. Lim, On the truth of nanoscale for nanobeams based on nonlocal elastic stress field theory: Equilibrium, governing equation and static deflection, in preparation, 2009.

Acknowledgement

The work described in this paper was supported by a grant from Research Grants Council of the Hong Kong Special Administrative Region (Project No. CityU 117406).

Influence of Different Curvature on Chaotic Vibrations of Cylindrical Shell-panels with Clamped Edges

Ken-ichi NAGAI, Shinichi MARUYAMA, Kouki HASEGAWA,
Naoki ONOZATO and Takao YAMAGUCHI

Department of Mechanical System Engineering, Graduate School of Engineering,
Gunma University, 1-5-1 Tenjin-cho, Kiryu, Gunma 376-8515, JAPAN, kennagai@gunma-u.ac.jp

1. Introduction Experimental results are presented on chaotic vibrations of cylindrical shell-panels subjected to periodic lateral excitation. Influences of the curvature of the shell-panel and the in-plane compressive force are examined on the chaotic responses. The panel is clamped along the cylindrical curved edges and simply supported along the other two. The cylindrical-panels are compressed by an in-plane elastic constraint at the clamped edges. Chaotic responses are examined with the Poincaré projections and the Lyapunov exponents. Contribution of vibration modes to the chaotic responses of the plate is inspected with the Karhunen-Loève transformation.

2. Test Panel and Test Procedure As shown in Fig.1, a cylindrical panel made of a phosphor-bronze sheet with thickness $h=0.24$ mm, square form of length $a=140$ mm is clamped along the curved edges by rigid blocks. The surfaces of the rigid blocks are cut to circular surface with the radius of curvature R . The other edges are simply supported by adhesive flexible films. The panel has an initial deflection inherently. The panel is initially compressed in the meridian direction with elastic plates at the clamped edges. In the experiment, chaotic responses of three cylindrical shell-panels with different curvatures are examined. Effect of the initial in-plane compressive force on the chaotic response is also investigated. The restoring force and the linear natural frequencies of the cylindrical shell-panels are measured. The shell-panels are excited laterally with an electromagnetic exciter. The shell-panels are subjected to gravitational acceleration and periodic acceleration $a_d \cos 2\pi f t$, where f is the exciting frequency and a_d is the peak amplitude of acceleration. Dynamic responses of the shell-panels at multiple positions are measured with laser displacement sensors for the data analyses. Chaotic responses are inspected with the frequency response curves, the Fourier spectra, the Poincaré projections and the maximum Lyapunov exponents. The contribution of vibration mode to the chaos is discussed with the K-L transformation.

3. Results and Discussion The experimental results are arranged with the following non-dimensional notations.

$$\begin{aligned} [\xi, \eta] &= [x, y] / a, \quad w = W / h, \quad n_c = N_c / N_{cr}, \quad [p_s, p_d] = [g, a_d] \rho a^4 / d, \quad q_s = Q_s a^2 / Dh, \\ \alpha &= a^2 / (Rh), \quad [\omega, \omega_{mn}] = [f, f_{mn}] (2\pi / \Omega_0), \quad \tau = \Omega_0 t \end{aligned} \quad (1)$$

In the above notations, $\Omega_0 = a^{-2} \sqrt{D / (Rh)}$ is the coefficient corresponding to lateral vibration of the shell-panel. Notation $D = Eh^3 / \{12(1 - \nu^2)\}$ is the bending rigidity, where E is Young's modulus and ν is Poisson's ratio. In Eq. (1), ξ and η are the non-dimensional coordinates, w is the lateral displacement normalized by the shell thickness h . The symbol n_c is the non-dimensional stress resultant of the compressive in-plane force, normalized by the buckling resultant N_{cr} . Notations p_s and p_d are the non-dimensional load intensities related to the accelerations of gravity g and of the periodic peak amplitude a_d , respectively. In the experiment, p_s is fixed as $p_s = 0.37 \times 10^3$. The restoring force of the shell-panel is obtained with the relation between static deflection and the static concentrated force Q_s . Notation q_s is the non-dimensional force. The symbol α is the nondimensional curvature of the shell-panel. Notations ω and τ are the nondimensional excitation frequency and the time, respectively.

Figure 2(a) shows the results of the characteristics of restoring force of the plate ($\alpha = 0$) and the shell-panel ($\alpha = 12$) under the pre-buckling force $n_c = 0.88$. The static deflection including the initial deflection shows twice that of the panel thickness opposite to the gravitational direction (negative z -direction). The static deflection w at the point $\xi = 0.6$ and $\eta = 0.4$ is presented under the

concentrated force q_s loaded at the center $\xi = 0.5$ and $\eta = 0.5$. When the force increases from the static equilibrium position to the negative z direction, the deflections show the characteristics of a hardening spring. As the force is loaded to the positive z direction, the spring characteristics change to the softening-and-hardening type. The gradient of the curve of plate ($\alpha = 0$) is almost zero from $w=1$ to $w=2$. The shell-panel ($\alpha = 12$) shows small deflection compared to that of the plate ($\alpha = 0$) in the positive z -direction. Figure 2(b) shows the characteristics of the restoring force of the shell-panels ($\alpha = 12$ and $\alpha = 20$) under the post-buckling conditions $n_c = 1.6$. When the compressive force is increased from $n_c = 0.88$ (Fig. 2(a)) to $n_c = 1.6$ (Fig. 2(b)) in the panel ($\alpha = 12$), the deflection w increases in the positive z -direction. For the panel with larger curvature $\alpha = 20$, the gradient of the spring characteristics around the static equilibrium is increased compared to that of the panel $\alpha = 12$. Table 1 shows the linear natural frequencies ω_{mn} where m and n denote the half-wave numbers of the vibration modes along the x -axis and the y -axis, respectively. In the table, many sets of natural frequencies satisfy the relation of internal resonance. For example, the lowest natural frequency $\omega_{11}=29.6$ of the shell-panel $\alpha = 12$ under $n_c = 1.6$ is close to half of the natural frequency $\omega_{12}=57.8$ of the vibration mode with one nodal line along the x -axis.

Fig. 3(a) shows the nonlinear response curves of the plate $\alpha = 0$ under the amplitude of periodic force $p_d = 0.38 \times 10^3$ and the initial compressive force $n_c = 0.88$. The amplitude of response at the position $\xi = 0.6$ and $\eta = 0.4$ is shown with the root mean square value. The resonance response is denoted by the symbol $(m, n; p)$ with the mode of vibration (m, n) and the type of resonance p . For example, $p = 1$ and $p = 1/2$ represent the principal resonance and the sub-harmonic resonance of 1/2 order, respectively. Internal resonance is denoted by the symbol $C[(m, n; p), (i, j; q)]$. The large amplitude response $(1, 1; 1)$ is generated from the principal resonance of the lowest mode of vibration. The nonlinear response exhibits the characteristics of a softening-and-hardening spring. The dominant chaotic responses are generated in four regions of the excitation frequency involving internal resonance, which are denoted by the symbol $C[(m, n; p), (i, j; q)]$. These chaotic responses are mainly generated from ultra-sub harmonic resonance of 2/3 order, sub-harmonic resonance of 1/2 or 1/4 order of the fundamental mode of vibration. Higher modes of vibration with one nodal line are also induced. Figure 3(b) presents the frequency response curve of the shell-panel $\alpha = 12$ under $p_d = 0.38 \times 10^3$ and $n_c = 0.88$. Compared to the results of plate, the dominant regions of chaotic response are decreased to two. The chaotic responses are generated by internal resonance involving the sub-harmonic resonance of the fundamental mode of vibration. When the in-plane compressive force is increased to $n_c = 1.6$, chaotic responses are generated in three frequency regions as shown in Fig. 3(c). In the figure, $C[(1,1;2/3),(1,1;2)+(2,1;2)]$ implies chaotic response generated from the internal resonance of the ultra-sub harmonic resonance $(1,1;2/3)$ and the combination resonance $(1,1;2)$ and $(2,1;2)$ where the combination resonance involves super-harmonic resonances of second order. In the other two regions, chaotic responses are generated from internal resonance. Figure 3(d) shows the response curves of the shell panel $\alpha = 20$ under $p_d = 0.75 \times 10^3$ and $n_c = 1.6$. Although the amplitude of periodic force is twice as large as that of the plate $\alpha = 0$ and the panel $\alpha = 12$, chaotic response cannot be observed. The foregoing results are confirmed by the following inspections.

Figure 4 shows the time progress, the Fourier spectrum and the Poincaré projection of the typical chaotic response $C[(1,1;1/2),(1,2;1)]$ of the shell-panel $\alpha = 12$, under the exciting frequency $\omega=55.6$, $p_d = 0.38 \times 10^3$ and $n_c = 1.6$. The time progress of the response w is presented by the number of excitation period τ_c . Irregular amplitude modulation of chaotic response is observed. In Fig. 4(b), broad band spectrum is observed. Dominant peaks of the spectrum correspond to the sub-harmonic resonance of order 1/2 with the lowest mode of vibration and to the principal resonance of the mode $(1,2)$. Therefore, the chaotic response is dominated by the internal resonance condition $2\omega_{11} \approx \omega_{12}$. In Fig. 4(c), the Poincaré projection shows the distinct figure in the space of deflection and velocity. To confirm the response is chaos, the maximum Lyapunov exponents of the chaotic responses are calculated. Furthermore, the Karhunen-Loève transformation estimates the contribution of vibration

modes in the chaotic response. These results are summarized in Table 2. The maximum Lyapunov exponents of the responses take positive values within $\lambda_{\max}=0.3$ and $\lambda_{\max}=1.0$, then the responses are confirmed as the chaos. In the most of the chaotic responses, the fundamental vibration mode contributes predominantly. Higher modes of vibration also contribute to the chaos with the ratio from 6% to 40%. According to the shell curvature and to the in-plane compressive force, the vibration modes induced in the chaos depend on the internal resonance condition.

4. Conclusion Experimental results are presented on chaotic vibrations of a shell-panel clamped at opposite edges. As the shell curvature is decreased or in-plane compressive force is increased, chaotic responses are easily induced from the internal resonance..

References

- 1) Nagai, K., Maruyama, S., Murata, T. and Yamaguchi, T.: Experiments and Analysis on Chaotic Vibrations of a Shallow Cylindrical Shell-panel, *Journal of Sound and Vibration*, Vol. 305, pp.492-520, (2007).
- 2) Maruyama, S., Nagai, K. and Tsuruta, Y.: Modal Interaction in Chaotic Vibrations of a Shallow Double-curved Shell-panel, *Journal of Sound and Vibration*, Vol. 315, pp.607-625, (2008).

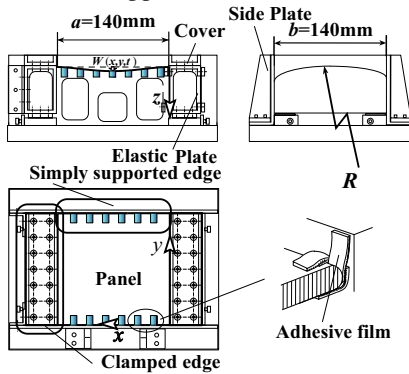


Fig. 1 Shell-panel and fixture

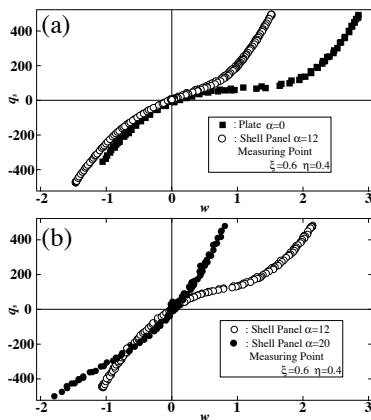


Fig. 2 Characteristics of restoring force

Table 1 Natural frequencies of the shell-panel

$\alpha=0, n_c=0.88$	$\alpha=12, n_c=0.88$	$\alpha=12, n_c=1.6$	$\alpha=20, n_c=1.6$
(m, n)	ω_{mn}	(m, n)	ω_{mn}
(1, 1)	26.8	(1, 1)	25.1
(2, 1)	43.0	(2, 1)	49.6
(1, 2)	63.5	(1, 2)	53.8
(3, 1) _a	76.5	(2, 2)	81.2
(3, 1) _b	97.3	(3, 1)	103
(3, 1) _c	107	(1, 3)	112
		(1, 1)	29.6
		(1, 2)	49.8
		(2, 1)	55.9
		(1, 2)	57.8
		(2, 1)	70.7
		(1, 3)	102
		(3, 1)	99.7
		(3, 1)	121
		(2, 2)	126

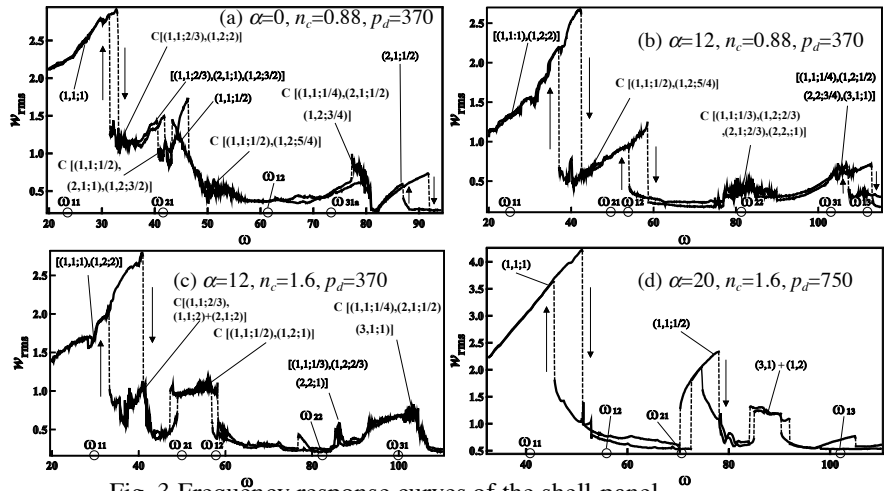


Fig. 3 Frequency response curves of the shell-panel

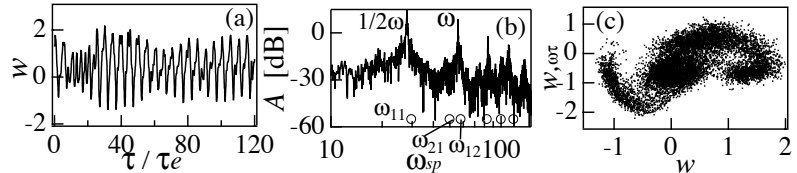


Fig. 4 Time history, Fourier spectrum and the Poincaré projection, $\alpha=12, n_c=1.6$

Table 2 Result of the principal component analysis and the maximum Lyapunov exponent

Curvature α	Compressive force n_c	Type of resonance (The maximum Lyapunov exponent)	Mode (m, n)	Contribution ratio [%]
0	0.88	C[(1,1;2/3),(1,2;2)]	(1,1)	80
		$(\lambda_{\max}=1.0)$	(1,2)	10
		C[(1,1;1/2),(1,2;5/4)]	(1,1)	89
		$(\lambda_{\max}=0.3)$	(1,2)	6
12	0.88	C[(1,1;1/2),(1,2;5/4)]	(1,1)	71
		$(\lambda_{\max}=0.9)$	(1,2)	20
		C[(1,1;1/3),(1,2;2/3), (2,1;2/3),(2,2;1)]	(1,1)	35
			(1,2)	24
			(2,1)	18
		$(\lambda_{\max}=0.7)$	(2,2)	16
12	1.6	C[(1,1;2/3),(1,1;2)+(2,1;2)]	(1,1)	79
		$(\lambda_{\max}=0.8)$	(2,1)	10
		C[(1,1;1/2),(1,2;1)]	(1,1)	66
		$(\lambda_{\max}=0.6)$	(1,2)	22
		C[(1,1;1/4),(2,1;1/2), (3,1;1)]	(1,1)	31
		(2,1)	45	
		$(\lambda_{\max}=1.0)$	(2,2)	14

Analysis and Design for Vibration of Laminated Composites by Using the Three-dimensional Theory

Yoshihiro Narita
School of Engineering, Hokkaido University, Sapporo, Japan
ynarita@eng.hokudai.ac.jp

1. Introduction

Advanced composites are traditionally used in the aerospace industries, and are expanding their applications to the fields of automobile, ocean and other engineering. Relative mechanical advantages are measured by two parameters, the specific modulus and specific strength that are high in composite materials. Another important advantage of the composite is the feasibility to produce the optimum or nearly optimum performance by designing the lay-up in the laminates. This class of optimization problem is called the stacking sequence problem or the lay-up design problem.

The present study deals with this design problem, but unlike in previous studies it uses the three dimensional elasticity theory. Comparison is made among sets of results obtained by 3D, FSDT (First-order Shear Deformation Theory) and CPT (Classical Plate Theory) for the optimum stacking sequence and corresponding natural frequency. The optimum solutions are obtained by the layerwise optimization method.

2. Outline of the Analysis

Figure 1 presents a very thick composite composed of a number of layers with the thickness h and a rectangular planform axb . The principal material axes 1 and 2 are taken along the fiber direction and the direction perpendicular to the fiber, and the thickness axis is given by the 3 axis. With these axis notations, the stress and strain relations are given by

$$\begin{Bmatrix} \sigma_1 \\ \sigma_2 \\ \sigma_3 \end{Bmatrix}^{(k)} = \begin{bmatrix} Q_{11} & Q_{12} & Q_{13} \\ & Q_{22} & Q_{23} \\ sym. & & Q_{33} \end{bmatrix} \begin{Bmatrix} \varepsilon_1 \\ \varepsilon_2 \\ \varepsilon_3 \end{Bmatrix}^{(k)}, \quad \begin{Bmatrix} \tau_{23} \\ \tau_{31} \\ \tau_{12} \end{Bmatrix}^{(k)} = \begin{bmatrix} Q_{44} & 0 & 0 \\ & Q_{55} & 0 \\ sym. & & Q_{66} \end{bmatrix} \begin{Bmatrix} \gamma_{23} \\ \gamma_{31} \\ \gamma_{12} \end{Bmatrix}^{(k)} \quad \dots(1)$$

where

$$\begin{aligned} Q_{11} &= (1 - \nu_{32}\nu_{23})E_1/\Delta, & Q_{12} &= (\nu_{21} + \nu_{31}\nu_{23})E_1/\Delta, & Q_{13} &= (\nu_{31} + \nu_{21}\nu_{32})E_1/\Delta \\ Q_{22} &= (1 - \nu_{31}\nu_{13})E_2/\Delta, & Q_{23} &= (\nu_{32} + \nu_{31}\nu_{12})E_2/\Delta, & Q_{33} &= (1 - \nu_{21}\nu_{12})E_2/\Delta \\ Q_{44} &= G_{23}, & Q_{55} &= G_{31}, & Q_{66} &= G_{12}, & \Delta &= 1 - \nu_{21}\nu_{13}\nu_{32} - \nu_{12}\nu_{23}\nu_{31} - \nu_{13}\nu_{31} - \nu_{32}\nu_{23} - \nu_{21}\nu_{12} \end{aligned} \quad \dots(2)$$

with E_1, E_2 and G_{12}, G_{23}, G_{31} being the normal and shear elastic modulus, respectively, and $\nu_{12}, \nu_{23}, \nu_{31}, \nu_{21}, \nu_{32}, \nu_{13}$ being Poison's ratios.

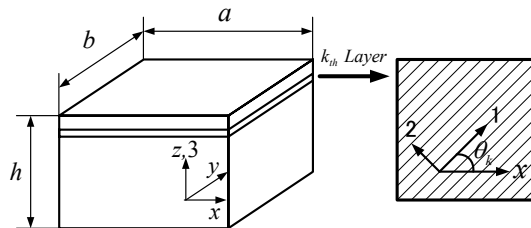


Figure 1. Coordinate system of the rectangular parallelepiped composed of fibrous layers.

The maximum displacements of x , y and z directions in the free vibration state are denoted by in $u(x, y, z)$, $v(x, y, z)$ and $w(x, y, z)$, respectively. The strain-displacement relations are given by

$$\left. \begin{aligned} \varepsilon_x &= \partial u / \partial x, \quad \varepsilon_y = \partial v / \partial y, \quad \varepsilon_z = \partial w / \partial z \\ \gamma_{yz} &= \partial w / \partial y + \partial v / \partial z, \quad \gamma_{zx} = \partial u / \partial z + \partial w / \partial x, \quad \gamma_{xy} = \partial v / \partial x + \partial u / \partial y \end{aligned} \right\} \dots(3)$$

After some algebraic manipulation, the maximum strain energy is written by

$$U_{\max} = \frac{1}{2} \sum_{k=1}^L \int_{V_k} \{\kappa\}^T [Q]^{(k)} \{\kappa\} dV_k$$

with $\{\kappa\} = \{\partial u / \partial x, \partial v / \partial y, \partial w / \partial z, \partial w / \partial y + \partial v / \partial z, \partial u / \partial z + \partial w / \partial x, \partial v / \partial x + \partial u / \partial y\}^T \dots(4)$

where $[Q]$ is a 6x6 matrix with elements given in (2). By denoting a radian frequency by ω , the maximum kinetic energy is given by

$$T_{\max} = \frac{1}{2} \sum_{k=1}^L \rho_k \omega^2 \int_{V_k} \{u \ v \ w\} \{u \ v \ w\}^t dV_k \dots(5)$$

where ρ_k is a mass per unit volume in the k -th layer. After introducing non-dimensional quantities, the displacement functions are defined by

$$u(\xi, \eta, \delta) = \sum_{i=0}^I \sum_{j=0}^J \sum_{k=0}^K A_{ijk} X_i(\xi) Y_j(\eta) Z_k(\delta), \quad v(\xi, \eta, \delta) = \sum_{l=0}^L \sum_{m=0}^M \sum_{n=0}^N B_{lmn} X_l(\xi) Y_m(\eta) Z_n(\delta)$$

$$w(\xi, \eta, \delta) = \sum_{p=0}^P \sum_{q=0}^Q \sum_{r=0}^R C_{pqr} X_p(\xi) Y_q(\eta) Z_r(\delta) \dots(6)$$

where ξ, η, δ are non-dimensional coordinates, X_i, Y_j, Z_k are admissible functions, and $A_{ijk}, B_{lmn}, C_{pqr}$ are unknown coefficients. These functions are substituted into the functional $F = T_{\max} - U_{\max}$ and the functional is minimized with respect to unknown coefficients as

$$\frac{\partial F}{\partial A_{\bar{i}\bar{j}\bar{k}}} = \frac{\partial F}{\partial B_{\bar{l}\bar{m}\bar{n}}} = \frac{\partial F}{\partial C_{\bar{p}\bar{q}\bar{r}}} = 0 \quad (\bar{i} = 0, 1, 2, \dots, I; \bar{j} = 0, 1, 2, \dots, J; \dots) \dots(7)$$

The frequency equation can be derived after this Ritz procedure as

$$\begin{bmatrix} E_{\bar{i}\bar{j}\bar{j}\bar{k}\bar{k}} & E_{\bar{i}\bar{l}\bar{j}\bar{m}\bar{k}\bar{n}} & E_{\bar{i}\bar{p}\bar{j}\bar{q}\bar{k}\bar{r}} \\ & E_{\bar{l}\bar{m}\bar{m}\bar{n}\bar{n}} & E_{\bar{l}\bar{p}\bar{m}\bar{q}\bar{n}\bar{r}} \\ sym. & & E_{\bar{p}\bar{q}\bar{q}\bar{r}\bar{r}} \end{bmatrix} \begin{Bmatrix} A_{\bar{i}\bar{j}\bar{k}} \\ B_{\bar{l}\bar{m}\bar{n}} \\ C_{\bar{p}\bar{q}\bar{r}} \end{Bmatrix} = 0$$

where

$$E_{\bar{i}\bar{j}\bar{j}\bar{k}\bar{k}} = \frac{1}{2} \Omega^2 I_{\bar{i}\bar{j}\bar{j}\bar{k}\bar{k}}^{(000000)} - 2q_{11} I_{\bar{i}\bar{j}\bar{j}\bar{k}\bar{k}}^{(110000)} - 2\alpha q_{16} \left(I_{\bar{i}\bar{j}\bar{j}\bar{k}\bar{k}}^{(011000)} + I_{\bar{i}\bar{j}\bar{j}\bar{k}\bar{k}}^{(100100)} \right) - 2\beta^2 q_{55} I_{\bar{i}\bar{j}\bar{j}\bar{k}\bar{k}}^{(000011)} - 2\alpha^2 q_{66} I_{\bar{i}\bar{j}\bar{j}\bar{k}\bar{k}}^{(001100)}$$

$$E_{\bar{i}\bar{l}\bar{j}\bar{m}\bar{k}\bar{n}} = -2\alpha q_{12} I_{\bar{i}\bar{l}\bar{j}\bar{m}\bar{k}\bar{n}}^{(011000)} - 2q_{16} I_{\bar{i}\bar{l}\bar{j}\bar{m}\bar{k}\bar{n}}^{(110000)} - 2\alpha^2 q_{26} I_{\bar{i}\bar{l}\bar{j}\bar{m}\bar{k}\bar{n}}^{(001100)} - 2\beta^2 q_{45} I_{\bar{i}\bar{l}\bar{j}\bar{m}\bar{k}\bar{n}}^{(000011)} - 2\alpha q_{66} I_{\bar{i}\bar{l}\bar{j}\bar{m}\bar{k}\bar{n}}^{(100100)}$$

Similarly for other elements $\dots(8)$

with $\Omega = \omega a^2 (\rho h / D_0)^{1/2}$, $D_0 = E_T h^3 / 12(1 - \nu_{12} \nu_{21})$ being a frequency parameter and $\beta (=a/h)$ being a thickness parameter. The optimum stacking sequences are determined to make the fundamental frequency maximum by using the layerwise optimization method [1], one of the practical and efficient approximate design methods developed by the present author.

3. Numerical Results and Discussions

Based on the three dimensional theory, a computation program was developed to calculate the natural frequencies and mode shapes of a laminated composite plate. The elastic constants of the composite in this study are for Graphite/epoxy material ($E_1=138\text{GPa}$, $E_2=8.96\text{GPa}$, $E_3=E_2$, $G_{12}=7.1\text{GPa}$, $G_{31}=G_{12}$, $G_{23}=E_2/2(1+\nu_{23})$, $\nu_{12}=0.30$, $\nu_{13}=\nu_{23}=\nu_{32}=\nu_{12}$, $\nu_{21}=\nu_{31}=\nu_{12}$) that has a large

degree of orthotropy ($E_2/E_1=15.4$). The boundary conditions are considered for eight typical combinations of clamped, simply supported and free edges. The thickness ratio is taken for $\beta(=a/h)=100$ (thin), 10(thick) and 1(cube, extremely thick). In addition to the 3D theory, the classical thin plate theory (CPT) and the first-order shear deformation theory (FSDT) are also used for studying the effects of using different plate and 3D theories.

Table 1 presents a comparative study of the optimum solutions obtained by using three different theories. Generally speaking, relatively good agreement is found among those results for the present range of thickness parameters and boundary conditions. It is shown that the use of different plate theories does not significantly affect the prediction of the optimum stacking sequences to maximize the fundamental frequencies, although slight discrepancy exists as the thickness is increased.

References

1. Y. Narita, Maximum frequency design of laminated plates with mixed boundary conditions, *International Journal of Solids and Structures*, Vol.43, (2006), pp.4342-4356
2. K. Murayama, Y. Narita and K. Sasaki, The shear deformable effect on optimum lay-ups of laminated plates, *Key Engineering Materials*, vol.334-335, (2007), pp.97-100

Table.1 Comparison of the maximum fundamental frequency parameters and optimum lay-ups obtained by the present 3D theory, FSDT and CPT for symmetric 8-layered square plates ($a/b=1$).

	$\Omega_{1,opt}$	Opt.Lay-ups	$\Omega_{1,opt}$	Opt.Lay-ups	$\Omega_{1,opt}$	Opt.Lay-ups
β	1		10		100	
CCCC						
3D	11.24	[90/90/90/90]s	67.70	[0/0/0/0]s	93.40	[-5/90/20/0]s
FSDT	11.18	[90/0/0/90]s	71.52	[0/90/90/0]s	93.33	[0/90/90/0]s
CPT	—	—	—	—	93.67	[0/90/90/90]s
SSSS						
3D	8.088	[40/65/30/-50]s	43.85	[-45/45/45/45]s	56.02	[45/-40/-45/-50]s
FSDT	8.780	[-75/15/-50/40]s	44.85	[-45/45/45/-45]s	55.72	[-45/45/45/45]s
CPT	—	—	—	—	56.32	[45/-45/-45/-45]s
CSFF						
3D	4.894	[25/20/5/5]s	14.95	[15/15/-50/5]s	15.52	[10/-10/-20/-35]s
FSDT	4.814	[25/-40/20/10]s	15.01	[15/15/-50/10]s	16.21	[15/15/-45/-50]s
CPT	—	—	—	—	16.40	[20/-45/20/25]s
CFFF						
3D	4.364	[0/0/0/0]s	13.19	[0/0/0/0]s	13.73	[-5/0/-5/5]s
FSDT	4.206	[0/0/0/0]s	13.18	[0/0/0/0]s	13.81	[0/0/0/5]s
CPT	—	—	—	—	13.75	[0/0/0/0]s
SSFF						
3D	2.098	[-45/-45/45/-45]s	9.368	[-45/45/-45/45]s	11.40	[-45/55/-80/-25]s
FSDT	2.216	[-45/45/-45/-45]s	9.442	[-45/45/-45/-45]s	11.19	[-45/45/-45/50]s
CPT	—	—	—	—	11.29	[-45/45/-45/45]s
CCFF						
3D	5.432	[50/55/50/55]s	17.11	[30/75/-35/60]s	19.69	[45/-45/50/-5]s
FSDT	5.485	[30/75/45/45]s	17.29	[30/75/-40/40]s	18.95	[40/-45/50/80]s
CPT	—	—	—	—	19.03	[45/-45/45/-35]s
SSCC						
3D	10.70	[50/-45/55/-45]s	53.34	[0/0/0/0]s	71.90	[45/-45/-45/40]s
FSDT	10.93	[40/-40/-85/-10]s	56.09	[45/-45/-45/45]s	71.47	[-45/45/45/45]s
CPT	—	—	—	—	72.01	[-45/45/45/45]s
SSSF						
3D	6.258	[0/0/90/0]s	36.15	[0/0/0/0]s	40.05	[0/0/5/15]s
FSDT	6.432	[0/90/0/0]s	36.12	[0/0/0/0]s	39.79	[0/0/0/0]s
CPT	—	—	—	—	39.84	[0/0/0/0]s

Dynamics of Circular Cylindrical Shells under Seismic Loads

Francesco Pellicano
Dept. of Mechanical and Civil Engineering
Univ. of Modena and Reggio Emilia

The present paper is focused on the dynamic analysis of circular cylindrical shells under seismic excitation: the excitation direction is the cylinder axis, the shell is clamped at the base and connected to a rigid body on the top and the base provides the seismic excitation which is supposed sinusoidal. The goal is to investigate the shell response when a resonant forcing is applied: the first axisymmetric mode is excited around the resonance at relatively low frequency and low excitation amplitude. A violent resonant phenomenon is experimentally observed as well as an interesting saturation phenomenon close to the previously mentioned resonance. A theoretical model is developed to reproduce the experimental evidence and provide an explanation of the complex dynamics observed experimentally.

The literature about vibration of shells is extremely wide and the reader can refer to Ref. [1] or more recently to Refs. [2-4] for a comprehensive review of models and results presented in literature.

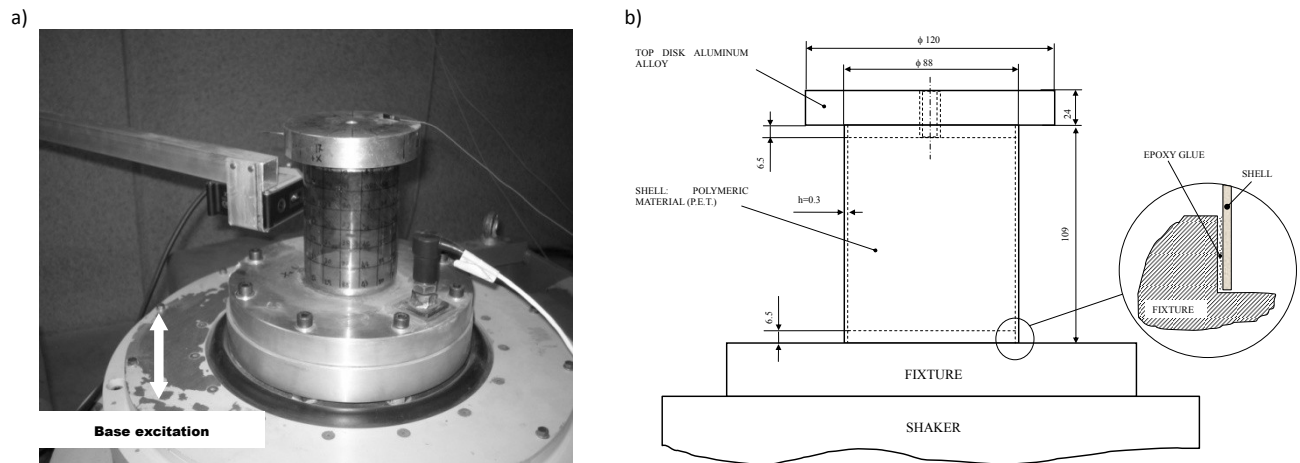


Figure 1. Setup.

The goal of the research is to investigate experimentally and numerically dynamic instabilities of circular cylindrical shells subjected to seismic excitation. The shell is vertically mounted on a shaking table (see Fig.1a) by means of clamping to the base (see Fig. 1b); an aluminium disk is clamped to the top of the shell. The base excitation furnishes energy in the axial direction and excites the shell through the inertia of the top disk. The axial loads primarily excite the axisymmetric modes and secondarily give a parametric excitation to shell like modes (see Fig. 2).

Figure 3 shows some results obtained by exciting the shell with $\approx 13g$ acceleration and decreasing the excitation frequency. Figure 3a shows clearly that the excitation level is not really constant; this is due to the shell-table interaction that made fine control of the table impossible during the experiment. Figure 3b shows that, close to 330Hz, the shell response rapidly grows to huge amplitudes, then it grows again at about 325 Hz and remains flat up to 295 Hz. The top disk behaves similarly in terms of maximum amplitude. The phenomenon is extremely violent and sudden and is accompanied by a strong noise.

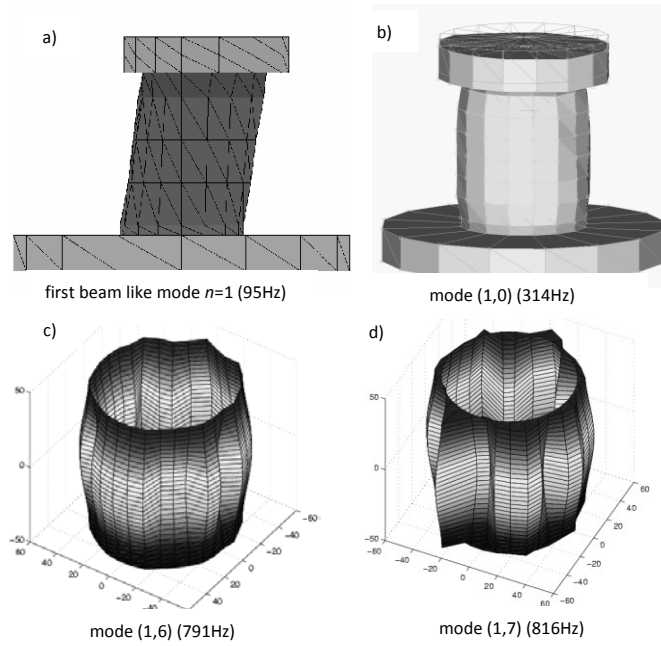


Figure 2. Experimental mode shapes. a) beam like mode; b) first axisymmetric mode; c,d) shell modes.

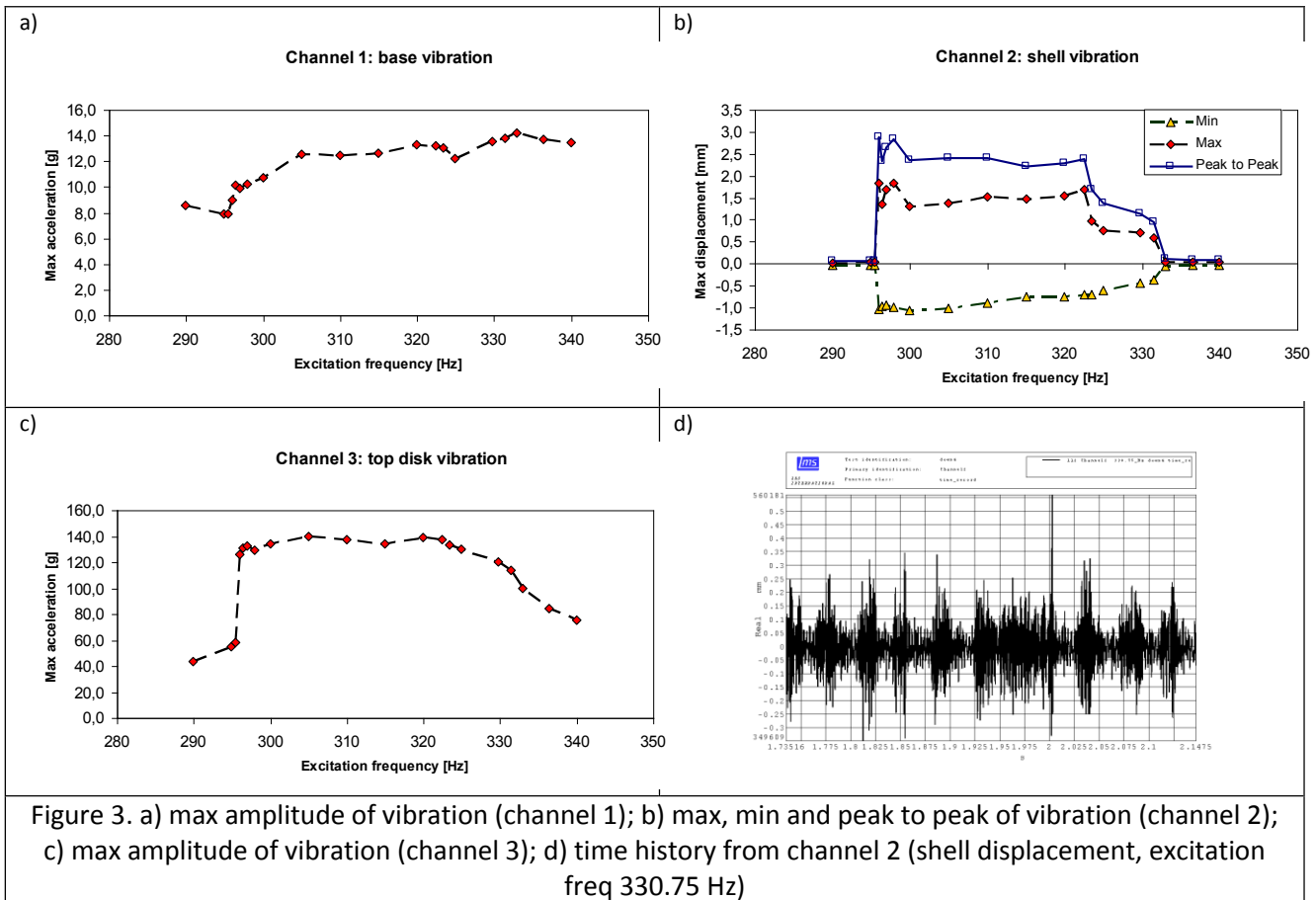


Figure 3. a) max amplitude of vibration (channel 1); b) max, min and peak to peak of vibration (channel 2); c) max amplitude of vibration (channel 3); d) time history from channel 2 (shell displacement, excitation freq 330.75 Hz)

A numerical model has been developed in order to explain the phenomenon. The model is based on the nonlinear Sanders-Koiter theory. The governing equations are solved by expanding the displacement fields using a mixed expansion based on harmonic functions and Chebyshev polynomials. Using Lagrange equations, a set of nonlinear ordinary differential equations is obtained and solved numerically. Details are omitted for the sake of brevity; see Ref. [5] for the application of the approach to linear problems.

Figure 4 shows the maximum amplitude of vibration simulated numerically: compared with Figure 3b it is clear that the numerical model captures an instability phenomenon, which is similar to the experimental one; however, the amplitude is larger than in the experiments and the instability zone is narrower (319-325 Hz numerical) (295-330 Hz experiments). Discrepancies are quantitatively relevant, they are probably due to several issues: i) geometric imperfections are not considered in the numerical model and these can change the linear frequencies of shell modes and modify the energy transfer from axisymmetric to asymmetric modes and enlarge the instability region; ii) the base excitation is constant for the numerical simulation, this is not true in experiments; iii) the shell-table interaction is not considered in the numerical model. The numerical method furnishes some interesting information about the instability mechanism: indeed, the modelling based on modal shapes reveals that the instability involves shell modes having from 4 to 10 nodal diameters (from 800 to 1250Hz natural frequency range); the mode having 9 nodal diameters (1050Hz natural frequency) is excited with the highest amplitude, central zone of Fig. 4. The onset of the instability (from 328 to 325 Hz of Fig. 4) is mainly dominated by the mode having 6 nodal diameters (800Hz natural frequency).

Such an embryonic numerical approach confirms the complexity of the phenomenon, which displays several high frequency resonant modes excited through internal energy transfer from the low frequency axisymmetric mode, which is the only one directly excited.

Further research will be needed for a full understanding of instability onset type and the energy transfer mechanism: shell imperfections as well as system-shaker interactions could be a first step for improving the model.

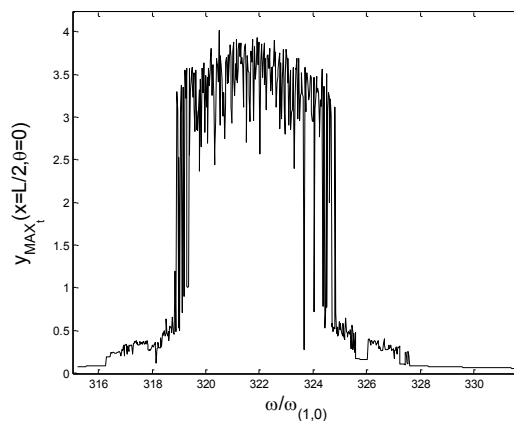


Figure 4. Shell response: numerical simulations.

- [1] A.W. Leissa, *Vibration of Shells*, NASA SP-288. Washington, DC: Government Printing Office. Now available from The Acoustical Society of America, 1993.
- [2] M. Amabili, M.P. Païdoussis, Review of studies on geometrically nonlinear vibrations and dynamics of circular cylindrical shells and panels, with and without fluid-structure interaction, *Applied Mechanics Reviews*, 56 (2003) 349-381.
- [3] V. D. Kubenko and P. S. Koval'chuk, Influence of Initial Geometric Imperfections on the Vibrations and Dynamic Stability of Elastic Shells, *International Applied Mechanics*, 40(8) (2004) 847-877
- [4] M. Amabili, *Nonlinear Vibrations and Stability of Shells and Plates*, Cambridge University Press, Cambridge, 2008.
- [5] F. Pellicano, "VIBRATIONS OF CIRCULAR CYLINDRICAL SHELLS: THEORY AND EXPERIMENTS", *J. of Sound and Vibration*, 2007, 303, 154-170. doi:10.1016/j.jsv.2007.01.022

FORCED VIBRATION OF COMPRESSOR AND TURBINE BLADES

Romuald Rządowski

Department of Aeroelasticity,
Institute of Fluid Flow Machinery,
Polish Academy of Sciences,
J. Fiszer st., 14, Gdansk, 80 952 Poland
E-mail: z3@imp.gda.pl

INTRODUCTION

The problem of unsteady flows in aerodynamic cascades arouses considerable interest mainly because of the effect of non-stationarity on the optimal design, efficiency and reliability of turbomachine operation. The energy transfer in a turbine stage is accompanied by the interaction of aerodynamic, inertial and elastic forces acting on the blades, which can cause excessive blade vibration, leading to structural fatigue failures. Taking into account the structural and mechanical damping, the mutual interaction of these forces determines the aeroelastic behaviour of the blades and represents an important problem not only for aircraft compressor and fan blade rows, but also for the last stages of steam and gas turbines that work in highly loaded off-design conditions.

The prediction of the unsteady pressure loads and aeroelastic behaviour of blades may involve the computation of shock waves, shock/boundary layer interaction and boundary layer separation although it cannot be used with inviscid methods. In order to overcome this limitation, complete Reynolds-averaged Navier-Stokes (RANS) equations are used to model complex and off-design cases of turbomachinery flows.

The unsteady prediction models for 3D viscous flutter and unsteady rotor blade forces in the stage have been discussed in literature over the last ten years (Sayma et al., 1998; Weber et al., 1998; Vasanthakumar et al., 2001; Chassaing and Gerolymus, 2001; Cinnella et al., 2004, Rządowski et al. 2006).

The aim of this paper is to present the mathematical model and the numerical analysis of the coupled fluid-structure solution for the 3-D viscous flow through the turbine stage while taking into account the blade oscillations, but without separating the outer excitation and unsteady effects caused by blade motion.

Here the 3D Reynolds-averaged Navier-Stokes (RANS) solver, coupled with a modified Baldwin and Lomax's algebraic eddy viscous turbulence model, has been applied to calculate three-dimensional unsteady viscous flow through mutually moving steam turbine stator and rotor blades while the rotor blades are vibrating.

The structural analysis used the modal approach and a 3D finite element model of the rotor blade.

To validate the developed numerical viscous code a comparison of the numerical calculations results with the measured data for 11th International Standard Configuration was performed. Moreover, the numerical results were also compared with the results of other authors (Fransson et al, 1999; Cinnella et al, 2004). These comparisons have shown sufficient quantitative and qualitative agreement for local unsteady performances (pressure amplitude and phase distribution).

The numerical analyses of aeroelastic characteristics of the steam turbine last stage in a nominal regime and the first stage compressor rotor blade of S0-3 aircraft engine are presented below.

COUPLED FLUID-STRUCTURE PROBLEM FORMULATION

In this study the partially integrated method was used to solve the coupled aeroelasticity problem for turbine and compressor stages. It involved separate solutions for fluid and structural equations, but the acquired data were exchanged at each time step, so that the solution from one domain was used as boundary condition for the other domain. In other words, at each time step a new rotor blade position was calculated using the aerodynamic forces obtained from a previous time step and this new position was used as the new fluid-structure boundary when computing the aerodynamic forces in the next time step.

The 3D transonic flow of viscous gas flow through an axial turbine stage was considered in the physical domain, including the nozzle cascade (NC) and the rotor wheel (RW), which was rotating at a constant angular velocity.

Normally, in an arbitrary configuration neither the NC nor the RW have an equal number of blades.

Figure 1 shows the calculated domain scheme in the tangential plane.

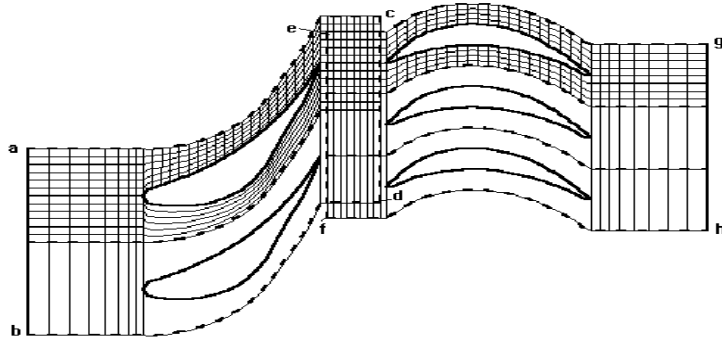


Figure 1. The calculated domain of turbine stage in tangential plane.

The calculated domain was divided into two subdomains (NC) and (RW), with an overlapping area. In each subdomain the cascade geometry and gas flow were described in absolute or relative coordinate systems rigidly connected with the NC and RW, stationary and rotating respectively.

The spatial viscous transonic flow, including generally strong discontinuities in the form of shock waves and wakes behind the exit edges of blades, is described in the relative Cartesian coordinate system rotating with constant angular velocity Ω , by non-stationary Reynolds-averaged Navier-Stokes (RANS) equations. These equations have been presented in the form of integral conservation laws of mass, impulse and energy (Gnesin et al., 2004):

$$\frac{\partial U}{\partial t} + \frac{\partial E}{\partial x} + \frac{\partial F}{\partial y} + \frac{\partial G}{\partial z} + H = \frac{\partial R}{\partial x} + \frac{\partial S}{\partial y} + \frac{\partial Q}{\partial z}, \quad (1)$$

where U - is the symbolic vector of conservative variables; E, F, G and R, S, Q are inviscid and viscous flux vectors respectively; H is the source term caused by an uninertial coordinate system.

The system of equations (1) is completed with the perfect gas law equation $\varepsilon = \frac{1}{\gamma-1} \frac{p}{\rho}$, where γ is the adiabatic exponent (specific heat ratio). The application of Reynolds-averaged equations required modelling of the Reynolds stress using closure relations based on empirical information. In this study a Baldwin and Lomax algebraic turbulence model was applied. At the solid wall, a no-slip condition is imposed $\bar{u} = \bar{u}_w$, where \bar{u}_w is the displacement velocity of the wall.

The dynamic model of the oscillating blade using the modal approach can be reduced to a set of decoupled differential equations with regard to the modal coefficients of natural modes:

$$\ddot{q}_i(t) + 2h_i \dot{q}_i(t) + \omega_i^2 q_i(t) = \lambda_i(t), \quad \lambda_i = \frac{\iint_{\sigma} p \bar{U}_i \cdot \bar{n} \, d\sigma}{\iiint_v \rho \bar{U}_i^2 \, dv}, \quad (2)$$

here h_i –mechanical damping i th -mode coefficient; ω_i – natural i th -mode frequency; λ_i – modal force relative to i th -mode displacement, calculated at every iteration by instant pressure distribution on the blade surface, p – blade surface pressure.

Having defined the modal coefficients q_i from the system of differential equations (2), blade displacement and velocity are obtained using modal superposition method.

NUMERICAL RESULTS

Due to the lack of experimental results, the numerical code developed to calculate the unsteady forces acting on the rotor blade in the stage was verified using the flutter calculation of turbine rotor blades. This was applied to the 11th Standard Configuration (Fransson et al, 1999). Three selected experiments were

proposed as test cases: a subsonic case ($M_2 = 0.69$) for code calibration, a transonic off-design case with a high incidence inlet flow angle 18 deg ($M_2 = 0.99$) and a separation bubble on the suction surface, and a supersonic off-design case ($M_2 = 1.42$) with incidence flow angle 33 deg. The details of these cases, including full blade geometry, are given by (Fransson et al, 1999). Viscous computations were performed using O-grids with 390×42 cells, and an average value of y^+ for the first cell near the wall of approximately 1.0. This code can also be used to analyse flutter in the compressor stage.

In literature unsteady forces acting on rotor blades were calculated using the unviscous code of real turbine stages, in the control stage (Rzadkowski and Soliński 2007), stages with steam extractions (Rzadkowski and Soliński 2007), the last steam turbine stage (Gnesin et al. 2004, Rzadkowski et al. 2006b, Rzadkowski and Soliński 2007) and an aircraft engine (Rzadkowski et al. 2008). The computational results of the viscous code presented here were carried out for the last stage of a steam turbine with a rotor blade length of 0.765 m, and the stator to rotor blades number ratio of 64 : 96 (2:3).

One of the important aspects of stator-rotor interaction is the effect of blade response when taking into account the excitation caused by both non-uniform flow and excitation caused by blade oscillations. The amplitude-frequency spectrum includes high frequency harmonics (3200 Hz, 6400 Hz) corresponding to pitch non-uniformity, and low frequency harmonics corresponding to non-uniformity along the entire stage circumference.

Here the 3D transonic flow of an inviscid non-heat conductive gas through the axial first compressor stage of an S0-3 aircraft engine was considered in the physical domain, including the nozzle cascade (S0), the rotor wheel (RW) rotating with constant angular velocity and the nozzle cascade (S1).

The blade vibration is defined by taking into account the first five natural mode shapes of the rotating blade.

The unsteady modal force includes high-frequency harmonics ($\nu_{rev} \times z_{st1} = 256 \times 35 = 8960 \text{ Hz}$ and $\nu_{rev} \times z_{st0} = 256 \times 42 = 10752 \text{ Hz}$, where ν_{rev} is rotation frequency, $z_{st0} = 42$ and $z_{st1} = 35$ are the number of stator S1 and stator S0 blades) corresponding to the rotor moving past stator S0 and the S1 blade pitch.

The amplitudes of harmonics are equal to 1-3 % of the averaged value for the F_y circumferential force component, 1.4-2.8 % for the F_z axial force, and 6.6-3.2 % for the aerodynamic moment.

The maximum values of the amplitude of the unsteady component for axial and circumferential loads occur in the periphery layer and decrease in the root, while maximum amplitude for aerodynamic moment occur in the mid section.

Apart from amplitudes with frequencies ($\nu_1 = 8960 \text{ Hz}$ and $\nu_2 = 10752 \text{ Hz}$), we observe amplitudes of unsteady loads with frequencies $\nu = 17920 \text{ Hz}$ ($2 \times 8960 \text{ Hz}$) and $\nu = 21504 \text{ Hz}$ ($2 \times 10752 \text{ Hz}$).

REFERENCES

- Cinnella P., Palma P.De., Pascasio G., Napolitano M., 2004, "A Numerical Method for Turbomachinery Aeroelasticity", *Journal of Turbomachinery*, Vol. 126, April 2004, pp.310-316.
- Cebeci T. and Smith A.M. Analysis of Turbulent Boundary Layers, N. Y., Academic Press, 1974.
- Chassaing J.C., Gerolymos G.A., 2001, "Compressor Flutter Analysis Using Time-Nonlinear and Time-Linearized 3-D Navier-Stokes Method", in book P. Farrand, S. Auber: Unsteady Aerodynamics, Aeroacoustics and Aeroelasticity of Turbomachines, *Proceedings of the 9th International Symposium held in Lyon, France*, 4-8 September 2000, Presses Universitaires de Grenoble, 666-677.
- Fransson T.H., Jöcker M., A. Bölcs, P. Ott., 1999, "Viscous and Inviscid Linear/Nonlinear Calculations Versus Quasi-Three-Dimensional Experimental Data for a New Aeroelastic Turbine Standard Configuration", *ASME Journal of Turbomachinery*, 121,717-725.
- Gnesin V.I., Kolodyazhnaya L.V. and Rzadkowski R., 2004, "A numerical modelling of stator- rotor interaction in a turbine stage with oscillating blades", *Journal of Fluid and Structure*, 19(8), 1141-1153.
- Rzadkowski R., Soliński M.: Unsteady Aerodynamic Forces Acting on the Rotor of Steam Turbines, Tom 29, Wydawnictwo IMP PAN Gdańsk, (in Polish) 2007.
- Rzadkowski R., Gnesin V., Kolodyazhnaya L., 2006, "3D Viscous Flutter in Turbomachinery Cascade by Godunov-Kolgan Method", *ASME paper GT-2006-90157*.
- Rzadkowski R., Gnesin V., Kolodyazhnaya L., 2008, "Effect of Stator Clocking on 3d Aeroelastic Characteristics of Compressor Rotor Blades", *ASME paper GT-2008-50767*.
- Sayma A.I., Vahdati M., Green J.S. Imregun M., 1998, "Whole -Assembly Flutter Analysis of a Low Pressure Turbine Blade", in book T.H. Fransson ed.: Unsteady Aerodynamics and Aeroelasticity of Turbomachines, *Proceedings of the 8th International Symposium held in Stockholm, Sweden*, 14-18 September 1997, Kluwer Academic Publishers, 347-359.
- Vasanthakumar P., Chen T., He L., 2001, "Three-Dimensional Viscous Computation of Blade Flutter and Forced Response Using Nonlinear Harmonic Approach", in book P. Farrand, S. Auber : Unsteady Aerodynamics, Aeroacoustics and Aeroelasticity of Turbomachines, *Proceedings of the 9th International Symposium held in Lyon, France*, 4-8 September 2000, Presses Universitaires de Grenoble, 649-665.
- Weber S., Gallus H.E., Peitsch D., 1998, "Numerical Solution of the Navier Stokes Equations for Unsteady Unstalled and Stalled Flow in Turbomachinery Cascade with Oscillating Blades", in book T.H. Fransson ed.: Unsteady Aerodynamics and Aeroelasticity of Turbomachines, *Proceedings of the 8th International Symposium held in Stockholm, Sweden*, 14-18 September 1997, Kluwer Academic Publishers, 478-491.

Tracking of Resonance Frequencies of Vibrating Beams by Phase-Locked Loops (PLL)

Wolfgang Seemann

Universität Karlsruhe (TH), Institut für Technische Mechanik, Germany
seemann@itm.uni-karlsruhe.de

Abstract

The use of phase-locked-loops (PLL) is wide spread in electronics. It is the basis e.g. of FM-radios and other applications. However, in mechanical systems in general a PLL is only applied if the system also contains electric parts like in some ultrasonic motors [1]. In the present paper the goal is to apply such a PLL to track the resonance frequency of a vibrating beam. These frequency changes may occur due to changing masses or due to a changing longitudinal force in the beam

1 Introduction

The use of phase-locked-loops is widespread in electronics. Such systems are used for example in FM radios to generate and reconstruct the original signal by tracking the frequency of the carrier wave. The principle is that the PLL consists of a voltage controlled oscillator (VCO) which has an output frequency which is proportional to its input voltage. This input voltage is the output of a controller which adjusts the phase of the VCO's output to a second signal. This second signal may be the signal of a sensor which measures the output of a mechanical system. The vibration of the mechanical part in return is excited by the VCO and an amplifier. In such a configuration both input signals of the controller do have the same frequency, but the phase shift between both signals is a function of the frequency. If there is a mechanical system in between, e.g. in form of a one dof oscillator, and the displacement is measured, then the phase difference may increase from zero (far below resonance) to 180 degrees (far above resonance).

In a cooperation between the Institute of Applied Mechanics of the University of Karlsruhe and the Institute of Production Technology, the goal was to develop an adaptive strut for a machine with parallel kinematics. Within this strut, the longitudinal force was first measured by the vibrating string principle. The changing frequency of the string was obtained by counting the maxima of the free vibration.

A second possibility, which is the topic of this presentation is to use a beam with piezoceramic patches to excite and sense the resonance vibration of the beam. The resonance frequencies of the beam change due to the changing longitudinal force. In other applications like bio sensors the resonance frequency may change if the mass along the beam changes, e.g. in microbeams where added molecules may stick to the beam, see figure 1.

2 Principle of a PLL

The principle of a phase locked loop is that a voltage-controlled oscillator (VCO) is driven by a controller which has the phase difference of two signals as its input signal. The output frequency of the VCO is proportional to the input voltage. The phase difference in general is detected by multiplying the two input signals of the phase detector and integrating the product. The phase of

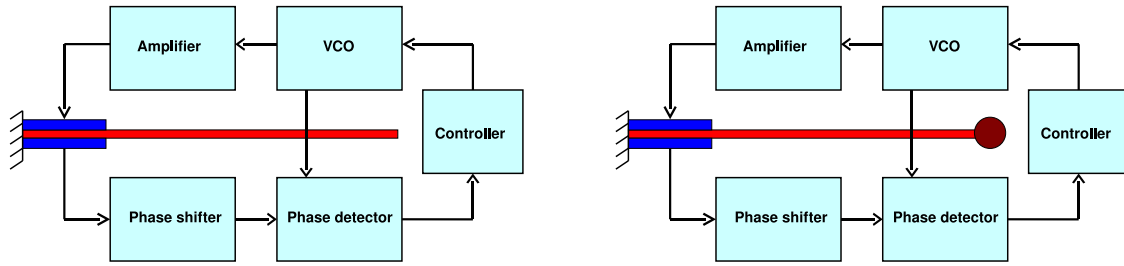


Figure 1: Principle of a phase locked loop (PLL) for a beam with changing mass

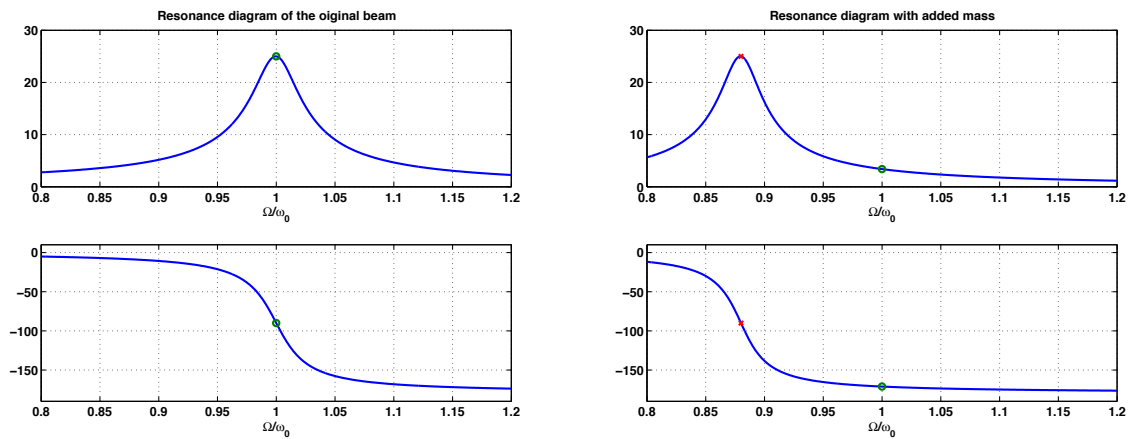


Figure 2: Sketch of the phase of the output signal with and without additional mass as a function of the excitation frequency

the mechanical system for a given excitation frequency with and without an additional mass e.g. are given in figure 2. In order to have the same phase of the mechanical system, the controller has to lower the excitation frequency of the beam with additional mass and this frequency change means that the input voltage of the VCO has to be changed, which can be measured very easily.

3 Phase relation between electric input of the beam and input signal of the phase detector

In order to track the resonance frequency of a beam, the phase difference between input and output of the mechanical part is important. Therefore, in this presentation the beam is modeled by Bernoulli-Euler theory and by assuming that the differential equation is given by the equation of motion for a beam with axial load and external damping. Damping may be important, because it affects the phase shift between excitation and output. The excitation of the beam may be modeled based on pin-force-models or on Bernoulli-Euler-models [2]. To sense the vibration, it is important to specify if the output voltage of a piezoelectric sensor is used or if the charge of the sensor is measured. In the first case, the output voltage has to be calculated based on the fact that between the sensor electrodes no charge is flowing while, in the second case, the electrodes of the sensor may be taken to be short circuited and the total charge between the electrodes corresponds to the

integral of the local electric displacement.

In order to do the analysis, a time harmonic solution is assumed in such a way that all quantities like voltage, displacement, stress, strain and charge are harmonic functions of time with given circular frequency of the excitation.

4 Results

At the moment results are not yet available. They will be presented at the conference. For several vibration modes, the frequency-phase plots will be given as well as the relation between axial force and phase for a fixed vibration frequency. For the application in a strut of a parallel machine, higher modes are of special interest in order to get a high dynamics of the measurement system.

References

- [1] W. Seemann, *Smart Motors in Germany*. In: Smart Materials, Structures and MEMS, Editors Aatre, K.V., Varadan, K.V., Varadan, V.V., SPIE-Vol. 3321, 1996, 472-483.
- [2] W. Seemann, *Exact Pin-Force Models for Piezoceramic Excitation*. In: ZAMM, Vol. 78, 1998, S727-S728.
- [3] P. V. Brennan, *Phase-locked loops: principles and practice*. Mcmillan, 1996.

Two Classical Problems on Stabilization of Statically Unstable Systems by Vibration

Alexander P. Seyranian

Institute of Mechanics, Moscow State Lomonosov University

Michurynski pr. 1, Moscow 119192, Russia

seyran@imec.msu.ru

Abstract. Two classical problems of stabilization of statically unstable systems by vibration are considered. First problem is the well known problem of stabilization of an inverted pendulum by high frequency excitation of the suspension point. The second problem is stabilization of an elastic rod compressed by an axial force, greater than the critical Euler's value, by longitudinal vibration (Chelomei's problem). Stabilization regions are found both analytically and numerically. It is shown that, in contrast to high-frequency stabilization of an inverted pendulum with a vibrating suspension point, the rod is stabilized at excitation frequencies of the order of the natural frequency of transverse oscillations of the free rod belonging to a certain region.

1. Stabilization of an inverted pendulum. Stabilization of the inverted vertical equilibrium position of a pendulum by high-frequency excitation of the suspension point was studied by many authors, see e.g., papers [1-3]. The difference between present paper and previous studies is that we assume existence of viscous damping forces, consider arbitrary periodic excitation function, and use the method of stability study of periodic systems based on analysis of the Floquet multipliers.

Oscillations of a physical pendulum with the vibrating suspension point about upper vertical (statically unstable) position is described by the equation

$$I\theta_{tt} + c\dot{\theta} - mr(g + z_{tt})\sin\theta = 0. \quad (1)$$

Here I and m are the moment of inertia and mass of the pendulum, θ is the angle measured from the vertical axis, c is the damping coefficient, r is the distance between suspension point and the center of gravity, g is the acceleration due to gravity, z is the vertical displacement of the suspension point following the law $z = a\phi(\Omega t)$, where Ω is the excitation frequency, and $\phi(\tau)$ is an arbitrary 2π -periodic function. The amplitude a and damping coefficient c are supposed to be small. For the sake of simplicity we use notation $\varphi = -\phi_{tt}$ and assume that the mean value of the periodic function $\varphi(\tau)$ is equal to zero.

Using non-dimensional time τ and parameters, linearized equation (1) takes the form of Hill's equation with damping

$$\ddot{\theta} + \beta\dot{\theta} + [\mu + \varepsilon\varphi(\tau)]\theta = 0, \quad \mu = -\omega^2. \quad (2)$$

The coefficients of this equation explicitly depend on the 2π -periodic function $\varphi(\tau)$ and three non-dimensional parameters $\varepsilon, \beta, \omega$. The amplitude and damping parameters ε and β are assumed to be small with respect to 1.

At $\varepsilon = 0, \beta = 0$ the upper vertical position of the pendulum $\theta = 0$ is unstable. Let us study possibility of stabilization of this position by high-frequency excitation of the suspension point. In this case we are close to the point $\varepsilon = 0, \beta = 0, \mu = 0$. To find the stability region we use the method based on calculation of derivatives of the monodromy matrix and analysis of Floquet multipliers. We show that the stability region for an arbitrary periodic function $\varphi(\tau)$ in the vicinity of the point $\mathbf{p}_0 = (0, 0, 0)$ in the first approximation is given by the inequality

$$\mu > F\varepsilon^2, \quad F = \left(\frac{1}{2\pi} \int_0^{2\pi} t\varphi(t)dt \right)^2 - \frac{1}{\pi} \int_0^{2\pi} \varphi(t) \int_0^t \tau\varphi(\tau)d\tau dt. \quad (3)$$

It can be shown that for most of the periodic functions the constant $F < 0$. In the formula for stabilization region the terms of higher order have the form of rather complicated multiple integrals. Using these relations we derive formulas for the stabilization frequency of the pendulum.

With introduction of the damping coefficient as $\beta_0 = c/(I\Omega_0)$ for the function $\varphi(\tau) = \cos \tau$ we obtain a formula for the stabilization frequency in the form

$$\frac{\Omega}{\Omega_0} > \sqrt{2} \left[\frac{1}{\varepsilon} + \frac{7\varepsilon}{32} + \frac{\varepsilon\beta_0^2}{4} - \frac{2389\varepsilon^3}{18432} \right]. \quad (4)$$

Thus, at rather high excitation frequency the upper vertical position of the pendulum becomes stable, and small damping increases the critical stabilization frequency. The first term in the right hand side of (4) agrees with that of known in the literature, see e.g. [1-3].

2. The Chelomei problem. Let us consider a straight elastic rod of constant cross section, loaded by a periodic axial force $P(t) = P_0 + P_t\phi(\omega t)$ applied at its end. The equation of transverse oscillations of the rod is

$$EJ \frac{\partial^4 u}{\partial x^4} + P(t) \frac{\partial^2 u}{\partial x^2} + 2\gamma m \frac{\partial u}{\partial t} + m \frac{\partial^2 u}{\partial t^2} = 0, \quad (5)$$

where x is the coordinate along the rod axis; t is the time; $u(x, t)$ is the rod deflection function; m is the mass per unit length; EJ is the flexural rigidity; γ is the damping coefficient; P_t and ω are the excitation amplitude and frequency of the longitudinal vibration, respectively. We consider the case in which both ends of the rod are simply supported. Then the solution can be found in the form of a series in eigenfunctions $u(x, t) = \sum \varphi_j(t) \sin(j\pi x/l)$. Substituting this series into Eq. (5), multiplying by $\sin(k\pi x/l)$, and integrating the result over the interval $[0, l]$, we arrive at an equation with respect to the functions $\varphi_k(t)$. With notation $\beta_k = \gamma/\Omega_k$ and new time variable $\tau = \omega t$ this equation takes the form

$$\frac{d^2 \varphi_k}{d\tau^2} + 2\beta_k \left(\frac{\Omega_k}{\omega} \right) \frac{d\varphi_k}{d\tau} + \left(\frac{\Omega_k}{\omega} \right)^2 \left\{ 1 - \frac{P_0}{P_k} - \frac{P_t\phi(\tau)}{P_k} \right\} \varphi_k = 0, \quad k = 1, 2, \dots, \quad (6)$$

where $\Omega_k = \pi^2 k^2 \sqrt{EJ/m} / l^2$ is the k -th eigenfrequency of transverse free oscillations of the unloaded rod, and $P_k = \pi^2 k^2 EJ / l^2$ is the k -th critical Euler's force. The trivial equilibrium of the rod $u(x, t) = 0$ is asymptotically stable if the functions asymptotically vanish $\varphi_k(t) \rightarrow 0$ as $t \rightarrow \infty$, $k = 1, 2, \dots$, and it is unstable if at least one of the functions $\varphi_k(t)$ exhibits unlimited growth as $t \rightarrow \infty$.

In his famous paper [4], Chelomei stated the problem of stabilization of an elastic rod loaded by a periodic longitudinal force exceeding in average the Euler's critical value $P_0 > P_1$, i.e., of a statically unstable rod, by means of longitudinal vibration bringing it to the straight position. Chelomei's results [4] were included with slight correction into the well-known monograph by Bogolyubov and Mitropol'skii [3]. In the present paper an obvious discrepancy in [4,5] is recognized concerning high-frequency stabilization formula: in derivations it was assumed that $\omega/\Omega_1 \gg 1$, while the critical stabilization frequency turns out to be of the order of the natural frequency. Besides, Chelomei [4] did not find a limitation on the stabilization frequency from below. The absence of this lower boundary leads to the paradoxical conclusion that the rod can be stabilized by applying an arbitrarily slow longitudinal vibration!

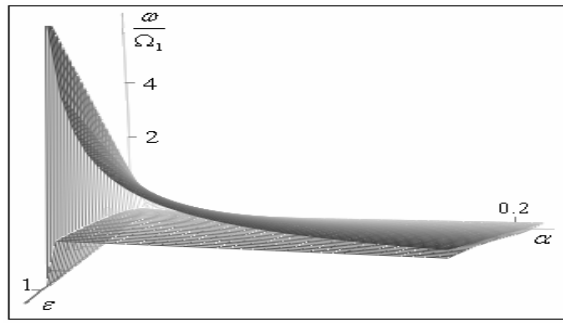


Fig. 1. Stabilization region.

For analysis of the rod stabilization, we use the results of investigation of the stability regions for the Hill equation with damping. Applying these results to Eq. (6) with $k=1$, assuming $0 < \alpha = P_0/P_1 - 1 \ll 1$ and small excitation amplitude $\varepsilon = P_i/P_1 \ll 1$ with $\phi(\tau) = \cos \tau$, we arrive at the two-sided inequality determining the stabilization frequency:

$$\varepsilon - 2\alpha + \sqrt{(\varepsilon - 2\alpha)^2 + \frac{\varepsilon^2}{2}} + \Delta < \left(\frac{\omega}{\Omega_1}\right)^2 < \frac{\varepsilon^2}{2\alpha} - \frac{7\alpha}{8} - 4\beta_1^2. \quad (7)$$

Here the term Δ is proportional to β_1^2 . Thus, the stabilization region boundaries depend on three small parameters, namely, ε , α and β_1 . Fig. 1 shows the dependence of the lower and upper boundaries of the stabilization frequency on the parameters ε , α calculated according to Eq. (7) at the damping coefficient $\beta_1 = 0.05$. Stabilization region found analytically in (7) agrees with the numerical results.

Conclusion. We considered two mechanical problems on stabilization of statically unstable systems by vibration. The difference between these problems is that, at small excitation amplitude, the pendulum in the upper vertical position is stabilized by an excitation frequency greater than the critical value and high as compared with the natural frequency of the pendulum, whereas the elastic rod is stabilized by excitation frequencies of the order of the natural frequency of transverse oscillations of the free rod belonging to a certain interval.

Acknowledgment. The author thanks Andrei A. Seyranian for his valuable assistance. This work was supported by INTAS, grant no. 06-1000013-9019.

References

1. Stephenson A. On a new type of dynamical stability. Mem. Proc. Manchester Lit. Phil. Soc. 1908. V. 52. N. 8. P. 1-10.
2. Kapitza P.L. Dynamical stability of a pendulum when its point of suspension vibrates, and pendulum with a vibrating suspension. In: Collected Papers by P.L. Kapitza (Haar D.T., Ed.). London, Pergamon, 1965, vol. 2, pp. 714-737.
3. Bogolyubov N.N. and Mitropol'skii Yu.A. Asymptotic Methods in the Theory of Nonlinear Oscillations. Moscow, Nauka, 1974.
4. Chelomei V.N. On possibility to increase stability of elastic systems by vibration. Doklady Akad. Nauk SSSR. 1956. V. 110. No. 3. P. 345-347.
5. Chelomei V.N. Paradoxes in mechanics caused by vibration. Doklady Akad. Nauk SSSR. 1983. V. 270. No. 1. P. 62-67.

On the vibrations of single - and multi - walled carbon nanotubes.

Anand V. Singh and Sina Arghavan
Department of Mechanical and Materials Engineering
The University of Western Ontario
London, Ontario, Canada, N6A 5B9

E-mail: avsingh@eng.uwo.ca

Introduction. Iijima [1] reported a new type of finite carbon structure composed of needle-like tubes which were produced in the soot by an arc-discharge evaporation technique and possessed amazing physical properties. Several synthetic methods were developed afterwards for preparing carbon nanotubes in the form of nanoscale whiskers that were seen to be light weight and stiff as graphite along the graphene layers. Because of this nanometric scale, such carbon fibers have a wide range of application in strengthening the current and future composite materials [2, 3]. To design with such materials, one requires a thorough understanding of the morphologies, length, thickness and number of concentric shells. Also desired is the clear understanding of the stiffness, strength, toughness, vibrational characteristics, etc.

Li and Chou [4,5] provided a concise review of the recent advances in carbon nanotubes and their composites along with the structural mechanics approach for the analysis. Harris [6,7] also reviewed the recent work on carbon nanotube composites and assessed successes in exploiting the full potential of the enhanced mechanical and electronic properties. Nanotubes are modeled as fullerenes (space frame like structures) of which the surfaces are essentially arrangements of hexagons around the circumference [8]. The arrangement pattern is chiral in which hexagons are arranged helically around the circumference. The chiral angles of 0° and 30° represent the two special cases known as “zigzag” and “armchair” respectively. The tubes are noted to be either as single-walled carbon nanotube (SWNT) or multi-walled carbon nanotube (MWNT) and generally are less perfect than their idealized versions. Within the last ten years, the buckling and vibrations of nanotubes, both single-walled and multi-walled, using conventional beam and shell theories were studied by some researchers [9-12].

This study aims at the understanding of the vibrational characteristics of the carbon nanotubes using the mechanical and material properties available in the literature. This will be achieved through thorough analysis of the free and transient vibration analyses. In addition, the performance of the numerical methods for the analyses of free and forced linear vibrations of single- and multi-walled nanotubes is being examined in detail. In the free vibration case, the natural frequencies and associated mode shapes are calculated and discussed briefly for the single-walled nanotubes (SWNTs) with clamped-free and clamped-clamped conditions at the two ends. In the forced vibration analysis, Newmark’s direct integration method is being used to obtain the transient response under different loading conditions. Subsequently the fast Fourier transform (fft) is performed on the transient response data to examine the contributions of individual natural modes to the overall response. This exercise produces the peaks at the dominant natural frequencies which are successfully compared with the same from the eigen-value/eigen-vector analysis of the model.

Modeling Procedure, Results and Discussions. Researchers have described a single-walled carbon nanotube (SWNT) as graphene sheet rolled into a tube with hexagonal cells around the circumference. In the case of graphene sheet, the carbon atoms are arranged in a hexagonal 2D array wherein each atom is shared by three hexagons. The atoms have covalent bonds between each other to keep them connected. These covalent bonds are considered as the connecting elements between

the carbon atoms; are characterized by their lengths and angles in a three dimensional space; and form hexagons on the wall of the tube [4]. Therefore, it is seen to be appropriate that a nanotube be simulated by a fullerene of carbon atoms, which act as joints of the connecting space frame elements with extensional, bending and torsional stiffness properties. Connecting frame elements are assumed to be circular in cross section and identical. Owing to the fact that the electrons of carbon atoms are of negligible mass as compared to the mass of the nuclei and that the radius of the nuclei (2.75×10^{-5} Å) is small as well, it is assumed that mass is concentrated at the joints with the atom. Though the present study is in its very early stage, a number of different types of single-walled carbon nanotubes have been modeled. Special programming is needed to define the nodal points, i.e. the locations of the carbon atoms, and then the orientations of space frame members representing sides of the hexagons are calculated one by one. Finally, the matrix equation of motion is obtained after assembling the stiffness and mass matrices which are calculated using the geometric and material properties as presented in the following table.

Table. Properties of the space frame elements

Cross sectional area, A	1.68794 Å ²
Length of bond, L	1.42 Å
Polar moment of inertia, J	0.45346 Å ⁴
Moment of inertia, I	0.22682 Å ⁴
Young's modulus of elasticity, E	5.488×10^{-8} N/ Å ²
Shear modulus of rigidity, G	8.711×10^{-9} N/ Å ²
Mass of each carbon atom, m_c	1.9943×10^{-26} Kg

Frequencies and the natural mode shapes of a clamped-free zig-zag nanotube are calculated and presented in this paper. The first eight values of the non-dimensional natural frequency parameter $\Omega = \omega \sqrt{(m_c / EI)}$ are found to be: 648.15, 3157.02, 3610.58, 5960.00, 8287.80, 8874.57, 11549.37 and 14473.04, all multiplied by 10^{-06} and their mode shapes are shown in the following figure. There are seven bending modes denoted by (B) in this group and one extensional mode which is the fourth denoted by (E). The deformed shapes are plotted in full lines on top of the undeformed geometry, shown by dotted lines. Subsequently, the tube is subjected to two impulsive loads one at a time in the horizontal and vertical directions respectively at the free end and transient responses are obtained by the Newmark's direct integration method. The fft of the horizontal transient response of a point shows as expected peaks at frequencies associated with the bending modes only and there is no peak for the fourth mode which is the extensional in this response's frequency spectrum. On the contrary the fft of the response due to the vertical load reveals peaks at the fourth modes and others way out of the range of the first eight modes. To check this, eigen analysis is carried out again for many modes and modes 11 and 31, also shown in the figure, are the second and third extensional ones. Frequency Ω of modes 11 and 31 are 17802.41×10^{-06} and 41704.60×10^{-06} respectively. In this particular case, the circumferential modes don't seem to be noticeable to a significant extent. In the case of the clamped-clamped armchair nanotube, the effects of the circumferential modes are found to be considerably significant, as the longitudinal modes are constrained. Again, the results and observations presented in this paper are quite preliminary and more elaborate results are expected to be presented at the conference. Research work will be extended further to accommodate the vibration analyses of multi-walled nanotubes (MWNTs).

Acknowledgement. This research has been made possible by the Shared Hierarchical Academic Research Computing Network (SHARCNET:www.sharcnet.ca) facilities.

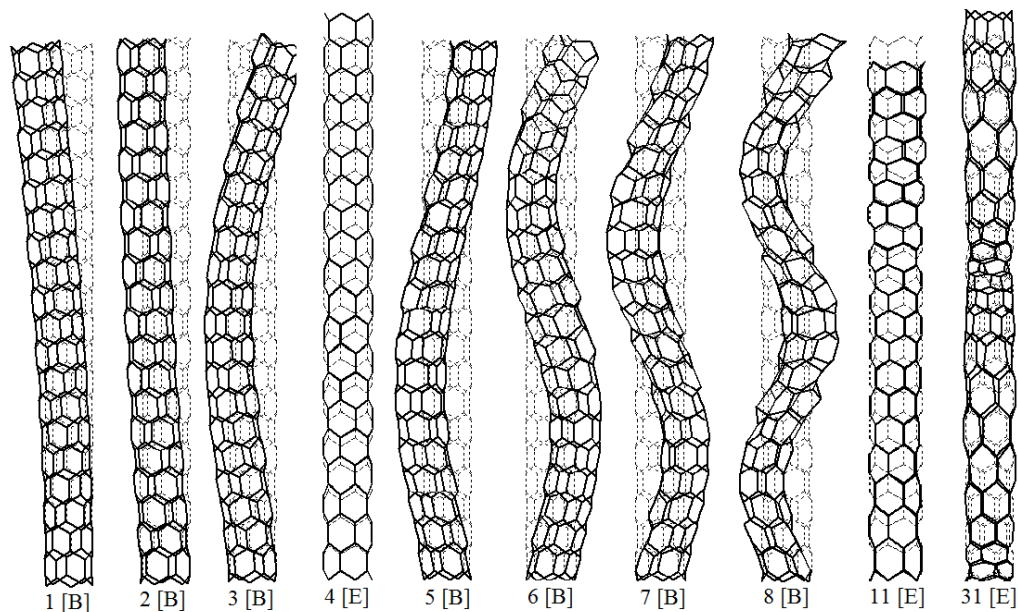


Figure. Bending and axial modes of a cantilevered nanotube.

References.

- [1] S Iijima, 1991, Helical microtubules of graphite carbon, *Nature*, 354, 56 – 58.
- [2] E W Wong, P E Sheehan, C M Lieber, 1997, Nanobeam mechanics: Elasticity, strength, and toughness of nanorods and nanotubes, *Science* 277, 1971 – 1975.
- [3] V N Popov, V E Van Doren, 2000, Elastic properties of single-walled carbon nanotubes, *Physical Review B*, 61(4), 3078 – 3084.
- [4] C Li, T-W Chou, 2003, A structural mechanics approach for the analysis of carbon nanotubes, *IJ Solids and Structures*, 40, 2487 – 2499.
- [5] C Li, T-W Chou, 2003, Elastic moduli of multi walled carbon nanotubes and the effect of van der Waals forces, *Composite Science and Technology*, 63, 1517 – 1524.
- [6] P J F Harris, 2004, Carbon nanotube composites, *Int. Materials Reviews*, 49(01), 31 – 43.
- [7] P J F Harris, 2005, New Perspectives on the structure of graphite carbons, *Critical Reviews in Solid State and Materials Sciences*, 30, 235 – 253.
- [8] E T Thostenson, Z. Ren, T-W Chou, 2001, Advances in the science and technology of carbon nanotubes and their composites: a review, *Composite Science and Technology* 61, 1899 – 1912.
- [9] L J Sudak, 2003, Column buckling of multiwalled carbon nanotubes using nonlocal continuum mechanics, *Journal of Applied Physics*, 94(11), 7281 – 7287.
- [10] J Yoon, C Q Ru, A. Mioduchowski, 2003, Vibration of an embedded multiwall carbon nanotubes, *Composite Science and Technology*, 63, 1533 – 1542.
- [11] Y Zhang, G Liu, X Han, 2005, Transverse vibrations of double walled carbon nanotubes under compressive axial loads, *Physics Letters A*, 340, 258 – 266.
- [12] M Aydogdu, M Cem ECE, 2007, Vibration and buckling of in-plane loaded double walled carbon nanotubes, *Turkish J. Eng. Env. Sci.*, 31, 305 – 310.

Stability of shells in frictional contact

Gottfried Spelsberg-Korspeter

Dynamics and Vibrations Group, Technische Universität Darmstadt, Germany

1 Introduction

Many technical systems contain parts that can be conveniently modeled as shells. Whereas their behavior is well investigated in the context of conservative loading, new phenomena arise if non-conservative loads are considered. This paper deals with shells subject to sliding friction. It turns out that sliding friction under certain circumstances can lead to self-excited vibrations that cause severe problems in many technical applications. The models dealing with rotating shells discussed in the paper explain the occurrence of barring in the process of paper calendering and also yield an explanation for the squealing of drum brakes. Very similar models dealing with moving frictional loads explain the famous phenomenon of singing wine glasses. Using perturbation theory for multiple eigenvalues in the context of FLOQUET theory [1] it is shown that multiple eigenfrequencies of shells make them particularly sensitive to self-excited vibrations [3]. This knowledge can be used as a constructive measure against self-excited vibrations. Using structural optimization shells are designed in such a way that multiple eigenfrequencies are avoided.

2 Mathematical model

We consider a shell in contact with an idealized friction pad which is pressed upon the shell by a spring as shown in figure 1. Two settings are investigated, first we consider a shell rotating at constant angular velocity and second we investigate a stationary shell in contact with a rotating pad. The equations for non-rotating shells are well known [2], interesting phenomena particularly arise due to rotation and friction forces. The geometry of the shell is described by two orthogonal curvilinear coordinates, i.e. a point M on the neutral surface with material coordinates ξ, η is described by

$$\mathbf{p}_0 = f_1(\xi, \eta, t)\mathbf{e}_x + f_2(\xi, \eta, t)\mathbf{e}_y + f_3(\xi, \eta, t)\mathbf{e}_z \quad (1)$$

in a global coordinate system where the explicit time dependence of the f_i originates from a prescribed motion of the undeformed shell. For a shell rotating about the \mathbf{e}_z axis at constant angular velocity Ω we can write

$$\mathbf{p}_0 = r(\xi, \eta) \cos(\Omega t + \eta)\mathbf{e}_x + r(\xi, \eta) \sin(\Omega t + \eta)\mathbf{e}_y + f_3(\xi, \eta)\mathbf{e}_z, \quad (2)$$

where we choose η to be an angle about the axis of rotation (c.f. figure 1), the coordinate ξ can be chosen as the z coordinate of the global coordinate system for example. If rotating shells or shells with moving loads are considered it can be beneficial to define non material coordinates α, ϕ with respect to artificial coordinate systems which in some cases can eliminate the explicit time dependence of the f_i in (2). It has to be noted however that when considering time derivatives the material coordinates have to be kept constant. In this paper we concentrate on shells which can be modeled by cylindrical coordinates. Three cases are of major interest in this paper and the relation of α, ϕ on ξ, η (c.f. figure 1) is stated accordingly

- a) rotating shell in nonrotating coordinates $\alpha = \xi, \phi = \eta + \Omega t$
- b) rotating shell in rotating coordinates $\alpha = \xi, \phi = \eta$
- c) nonrotating shell in rotating coordinates $\alpha = \xi, \phi = \eta - \Omega t$

We note that for the case of a rotationally symmetric shell $r(\alpha, \phi) = a$ is constant and $f_3(\alpha, \phi) = f_3(\alpha)$. The curvilinear coordinates define a local coordinate system given by

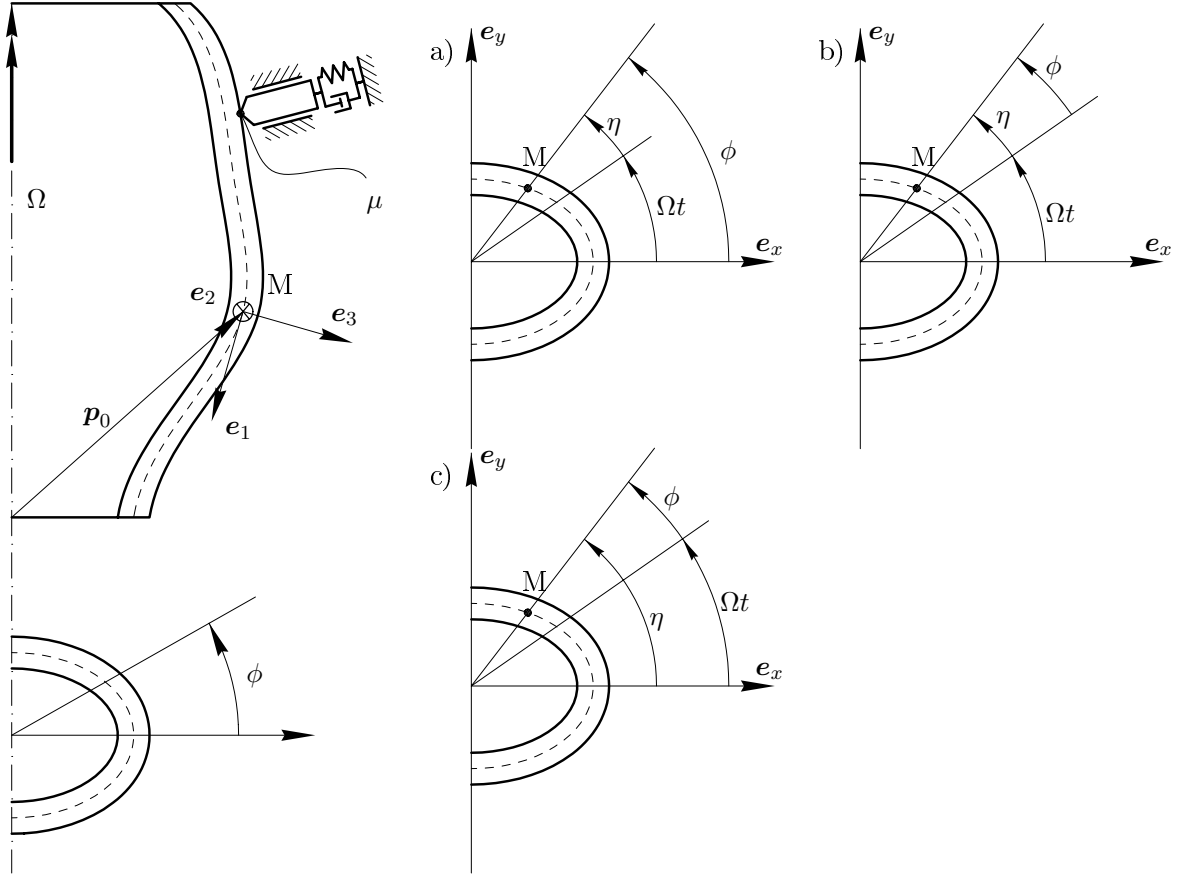


Figure 1: rotating frame in different reference frames

$$\mathbf{e}_1 = \frac{\mathbf{p}_{0,\alpha}}{\|\mathbf{p}_{0,\alpha}\|}, \quad \mathbf{e}_2 = \frac{\mathbf{p}_{0,\phi}}{\|\mathbf{p}_{0,\phi}\|}, \quad \mathbf{e}_3 = \mathbf{e}_1 \times \mathbf{e}_2. \quad (3)$$

We assume that points on the neutral surface of the shell have a degree of freedom in each direction of the corresponding local coordinate system, i.e. in the deformed configuration of the shell the position vector of a point on the neutral surface of the shell is given by

$$\mathbf{p}_M = \mathbf{p}_0 + u(\alpha, \phi, t)\mathbf{e}_1 + v(\alpha, \phi, t)\mathbf{e}_2 + w(\alpha, \phi, t)\mathbf{e}_3. \quad (4)$$

A point on the surface of the shell, which is needed to incorporate the contact forces into the equations of motion, is parameterized through a point on the neutral surface, i.e.

$$\mathbf{p}_P(\alpha, \phi, t) = \mathbf{p}_M(\alpha, \phi, t) + \frac{h}{2}\mathbf{e}_\nabla(\alpha, \phi, t), \quad (5)$$

$$\mathbf{e}_\nabla(\alpha, \phi, t) = \frac{\frac{\partial \mathbf{p}_M}{\partial \alpha} \times \frac{\partial \mathbf{p}_M}{\partial \phi}}{\left\| \frac{\partial \mathbf{p}_M}{\partial \alpha} \times \frac{\partial \mathbf{p}_M}{\partial \phi} \right\|}. \quad (6)$$

In order to obtain velocities of material points of the shell their corresponding position vectors have to be differentiated with respect to time with the material coordinates kept constant. The equations of motion can now be derived from the principle of virtual work employing classical stress and strain expressions from [2] and introducing the virtual work of the contact forces.

3 Interaction of symmetry and stability

For rotationally symmetric shells when neglecting in-plane displacements (i.e. $u(\alpha, \phi, t) = 0$, $v(\alpha, \phi, t) = 0$) and working with a coordinate system attached to the undeformed shell the equations

of motion obtained from a RITZ discretization can be brought into the form

$$M\ddot{\mathbf{q}} + \varepsilon\Delta\mathbf{D}(t)\dot{\mathbf{q}} + (\mathbf{K} + \varepsilon\Delta\mathbf{K}(t))\mathbf{q} = \mathbf{f}(t), \quad (7)$$

where $M = \text{diag}(1, 1, \dots, 1)$ and $\mathbf{K} = \text{diag}(\omega_1^2, \dots, \omega_N^2)$ correspond to the shell and $\Delta\mathbf{D}(t)$, $\Delta\mathbf{K}(t)$ originate from the contact forces. The matrices $\Delta\mathbf{D}(t) = \Delta\mathbf{D}(t + 2\pi)$, $\Delta\mathbf{K}(t) = \Delta\mathbf{K}(t + 2\pi)$ are periodic where without loss of generality we introduced a dimensionless time scale. The parameter $\varepsilon \ll 1$ can be interpreted as the magnitude of the contact forces. In figure 2 the stability and

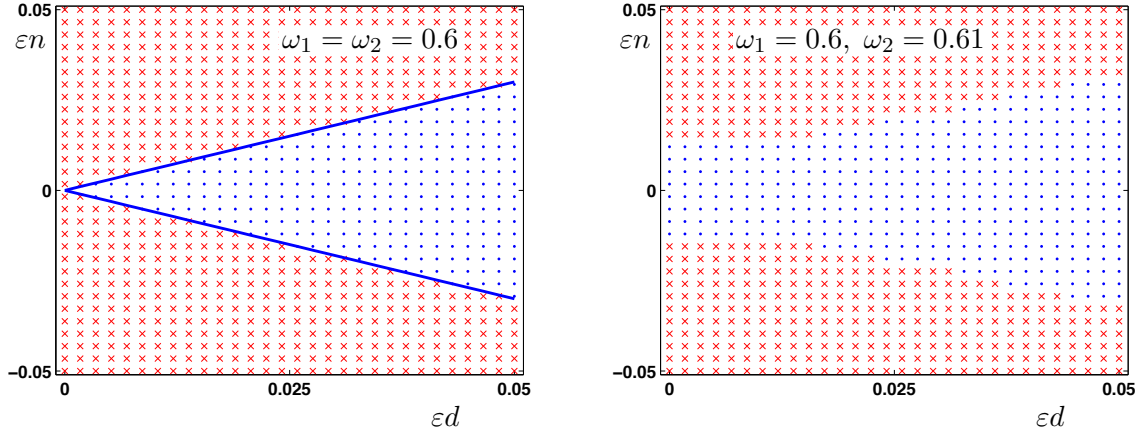


Figure 2: Stable regions for a symmetric and an asymmetric system (dot: stable, cross: unstable)

instability regions for the trivial solution of (7) in the parameter space are calculated using the matrices

$$\Delta\mathbf{D}(t) = d \cos^2 t \begin{bmatrix} 1 & 0 \\ 0 & 1 \end{bmatrix}, \quad \Delta\mathbf{K}(t) = n \cos^2 t \begin{bmatrix} 0 & -1 \\ 1 & 0 \end{bmatrix}, \quad \mathbf{K} = \begin{bmatrix} \omega_1^2 & 0 \\ 0 & \omega_2^2 \end{bmatrix}. \quad (8)$$

with a dissipative parameter d and a circulatory parameter n . It is seen that the stability region is significantly enlarged when the ω_1 and ω_2 are split up. This is also proved by analytically calculating the derivatives of the FLOQUET multipliers.

4 Conclusion

The stability behavior of shells loaded by friction forces is studied. The investigation of the equations of motion explains the occurrence of self-excited vibrations. An analytical understanding of the interaction of symmetry and stability of shells can be used for structural optimization to avoid self-excited vibrations and is in this paper considered in the context rotationally symmetric shells with negligible in-plane vibrations. A more general setting including in-plane vibrations is subject to future work.

References

- [1] Seyranian, A.P.; Mailybaev, A.A.: *Multiparameter Stability Theory with Mechanical Applications*, World Scientific, 2003.
- [2] Soedel, W.: *Vibrations of shells and plates*, Marcel Dekker, Inc. New York and Basel, 1981.
- [3] Spelsberg-Korspeter, G.: Breaking of symmetries for stabilization of rotating continua in frictional contact. *Journal of Sound and Vibration*. 322:798–807. 2009.

Simulation of Pyroshocks

Utz von Wagner, Nikolas Jüngel and Alexander Lacher

Department of Applied Mechanics, Technische Universität Berlin, Germany

1. Introduction

Pyroshocks are transient motions of structural elements due to explosive loading induced by the detonation of ordnance devices incorporated into or attached to the structure. In space programs the simulation of pyroshocks is a fixed part of the test requirement for instruments and equipment of space vehicles. Therefore, by the use of various test devices such as hammer pendulums, the excitation of a pyroshock has to be reproduced which, so far, has led to rather empirical knowledge. In the current work, a test set up containing a hammer pendulum and a rod or a plate is modeled in order to get a better predictability of pyroshock simulations. Numerical and analytical calculations are used for the simulation of in-plane wave propagation due to impact loading. Furthermore, the results obtained are compared with data received from conducted experiments.

2. The Shock Response Spectrum (SRS)

The properties of a pyroshock are usually given by the customer (using e.g. NASA standards) defining a frequency spectrum of the acceleration signal by the Shock Response Spectrum (SRS), the maximum acceleration and the duration of the shock signal. For calculating the SRS, an acceleration time signal is imagined to excite a damped one mass oscillator with a certain eigenfrequency. The resulting maximum acceleration amplitude in combination with the corresponding eigenfrequency leads to one point in the SRS diagram. The aim is to produce pyroshocks that show an SRS within a tolerance prescribed by the customer (Fig. 1).

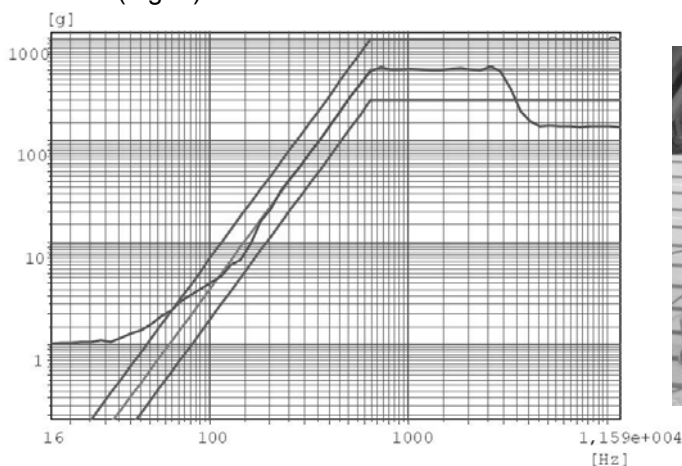


Fig. 1 Example of an SRS with tolerance lines

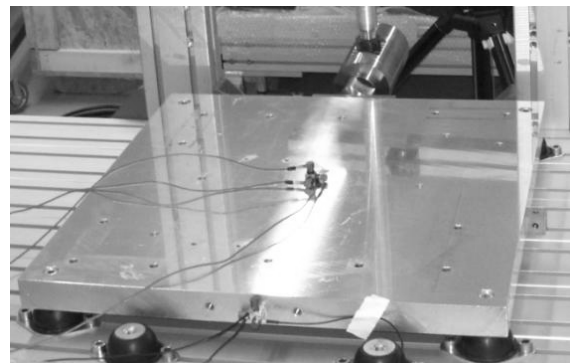


Fig. 2 Test Setup (aluminum plate with pendulum hammer)

3. Test Setup

Figure 2 shows a standard pyroshock test set up. An aluminum plate (1m x 1m x 3cm) is supported on soft pads in order to allow the free boundaries at the edges. The plate is excited by a pendulum hammer including a load cell. Velocity and acceleration data due to the impact are measured at the edges by using a laser-vibrometer or at arbitrary points of the plate by accelerometers using special fixing devices.

4. 1-D modeling and experimental results

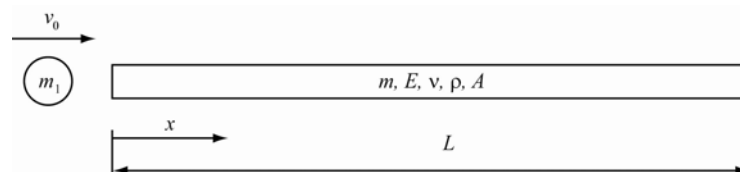


Fig. 3 One dimensional mechanical model

A one dimensional model of in-plane wave propagation excited from a hit of a sphere has been examined first (Fig. 3). The force due to the impact is calculated with the help of Hertzian contact theory while the resulting wave propagation can be described according to d'Alembert as described in [1].

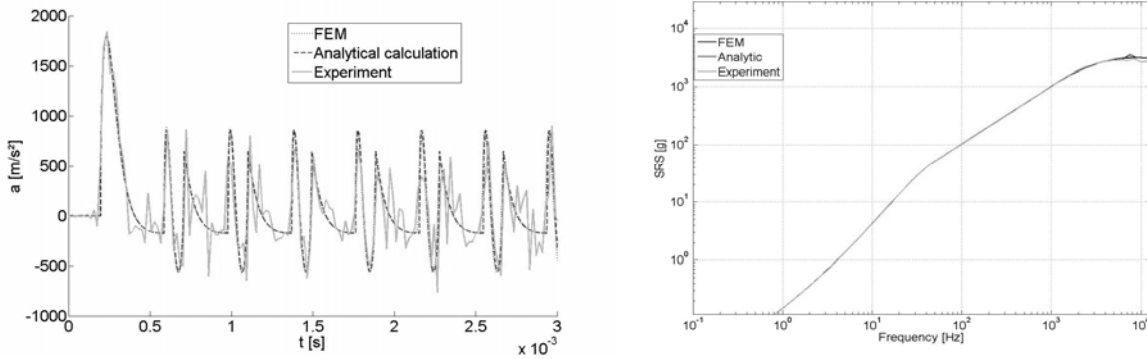


Fig. 4 Comparison of acceleration time signals (left) and SRS obtained (right) at $x = L$

Experiments conducted have been compared with both numerical, i.e. finite element, as well as the analytical results. Fig. 4 shows a very good agreement between measured and calculated accelerations at the end of the bar, while the SRS of all signals also coincide see Fig. 4.

5. 2-D modeling and experimental results

A more difficult task is to compute the in-plane acceleration of a certain point in a free rectangular disk due to impact loading. Therefore, an initial boundary value problem can be formulated in the x - y -plane of the disk with the coupled linear field equations

$$\frac{\rho}{C} \frac{\partial^2 u}{\partial t^2} - \frac{\partial^2 u}{\partial x^2} - \frac{(1-\nu)}{2} \frac{\partial^2 u}{\partial y^2} - \frac{(1+\nu)}{2} \frac{\partial^2 v}{\partial x \partial y} = \frac{1}{Ch} F(t) \delta(x+a) \delta(y) \quad (1)$$

$$\frac{\rho}{C} \frac{\partial^2 v}{\partial t^2} - \frac{(1-\nu)}{2} \frac{\partial^2 v}{\partial x^2} - \frac{\partial^2 v}{\partial y^2} - \frac{(1+\nu)}{2} \frac{\partial^2 u}{\partial x \partial y} = 0, \quad \text{with } C = \frac{E}{1-\nu^2}$$

where $u(x, y, t)$ and $v(x, y, t)$ are the displacement fields in x and y directions and ν, E, ρ describe Poisson's ratio, Young's modulus and the mass density respectively. F denotes the impact force measured (Fig. 5). The boundary conditions are given by

$$\frac{\partial u}{\partial x} + \nu \frac{\partial v}{\partial y} = 0 \text{ at } x = \pm a; \quad \frac{\partial v}{\partial y} + \nu \frac{\partial u}{\partial x} = 0 \text{ at } y = \pm b; \quad \frac{\partial u}{\partial y} + \frac{\partial v}{\partial x} = 0 \text{ at } x = \pm a \text{ and } y = \pm b \quad (2)$$

where a, b, h are half of the length and width of the disk as well as its thickness respectively. The eigenmodes of the disk are calculated analytically according to [2]. Using these as shape functions in a Galerkin procedure for calculating the excited vibrations leads to a simple decoupled system of time dependent differential equations based on (1) and (2) which can be solved by applying the initial conditions. The acceleration SRS signal obtained at any arbitrary point of the disk can then be used to compute the corresponding SRS.

For comparison, again a FE model was prepared using shell elements. The use of the measured force data (Fig. 5) as excitation leads to the desired time signal (see Fig. 6) within a reasonable amount of time. Due to the high wave speed and the large dimensions of the system ($a = b = 0.5m$) a high performance is needed. In Figures 6 and 7 a comparison of the results obtained from measurements, FEM and analytical solution is shown. Further experiments with different impact velocities of the hammer pendulum have been

conducted. Additionally, the accelerations at several different points on the edge of the disk were measured. The results of those experiments have shown comparable coincidences to the results in this paper.

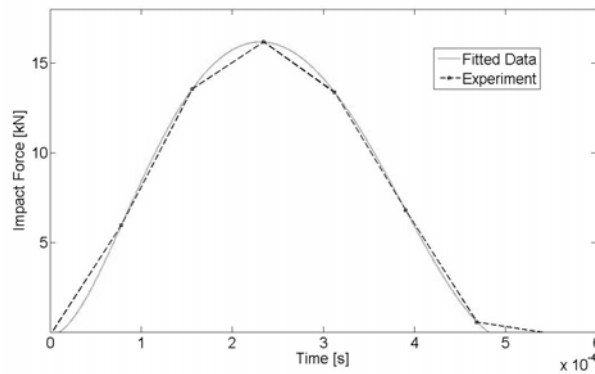


Fig. 5 Impact force measured

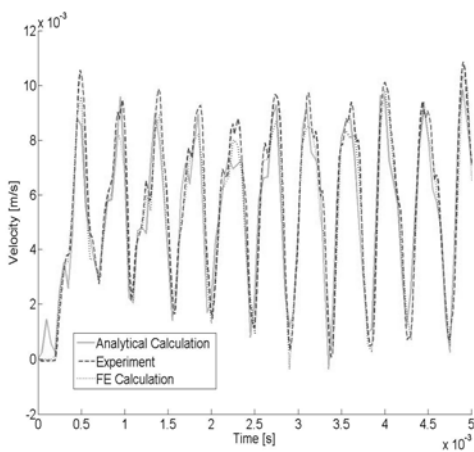


Fig. 6 Comparison of velocities at $x = a, y = 0$ obtained experimentally, by FEM and analytically

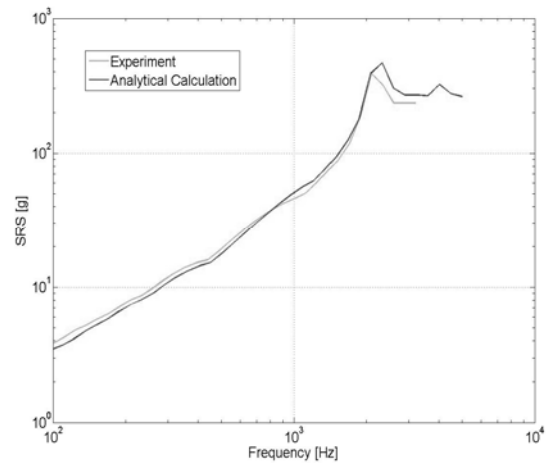


Fig. 7 Comparison SRS at $x = a, y = 0$ obtained experimentally, by FEM and analytically

6. Conclusions

A 1-D and a 2-D model for the simulation of pyroshocks are investigated respectively in order to obtain Shock Response Spectra. The in-plane wave propagation due to the impact between a rigid body and an unsupported beam or disk respectively can be described with the help of the Galerkin procedure as well as using the FEM. In both cases, all approaches show very good coincidence with respect to experimental results. In future, alternative excitation methods such as piezo actuators or electrodynamic shakers are to be investigated in order to achieve a better controllability and higher energy amount of the impact.

7. References

- [1] Hu, B., Schiehlen, W. and Eberhard, P.: Comparison of Analytical and Experimental Results for Longitudinal Impacts on Elastic Rods. *Journal of Vibration and Control* 9, 157-174, 2003.
- [2] Pelchen, C.: Schwingungen von Scheiben mit Eigenspannungen. *Diploma thesis* Universität Karlsruhe, 1987.

Dynamics of a 1-dimensional Wave Guide with Point-wise Defects

Jörg Wauer, Natalia Glushkova and Evgeny Glushkov

Institut für Technische Mechanik, Universität Karlsruhe (TH), Germany and

Institute for Mathematics, Mechanics and Informatics, Kuban State University, Krasnodar, Russia

Introduction

The first of the co-authors is very interested in the dynamics of circular ring structures with defects because he expects locally concentrated resonance phenomena. Since the vibrations of such a ring structure can be considered as waves propagating forward and backward and superposing to standing waves, i.e., vibrations, he basically is very interested to study the dynamics of non-homogeneous 1-dimensional wave guides and the appearing resonance effects, also known as trapped modes, wave blocking, etc. The work of Glushkov and Glushkova (see [1] and the references listed there, for instance) obviously provides a good basis to discuss the problem relying on a specific wave approach in semi-analytical form. Since the ring is governed by coupled wave equations, it seems to be the way to succeed is first to study the simplest preliminary problem, i.e., the dynamics of a straight infinite string with point-wise defects at one, two or more locations.

Formulation

Consider a straight infinite string $-\infty < x < \infty$ lying on a spring foundation (Fig. 1). Dynamic processes in the string are caused by a given incident force $p(x, t)$. The load gives rise to the transverse

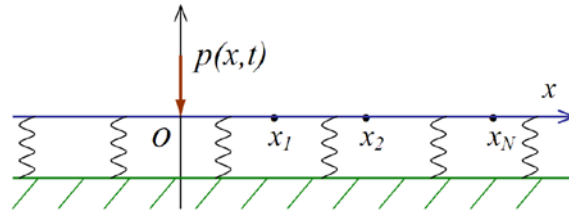


Figure 1: Layout of the 1-dimensional wave guide

string displacement $w(x, t)$ that obeys the governing partial differential equation

$$\rho A w_{,tt} + cw - S w_{,xx} = p(x, t) \quad (1)$$

with the homogeneous initial conditions $w(x, 0) = w_{,t}(x, 0) = 0$. Here ρ is string density, A is its cross-section area, c is the spring constant of the foundation, and S is axial pre-stress of the string, assumed to be constant.

It is assumed that this waveguide structure may have a set of defects modeled by the point-wise variation of the spring constant, c and/or the cross-section mass ρA :

$$c(x) = c_0 [1 + \sum_{j=1}^N \varepsilon_j \delta(x - x_j)], \quad \rho A(x) = \rho_0 A_0 [1 + \sum_{j=1}^N \alpha_j \delta(x - x_j)]. \quad (2)$$

N is a number of defects, x_j are points of defects' location. ε_j and α_j are dimensionless defects' characteristics; formally they vary in the limits

$$-1 < \varepsilon_j, \alpha_j < \infty;$$

with $\varepsilon_j = 0$ (or $\alpha_j = 0$) there is no any spring (or cross-section) defect at the point x_j .

For simplicity, the incident force is assumed to be a point load applied at the origin:

$$p(x, t) = p_0 \delta(x) f(t), \quad (3)$$

$f(t)$ is a time-shape function of the load. In the numerical examples below we will usually take it in the form of n -cycle sine burst:

$$f(t) = \begin{cases} \sin \omega c t, & 0 \leq t \leq nT, \\ 0, & t > nT \end{cases} \quad (4)$$

where $T = 2\pi/\omega_c$ is the sine period. With $n = 1/2$ this function describes also a half-period shock pulse of duration $T/2 = \pi/\omega_c$. The frequency spectrum of this time-function is

$$F(\omega) = -\frac{\omega_c}{\omega^2 - \omega_c^2}(1 - e^{2i\omega nT}). \quad (5)$$

The Fourier transform

$$\mathcal{F}_t[w(x, t)] \equiv \int_{-\infty}^{\infty} w(x, t)e^{i\omega t} dt \stackrel{Df}{=} w(x, \omega) \quad (6)$$

converts eq. (1) into the frequency domain equation

$$Sw_{,xx} + (\omega^2 \rho A - c)w = -p_0 F(\omega) \delta(x) \quad (7)$$

with respect to the frequency spectrum (or time-harmonic complex amplitude) $w(x, \omega)$ (it was assumed $w(x, t) \equiv 0$ for $t \leq 0$).

Using the inverse Fourier transform \mathcal{F}_t^{-1} the transient solution $w(x, t)$ may be represented in terms of its frequency spectrum $w(x, \omega)$:

$$w(x, t) = \mathcal{F}_t^{-1}[w(x, \omega)] \equiv \frac{1}{2\pi} \int_{-\infty}^{\infty} w(x, \omega) e^{-i\omega t} d\omega \equiv \frac{1}{\pi} \text{Re} \int_0^{\infty} w(x, \omega) e^{-i\omega t} d\omega. \quad (8)$$

In view of the general δ -function property

$$f(x)\delta(x - a) = f(a)\delta(x - a),$$

the δ -constituents in the equation coefficients induced by the defects (see (2)) may be replaced by the terms $w_j(\omega^2 \rho_0 A_0 \alpha_j - c_0 \varepsilon_j) \delta(x - x_j)$ with unknown constant factors $w_j = w(x_j)$. After transferring those terms into the right-hand side we arrive at the equation

$$Sw_{,xx} + (\omega^2 \rho_0 A_0 - c_0)w = -p_0 F(\omega) \delta(x) + \sum_{j=1}^N w_j (c_0 \varepsilon_j - \omega^2 \rho_0 A_0 \alpha_j) \delta(x - x_j) \quad (9)$$

To reduce the number of input parameters it is worth carrying out further calculations in a dimensionless form. After some calculation, we obtain the dimensionless equation

$$\bar{w}'' + k_0^2 \bar{w} = -\bar{p} \delta(\bar{x}) + \sum_{j=1}^N \bar{w}_j (\bar{c}^2 \varepsilon_j - \bar{\omega}^2 \alpha_j) \delta(\bar{x} - \bar{x}_j) \quad (10)$$

with

$$k_0^2 = \bar{\omega}^2 - \bar{c}^2 = \frac{h^2 \rho_0 A_0}{S} \omega^2 - \frac{h^2}{S} c_0, \quad \bar{p} = \frac{p_0 F(\omega) h}{S t_0}, \quad \bar{w}_j = \frac{w_j}{h t_0}$$

where h is a reference length and $t_0 = h\sqrt{\rho_0 A_0/S}$ a unit of time.

In fact, $\bar{w}(\bar{x}, \bar{\omega})$ is proportional to \bar{p} , which enters into the right-hand side of the initial equation as a constant factor. Thus, the load independent dynamic response of a string with defects (frequency-response characteristic) is the solution of equation

$$\bar{w}'' + k_0^2 \bar{w} = \delta(\bar{x}) + \sum_{j=1}^N \bar{w}_j (\bar{c}^2 \varepsilon_j - \bar{\omega}^2 \alpha_j) \delta(\bar{x} - \bar{x}_j) \quad (11)$$

which is a special case of (10) with $\bar{p} \equiv 1$.

In the following, the overline above the dimensionless quantities are generally omitted.

Solution

The function g within

$$g'' + k_0^2 g = \delta(x) \quad (12)$$

is a fundamental solution to eq. (11). From the variety of partial solutions to eq. (12) we conventionally choose that satisfying zero and wave radiation conditions at infinity:

$$g(x) = \frac{e^{ik_0|x|}}{2ik_0} \quad (13)$$

where with real ω

$$k_0 = \begin{cases} \sqrt{\omega^2 - c^2}, & \omega > c \\ i\sqrt{c^2 - \omega^2}, & |\omega| \leq c \\ -\sqrt{\omega^2 - c^2}, & \omega < -c \end{cases} . \quad (14)$$

The first of these inequalities provides propagation of undamped harmonic waves $e^{i(k_0|x| - \omega t)}$ from the source to infinity (Sommerfeld's radiation condition), while the second one implies zero behaviour at infinity ($g \rightarrow 0$ as $|x| \rightarrow \infty$, $|\omega| < c$). The third condition for $\omega < -c$ follows from the general property $g(\tilde{\omega}) = g^*(\omega)$ where $\tilde{\omega} = -\omega_1 + i\omega_2$ is the point symmetric to a point $\omega = \omega_1 + i\omega_2$ with respect to the imaginary axis $\text{Re } \omega = 0$ of the complex ω -plane. Any harmonic solution (frequency spectrum) $w(\omega)e^{-i\omega t}$ must obey this property to assure the corresponding transient solution $w(t)$ expressed in terms of the inverse Fourier transform (8) to be a real function. More precisely, it assures identity between the integrals in eq. (8).

To meet the condition (14), it is enough to fix the branches of square-root functions in $k_0 = \sqrt{\omega - c}\sqrt{\omega + c}$ so that $\sqrt{1} = 1$ and the cuts drawn in the complex ω -plane from the branch points $\pm c$ to infinity beneath the integration contour \mathcal{L}_ω in the inverse Fourier transform \mathcal{F}_t^{-1} .

Then, a general solution to eq. (11) may be written in the form

$$w(x, \omega) = g(x) + \sum_{j=1}^N w_j (c^2 \varepsilon_j - \omega^2 \alpha_j) g(x - x_j). \quad (15)$$

The generalized vector of unknown coefficients $\mathbf{w} = [w_1, w_2, \dots, w_N]^T$ are obtained from the linear algebraic system

$$A\mathbf{w} = \mathbf{g} \quad (16)$$

which results from the substitution w of form (15) into the N conditions $w(x_j) = w_j$, $j = 1, 2, \dots, N$. The matrix and the right-hand side of this system are

$$A = 2ik_0 I - B, \quad I \text{ is unitary matrix,} \quad B = [b_{ij}]_{i,j=1}^N, \quad b_{ij} = d_j e_{ij}, \\ d_j = c^2 \varepsilon_j - \omega^2 \alpha_j, \quad e_{ij} = e^{ik_0|x_i - x_j|}, \quad \mathbf{g} = [e_1, e_2, \dots, e_N]^T, \quad e_i = e^{ik_0|x_i|}.$$

Evaluation and Results

Essentially it is sufficient to discuss the dynamics in the frequency domain since all essential conclusions regarding resonance effects, etc. can be drawn. In detail, all results obtained up to now will be presented at the symposium. To give an idea, one result for the straight infinite string on elastic

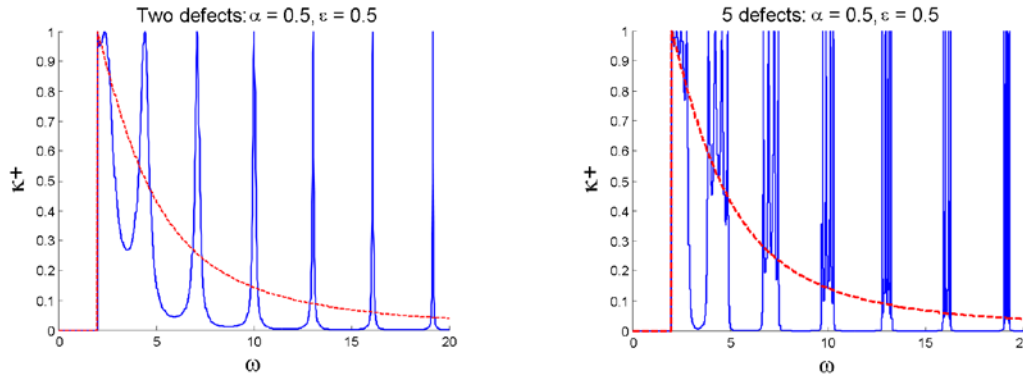


Figure 2: Wave transmission through systems of 1, 2 and 5 defects.

foundation with defects at one, two or five locations is shown in Fig. 2 where the transmission coefficient $\kappa^+ = |w(x^+, \omega)|^2 / |g(x^+, \omega)|^2$, $\omega > c$ for a specific defect situation is drawn. $x^+ > x_N$ is any point at the right-hand side of defects and this ratio shows how much the squared amplitude of the string oscillation behind the defects becomes less than the oscillation of the defect-free string.

References

1. Glushkov, E., and Glushkova, N., *Trapped Mode, Pass-band and Gap-band Effects in Elastic Wave Guide Structures with Single and Multiple Obstacles*, in: Proc. Int. Symp. on Vibrations of Continuous Systems, July 2009, Zakopane, Poland.

Accurate Free Flexural Analysis of a Cantilever Piezoelectric Plate Carrying a Rigid Mass

S. D. Yu

Department of Mechanical and Industrial Engineering, Ryerson University
350 Victoria Street, Toronto, Ontario, Canada M5B 2K3

Email: syu@ryerson.ca; Tel: (001) 416-979-5000 ext. 7687; Fax: (001) 416 979 5265

Abstract

In this paper, the method of superposition is employed to obtain an accurate analytical solution for free flexural vibration of a cantilever piezoelectric plate carrying a rigid mass.

1. Introduction

A class of vibrational energy harvesting devices operating in the {3-1} mode consists of a laminated structure with two identical piezoelectric layers separated by a shim material (bimorph). A large rigid mass is often attached to the free end of the piezoelectric structure to obtain a desired natural frequency for maximizing the electrical output for a base excitation frequency. The rigid mass is usually made of heavy material such as tungsten. The common shapes are block, L-shaped, U-shaped, etc. Figure shows a piezoelectric cantilever carrying a block rigid mass.

Many of the bimorph cantilever type energy harvesting devices are modeled as beams in the literature ([1]-[4]). This may be acceptable for certain piezoelectric cantilevers having large length to width ratios. However, often the aspect ratios of practical piezoelectric cantilevers are in the vicinity of unity. The assumption of cylindrical bending of such plate structures often over-predicts the natural frequency as the bending in the width direction is ignored. As a result, the theoretical predictions of the dynamic behaviors of the electro-mechanical system based on beam bending theories may not be accurate.

In this paper, the equation of transverse bending vibration of the piezoelectric structure and boundary conditions are derived in accordance with the classical plate theory. Small amplitude vibrations are assumed for both the structure and the mass. To obtain an analytical solution for free vibration of a piezoelectric plate subjected to the boundary and interface conditions, Gorman's method of superposition [5] is employed. A superposition strategy is developed to handle the solid-rigid interface conditions. Numerical results show that the proposed method is convergent and accurate.

2. Equations of Motion of the Piezoelectric Plate and the Rigid Mass

According to duToit et al. [3], the equation of motion for the piezoelectric structure may be obtained from the following Hamilton's principle

$$\int_{t_1}^{t_2} (\delta T - \delta V + \delta U + \delta W_e + \delta W_{nc}) dt = 0 \quad (1)$$

where T is the kinetic energy of the piezoelectric structure; V is the potential energy of the piezoelectric structure associated with lateral bending; U is the Rayleigh dissipation function; W_e is the electric energy (considered as the resistance load to the mechanical system); and W_{nc} is the work done by all external forces. Implementation of the classical plate theory and the electrical potential field yields the following equation of transverse bending vibration and the electrical charge balance equations for the electromechanical system mounted on a vibrating base

$$\bar{\rho} \ddot{w} + \bar{D} \left[\frac{\partial^4 w}{\partial x^4} + 2 \frac{\partial^4 w}{\partial x^2 \partial y^2} + \frac{\partial^4 w}{\partial y^4} \right] + \beta \bar{D} \left[\frac{\partial^4 \dot{w}}{\partial x^4} + 2 \frac{\partial^4 \dot{w}}{\partial x^2 \partial y^2} + \frac{\partial^4 \dot{w}}{\partial y^4} \right] + \gamma v \frac{\partial^2 R_{ab}(x, y)}{\partial x^2} \frac{\partial^2 w}{\partial x^2} = -\bar{\rho} \ddot{w}_b \quad (2)$$

$$\int_A \left\{ \gamma \frac{\partial^2 w}{\partial x^2} \right\} dA - 2c_0 v - q = 0 \quad (3)$$

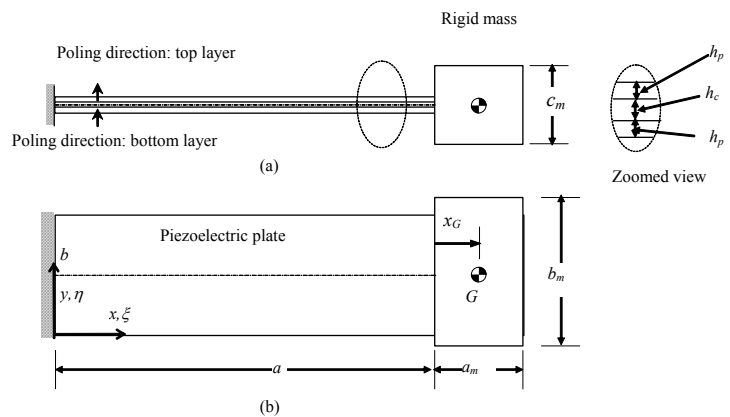


Figure 1 Sketch and dimensioning of a bimorph piezoelectric structure and a rigid mass: (a) front view, (b) top view

where w is plate lateral displacement; w_b is the lateral base motion; $\bar{D} = D_{11} = D_{22}$; $\bar{v} = D_{12} / D_{11}$
 $D_{ij} = \frac{1}{12} [c_{ij}^{(1)} (h^3 - h_s^3) + c_{ij}^{(2)} h_s^3]$, $i, j = 1, 2, 6$ $\gamma = e_{31}^{(1)} (h_p + h_s)$; $c_0 = \eta_{33} ab / h_p$; $R_{ab}(x, y)$ is a unit step function defined in
the rectangular region, $0 \leq x \leq a, 0 \leq y \leq b$; q is the charge; v is the voltage across each piezoelectric layer; $e_{31}^{(1)}$ is the
electro-mechanical coupling coefficient; η_{33} is the Dielectric constant; h_p is the thickness of each piezoelectric layer; h_s
is the thickness of the shim core.

The rigid mass attached to the cantilever piezoelectric structure for harvesting ambient mechanical energy is significantly
stiffer than the piezoelectric structure. The mass itself can be regarded as a rigid body. Because the in-plane rigidity of
the piezoelectric structure is significantly higher than its flexural rigidity, only the lateral displacement along the x_G -axis,
the rotation about the y_G -axis, and rotation about the x_G -axis need to be considered. The equations of (small amplitude)
motion of the rigid mass subjected to the distributed lateral reaction and the distributed bending moment along the
interface may be written as

$$m(\ddot{w}_b + \ddot{z}_a + a_o \ddot{\theta}_G) = -\int_0^b V_x dy, \quad I_x \ddot{\psi}_a = -\int_0^b V_x (y - \frac{b}{2}) dy, \quad I_y \ddot{\theta}_a = -\int_0^b M_x dy + \int_0^b V_x a_0 dy \quad (4)$$

where m is the mass of the rigid mass; I_x and I_y are the mass moments of inertia of the rigid mass about the x_G and y_G
axes, respectively; G refers to the mass centre of the rigid mass; a_0 is the axial coordinate of the mass centre of the rigid
mass with respect to the interface; z_a is the lateral displacement of the rigid mass at the midpoint of the interface; θ_a and
 ψ_a are the angles of rotations of the rigid mass about the x_G and y_G axes, respectively.

Within the context of the classical plate theory, the interactions between the piezoelectric structure and the rigid mass
along the interface are the distributed lateral force and the distributed bending moment. When deriving the equation of
the motion for the piezoelectric structure, these forces may be considered as the external forces and be incorporated into
the partial differential equation. However, such distributed lateral force and bending moment act on the boundary edge x
 $= a$, they can also be handled as the boundary constraints to the piezoelectric structure. The latter approach is adopted in
this paper. Along the clamped edge ($x = 0$), the relative lateral displacement and the slope taken normal to the edge are
zero. Along the two free edges ($y = 0, b$), the bending moment and the lateral edge reaction are zero. Finally, there are
two corner conditions at the extremities of the structure-mass interface, which need to be checked as the displacements at
the two locations are not prescribed.

The conditions across the structure-mass interface include the balance of forces and the continuity of displacements.
Since the force and moment balance is already implemented into the equations of motion for the rigid mass, one only
needs to ensure the following continuity of the lateral displacement and the slope taken normal to the interface

$$w|_{x=a} = z_a + (y - \frac{b}{2})\psi_a, \quad \frac{\partial w}{\partial x}|_{x=a} = \theta_a \quad (5)$$

The boundary conditions for a piezoelectric plate are similar to those for a regular plate. For a bimorph piezoelectric
plate in the {3-1} mode, the bending moment and the lateral edge reaction are given below

$$M_x = \bar{D} \left[\frac{\partial^2 w}{\partial x^2} + \bar{v} \frac{\partial^2 w}{\partial y^2} \right] + \gamma v R_{ab}(x, y), \quad V_x = -\bar{D} \frac{\partial}{\partial x} \left[\frac{\partial^2 w}{\partial x^2} + \bar{v} \frac{\partial^2 w}{\partial y^2} + \gamma v R_{ab}(x, y) \right] \quad (6)$$

3. Free Vibration of Cantilever Plate Carrying a Rigid Mass

It is useful to study first the free vibration of an undamped piezoelectric structure without considering the
electromechanical coupling. Dropping the terms associated with damping, electromechanical coupling and base motion,
the governing equation for free vibration is reduced to

$$\phi^2 \frac{\partial^4 W}{\partial \xi^4} + 2 \frac{\partial^4 W}{\partial \xi^2 \eta^2} + \phi^{-2} \frac{\partial^4 W}{\partial \eta^4} - \bar{\lambda}^4 W = 0 \quad (7)$$

where $\xi = x/a$, $\eta = y/b$, $\phi = b/a$, and $\bar{\lambda}^2 = \omega_n ab \sqrt{\rho / \bar{D}}$.

In the case of free vibration, the three governing equations for the rigid mass are

$$\int_0^1 \tilde{M}_\xi|_{\xi=1} d\eta + e \int_0^1 \tilde{V}_\xi|_{\xi=1} d\eta - i_y \bar{\lambda}^4 \Theta_a = 0, \quad \int_0^1 \tilde{V}_\xi|_{\xi=1} d\eta + \tilde{m} \bar{\lambda}^4 Z_a + e \tilde{m} \bar{\lambda}^4 \Theta_a = 0, \quad \int_0^1 \tilde{V}_\xi|_{\xi=1} (\eta - 0.5) d\eta + i_x \bar{\lambda}^4 \Psi_a = 0 \quad (8)$$

where $e = a_0 / a$, $\tilde{m} = m / \bar{\rho} ab \phi^2$, $i_x = I_x / \bar{\rho} b^4$, $i_y = I_y / \bar{\rho} ab^3$.

The cantilever piezoelectric structure carrying a proof mass has three ordinary edges (one clamped and two free) and one interface edge. Boundary conditions for the ordinary edges are well-defined. For the interface edge, it is assumed that the proof mass width is equal or greater than the plate width. This covers all piezoelectric designs available in the literature. Otherwise, one needs to deal with partial boundary conditions. Along the interface, we assume that the bonding (welding) is strong enough to withstand the force and moments transferred from the plate to the mass. As a result, continuity in the displacement and slopes across the structure-mass is satisfied. The following interface conditions are everywhere satisfied

To obtain an analytical solution for free lateral vibration of a cantilever plate carrying a rigid mass, four building blocks shown in Figure 2 are employed. The first three building blocks are designed to handle the clamped and free edges in the cantilever plate. The fourth building block is designed to handle the interface conditions between the plate and mass. It is noted that, because of the continuous displacement requirement across the interface, the solution for the plate-mass structure does not reduce itself to that for the cantilever plate even if the mass of the rigid mass becomes zero. However, the differences may be very small for certain modes, symmetric with respect to the plate major centerline because of the small straightening edge effect.

Each of the four building blocks has a driving edge and three non-driving edges. For a non-driving edge, the boundary conditions are either simple support (represented by a dashed line beside an edge) or slip-shear (represented by a pair of small circles at the middle of an edge). For a driving edge corresponding to a free edge in the original cantilever plate, the conditions are zero lateral edge reaction and prescribed slope of plate taken normal to the edge. For a driving edge corresponding to the clamped edge in the original cantilever plate, the boundary conditions are zero lateral displacement and prescribed bending moment. For the interface edge in the original plate, the conditions are the prescribed slope for continuous slope requirement and prescribed lateral edge reaction for vertical force balance. For each of the four building blocks employed, a Levy type solution can be obtained as there are two opposite edges with combinations of simply supported and slip-shear boundary conditions.

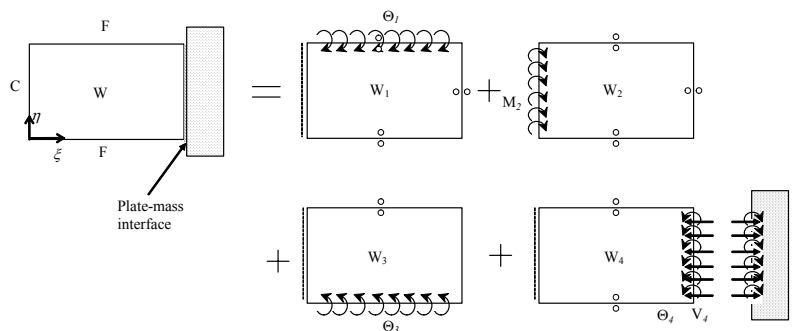


Figure 2 Building blocks employed for obtaining an analytical solution for a plate-mass system

4. Conclusions

An analytical solution for free flexural vibration of a piezoelectric cantilever carrying a rigid mass is obtained using Gorman's method of superposition. Comparisons with the previously published results indicate that the procedure presented in this paper is accurate and convergent for free vibration. The procedure is also extended to deal with the mechanical and electrical responses of the piezoelectric system due to harmonic base motion. The simulation results are found to be in excellent agreement with the experimental data.

References

- [1] S. Roundy, P. K. Wright, and J. M. Rabaey, Energy Scavenging for Wireless Sensor Networks with Special Focus on Vibrations, Kluwer Academic Publishers, New York, NY, 2003.
- [2] H. A. Sodano, D. J. Inman and G. Park, A review of power harvesting from vibration using piezoelectric materials, The Shock and Vibration Digest 36(3) (2004) 197–205.
- [3] N. E. duToit, B.L. Wardle, and S.-G. Kim, Design consideration for MEME-Scale Piezoelectric Mechanical Vibration Energy Harvesters, Integrated Ferroelectrics 71 (2005) 121-160.
- [4] S. R Anton and H. A. Sodano, A review of power harvesting using piezoelectric materials (2003–2006), Smart Mater. Struct. 16 (2007)1-21.
- [5] D. J. Gorman, The free vibration analysis of rectangular plates, Elsevier North Holland, Inc., N.Y., 1982.

Biographical Sketches of Participants

Eberhard W. Brommundt
Professor Emeritus
Institut für Dynamik und Schwingungen
Technische Universität Braunschweig, Germany

After an apprenticeship as a mechanic with German Railways I got an education as a mechanical engineer at the Mannheim Polytechnic. Working in the group of strength and vibrations in the department of steam turbine design of Brown, Boveri & Cie, Mannheim, I realized insufficient knowledge of Mathematics and Mechanics. Thus, I studied these fields at Technical University Darmstadt and got a diploma in mathematics.

As research assistant at the Institute of Mechanics and Vibrations of TU Darmstadt I worked mainly on linear and nonlinear vibrations, got my PhD and Habilitation in these fields. I became a docent of mechanics, and spent one year as Visiting Assistant Professor at the Department of Aerospace Engineering and Mechanics, University of Minneapolis, Minnesota.

From 1970 till 2000 I worked as professor of mechanics of the Institute of Technical Mechanics in the Department of Mechanical Engineering of Technical University Braunschweig. Research topics: Basic and applied problems from dynamics, linear and nonlinear oscillations, stability of motion, mechanisms of self-excitation. The areas of application comprise, e.g., rotor dynamics, rail-wheel dynamics, stability of fluid centrifugals, drill-string dynamics.

As Professor Emeritus I still like to ponder about intricate technical problems, although the rate of efficiency is low, and detecting the own flaws and errors is rather tedious, gardening does not really help, cycling a bit more.

Biosketch of Erasmo Carrera

After earning two degrees (Aeronautics, 1986 and Aerospace Engineering, 1988) in the Politecnico di Torino, Carrera received his PhD in Aerospace Engineering in 1991, at the Politecnico di Milano – Politecnico di Torino – Universit di Pisa. He began working as a Researcher at the Dep of Aerospace of Politecnico di Torino in 1992 holding courses on Missiles and Aerospace Struc Design, Plates and Shells, FEM and since 2000 is associate Prof of Aerospace Structures and Aeroelasticity. He visited twice the Institute fuer Statik und Dynamik, Universitaet Stuttgart, the first time as a PhD student (6 months in 1991) and then as visiting Scientist under GKKS Grant (18 months in 1995-96). In the Summer of '96 he was Visiting Prof at ESM Dept of Virginia Tech. In the 2004 he has also been visiting prof for two mounths at SUPMECA, Paris. His main research topics are: composite materials, FEM, plates and shells, postbuckling and stability, smart structures, thermal stress, aeroelasticity, multibody dynamics, non classical lifting systems and Multifield Problems. On these topics dr Carrera has bring significant contributions. In particular he has proposed the Carrera Unified Formulations to developed hierarchical plate/shell theories and Finite Elements for multilayered structures analysis as well as the generalization of classical and advanced variational methods for multifield problems. Carrera has been responsible of various research contracts with EU and national and international agencies/industries. He has been appointed for various Academic responsibility. Presently Carrera is deputy director of his Dep. He his an author of more than one hundred articles, many of which have been published in international journals. He serves as a referee for many journals such as J of Appl Mech, AIAA J, J Sound Vibr, Int J Sol and Str, Int J Num Meth Eng, and as contributing editor for Mech of Adv Mat and Str. He has served the Ed. Board of many int. conferences.

Li-Qun Chen

Graduating with the B. Sc. degree in Mechanical Engineering from Anshan University of Science and Technology (Anshan, Liaoning, China) in 1984. I worked there as a teaching assistant until 1986. I taught mechanics for students majoring in engineering and did some research on analytical dynamics. From 1986 to 1989, I was a graduate student in Northeastern University (Shangyang, Liaoning, China). My thesis is on chaotic behaviors of a few typical nonlinear oscillators. After receiving the M. Sc. Degree, I returned AUST where I was promoted to Instructor in 1990 and Associate Professor in 1992.

Leaving AUST in 1995, I investigated controlling chaos in Shanghai Jiao Tong University until I was awarded the Ph. D. degree in Mechanics in 1997.

From 1997 to 1999, I was a postdoctoral fellow in Shanghai Institute of Applied Mathematics and Mechanics, working on chaotic vibration of viscoelastic structures and its control.

I joined Department of Mechanics, Shanghai University as Professor in 1999 and hold the position until now. My main research interests are control and synchronization of chaos, dynamics and control of spacecraft, and vibration of continuous systems especially transverse vibration of axially moving materials and vibration of continua under nonlinear boundary conditions.

On leave of Shanghai University, I once served as Research Associate, Visiting Scholar, Research Fellow or Visiting Professor in University of Toronto (2 times), University of California at San Diego, and City University of Hong Kong (3 times).

I am married to Qi Hong, have a daughter who is a university student now. My personal hobbies include reading, traveling, badminton, and cooking.

Piotr Cupiał

I graduated in 1987 in the field of applied and computational mechanics. Still as a student I began work at the Institute of Physics of the Cracow University of Technology. After three years I moved to the Institute of Mechanics and Machine Design (now the Institute of Applied Mechanics). In 1997 I obtained my PhD from the Cracow University of Technology in the field of the application of damping polymers in the vibration suppression of composite structures.

Recently, my main research activities have concentrated on the vibration analysis and control of electromechanical systems, particularly of piezoelectric- and smart structures. In 2008 I published a monograph "Coupled electromechanical problems for piezoelectric distributed-parameter systems". This research should allow me to obtain soon the title of "habilitated doctor" (similar to the DSc degree) (the habilitation colloquium is scheduled to take place in June).

In 1991 I spent three months at Universite de Technologie de Compiègne (France), within the European Union program TEMPUS, working on experimental modal analysis of large structures. During the years 1998-2001 I spent three years at the European Organization for Nuclear Research (CERN) in Geneva. For one year, starting in October 2000, I was awarded an appointment as scientific associate at CERN, a position granted to "researchers with established position in their field". At CERN I worked on the finite element analysis and dynamic measurements in connection with the Large Hadron Collider (LHC) and the four particle physics experiments to start there soon.

In 1990 I was secretary of the IX International Conference on Non-Linear Oscillations (ICNO'90) held in Cracow. Since 2007 I have been acting on the editorial board of Journal of Sound and Vibration. I am glad that the 7th International Symposium on Vibrations of Continuous Systems takes place in Zakopane, and that I can act as local arrangements chairman.

In my free time I enjoy listening to various kinds of music and reading history books. I have always liked the mountains a lot, hiking in the summer and skiing in winter. I am married to Gabriela and have one son who is four and a half years old.

Stuart M. Dickinson

**Professor Emeritus
The University of Western Ontario
London, Ontario, Canada**

The above served an engineering apprenticeship with Ford Motor Company, Dagenham, UK, before attending the University of Nottingham, where he obtained both his B.Sc. and Ph.D. in Mechanical Engineering. After spending three years as a lecturer at the University of Liverpool, he immigrated to Canada in 1969 to take up a faculty position at The University of Western Ontario, becoming Professor Emeritus upon his early retirement in 1997. Whilst at Western, he had the opportunity of spending sabbatical leaves at the Institute of Sound and Vibration Research, Southampton, UK, the University of Canterbury, Christchurch, New Zealand, and Monash University, Melbourne, Australia.

His research interests have mainly been in the vibration of beams, plates and shells, with brief excursions into acoustics. He enjoyed working with one or two graduate students at a time and found their contributions to his research invaluable. Most of the research was of a theoretical or numerical nature, primarily employing "classical" approaches, although some experimental work was conducted and, in the early years, some work was done on the development of finite element methods.

His recreational interests, shared with his wife Rosemary, include curling, badminton and dinghy sailing. He also plays the euphonium, though not very well, and participates in a concert band program run at the university.

Stanley B. Dong

University of California at Los Angeles

My entire college education occurred at the University of California at Berkeley, where I began in 1953 and completed in 1962 in the Department of Civil Engineering. I was quite fortunate to have Karl Pister as my advisor upon entering in my freshmen year. He remained my advisor throughout and was my doctoral dissertation supervisor, which dealt with various aspects of anisotropic mechanics with a primary emphasis on laminated anisotropic shells and plates.

After receiving my degree in 1962, I worked at Aerojet-General Corporation in Sacramento, California, with primary duties concerned with the analysis of filament-wound pressure vessels to be used as rocket motor cases in Polaris/Poseidon missiles. I was extremely fortunate to have some very distinguished co-workers, Leonard Herrmann and Edward Wilson. Our interactions (or more accurately, their tutelage) enabled me to learn to code in FORTRAN, and it was at Aerojet-General that I was able to develop my first finite element code for the analysis of laminated composite shells of revolution under axisymmetric loading. To mention that we worked on an IBM 7094 with 32K memory is a stark reminder of the digital Neanderthal period.

In 1965, I joined the faculty at UCLA in the then Engineering College, where I have since remained. This College (with only one department) was a brainchild of our late founding Dean L.M.K. Boelter, who was known for the *unified curriculum*. In 1970, the Engineering College was re-organized as the School of Engineering and Applied Science with seven departments based on technical disciplines rather than the conventional monikers of civil, mechanical, electrical, etc. In 1982, because of the confusion between these discipline names with the conventional departmental names, the School of Engineering and Applied Science regrouped itself into conventional departments. I was first affiliated with the Mechanics and Structures Dept., where I served as its Chair from 1973-76, and then with Civil and Environmental Engineering Dept., where I served another stretch as Chair from 1989-92. In 1994, the UC System offered an unusual and lucrative early retirement plan, which I (and about 10% of the entire UC faculty) opted for, and thus earning my present title as Professor Emeritus. My days in retirement have enabled me to pursue various topics at leisure.

Moshe Eisenberger

Faculty of Civil and Environmental Engineering

Technion – Israel Institute of Technology

Technion City, 32000, Israel

e-mail: cvrmosh@technion.ac.il

I got my B.Sc. at the Technion, Haifa, Israel (1977), and Stanford, California, USA (M.Sc., 1978, and Ph.D., 1980), all in Civil Engineering. Following the completion of my studies I received a tenure track appointment at the Technion. Since then I am at the same department with sabbatical leaves in Carnegie Mellon, USA, (1987-9, 1993-4) and City University of Hong Kong (2006).

My professional interests have shifted within the broad discipline of computational mechanics: in the early 80's, at the beginning of the PC era I was mostly involved in structural analysis and computer methods for frames and finite elements calculations. Then I became more interested in stability and vibration analysis of continuous systems, starting with rods and beams with variable cross section, and moving to plates and shells with variable thickness, made of isotropic, composite, and functionally graded materials. All the analyses were made using the dynamic stiffness method and thus produced exact results, which have since served as benchmark values for comparison by other researches that developed various computational methods.

I am married to Dorit and have two children, Gilad and Yarden, and all have been with me in some of the previous ISVCS meetings. For many years I have been biking (mostly road), and hiking and climbing mountains. Two years ago I had a biking accident, my own mistake, and broke my collar bone into 4 pieces. A relatively large titanium fixing repaired it completely – and very shortly after the surgery I was back on my bikes. The human body design – relatively weak collar bone that will protect the shoulder from damage in case of injury, worked perfectly in my case!

Mark S. Ewing
University of Kansas

I grew up interested in science and mathematics, largely due to my fascination with the spacecraft I used to watch as they were launched from nearby Cape Canaveral. I was “energized” for science when I attended a National Science Foundation summer school at Rollins College in the summer of 1966. The next year, I was energized for engineering when I attended the JETS summer program at the University of Illinois. In 1972, I received my BS in Engineering Mechanics from the U.S. Air Force Academy, then began a 20-year career in the Air Force. I served for four years in turbine engine stress and durability analysis where I was an “early” user of finite element analysis for hot, rotating turbomachinery. I then served a two-year assignment in turbine engine maintenance and support, which was less technical, but eye-opening. During these early years—and in my spare time—I earned an MS in Mechanical Engineering from Ohio State University.

With an MS in hand, I returned to the Air Force Academy to serve on the faculty as an Assistant Professor. After two years, I returned to Ohio State to complete a PhD. As a student of Art Leissa’s, I focused on the combined bending, torsion and axial vibrations of beams, thereby establishing my interest in the vibrations of continuous systems.

After returning to and teaching at the Air Force Academy for six years, I was assigned to the Air Force Flight Dynamics Lab, where I worked on two interesting projects. The first was the development of a structural design algorithm capable of, among other things, “maximizing” the separation of two natural frequencies in a built-up structure. The utility of this endeavor was to allow the design of aircraft wings for which the bending and torsional natural frequencies are sufficiently separated (in frequency) to avoid flutter. The other interesting project was the analysis of the effect of convected aerodynamic loads on a missile.

I am now on the Aerospace Engineering faculty at the University of Kansas. My current research interests are in structural dynamics and structural acoustics, the latter of which is a topic of increasing interest to aircraft manufacturers. In recent years, I have focused on the ability to analyze, design and measure structural damping for built-up fuselage structures. All of the test articles I’ve used to validate my work through experimentation are simple structural elements, namely beams and plates.

I have a great love of the outdoors, and of the mountains in particular. When Art Leissa asked me to help organize the first International Symposium on Vibrations of Continuous Systems, and he told me he wanted to meet in the mountains, I was really excited. I look forward to attending the Symposium this year after missing the last three.

Evgeny Glushkov

Institute for Mathematics, Mechanics and Informatics
Kuban State University, Krasnodar, Russia

After the graduation from the Mechanics and Mathematics Department of the Rostov State University (RSU) in 1975, I continued my research in the Wave Processes group of the Institute for Mechanics and Applied Mathematics, RSU, having defended my Kand. Sc. (PhD) thesis in 1978. At that time the group dealt mostly with the problems coming from geophysics and vibroseismic prospecting. In 1982 I was suggested to relocate 300 km south for establishing and leading similar wave dynamics group at the Kuban State University, Krasnodar. Hence, we (together with Dr. Sc. **Natalia Glushkova**, with whom we have been working jointly as a family team) are disciples of the so-called South-Russian school of mechanics and applied mathematics. In accordance with its spirit we have been elaborating computer models basing on a thorough preliminary analytical study that involves such tools as integral transforms, complex variables, asymptotic analysis, residual technique, etc.

In the 1980s we were focused on the development of analytically-based methods for the dynamic contact problem solution and Green's matrix calculation in the cases of elastic multilayered, functionally-gradient and arbitrarily anisotropic media; on the calculation of wave energy fluxes emitted by harmonic sources into elastic structures; on obtaining the orders and eigenforms of 3D stress singularities at the top of polyhedral corners, wedge-shaped cracks and contact areas. Those results have been summarised in the second, Dr. Sc. (Habilitation) dissertation defended in the Leningrad State University in 1988.

In spite of the financial collapse of 1990s, we managed to keep researching owing to the development of international cooperation. Since that time we have established close links with our colleagues in Europe and the USA, took part in international projects and won research and visiting grants. Among them, we have appreciably benefited from the collaboration with the colleagues from Chalmers University of Technology, Sweden (NDE modelling), Forschungszentrum Karlsruhe, Germany (3D stress singularity), Kaiserslautern and Karlsruhe Universities (piezo-electrically based devices and smart structures), and others.

In general, our interests touch upon the development and computer implementation of mathematical models for dynamic systems and structures, as well as in search for new nice effects and phenomena. We also like very much when our numerical results coincide with experimental measurements and, even more, when they explain the latter.

Currently we deal with smart structures and damaged composite materials (anisotropic laminates), with the diffraction problems relating to NDE and SHM, with cylindrical laminate borehole waveguides in porous-elastic stratum, with resonance trapped-mode, gap-band and pass-band effects.

Along with research I like history and historical literature. Since Natalia and I have met during a mountain hike over Caucasus, we like hiking with rucksacks and tent. Every year we try to spend several summer weeks in hiking or in the wild tent camp still existing on the Black Sea beach not far from our city. While travelling I enjoy photographing and have already collected a bulk of pictures, when Natalia is keen on collecting mushrooms, berries and medicinal herbs.

Peter Hagedorn
Technische Universität Darmstadt

I received most of my education in Sao Paulo, Brazil, where I obtained a degree in mechanical engineering and later a doctor's degree (in 1966) at the Escola Politecnica da Universidade de Sao Paulo. Later I did my 'Habilitation' (similar to a D.Sc. degree) at Karlsruhe in Germany. My main professional interests are vibrations and stability of discrete and continuous systems (such as beams, plates and cables), and vibration control. While my early work was more analytical (e.g. the converse of the Lagrange-Dirichlet theorem, differential games, etc.), during the last 30 years I have worked more and more also with problems related to industrial applications, including experimental work, the emphasis however usually being on producing practical mathematical models.

Recently I have been working with piezoelectric ultrasonic travelling wave motors, wind excited vibrations of overhead transmission lines (including cfd calculations), and with the dynamics and active noise control in disk brakes. I am the author of several books on linear and nonlinear vibrations as well as a three volume German textbook on elementary statics, strength of materials and dynamics. I have also organized several workshops dealing with the question of how we should teach engineering mechanics to our students today.

I have been a visiting professor and research fellow at Stanford, Berkeley, Paris, Irbid (Jordan), Rio de Janeiro and Christchurch (New Zealand). At the University of Canterbury at Christchurch, New Zealand, I also hold the position of an Adjunct Professor, and we usually spend about a month there every year (also seeing the family and enjoying the grandchildren). My personal hobbies are travelling, reading, photography and hiking (mainly day hikes).

Hartmut Hetzler

Institut für Technische Mechanik, Universität Karlsruhe (TH), Karlsruhe, Germany
Karlsruhe Institute of Technology

I was born on 11 January, 1977 in Heidelberg (Germany). After finishing high-school (Gymnasium) in 1996 and passing 10 months of compulsory military service, I studied mechanical engineering from 10/1997 to 03/2003, focusing on applied mechanics and control. I received my diploma (Dipl.-Ing.) in 03/2003.

From 03/2003 to 03/2008 I was research assistant at the Institute of Engineering Mechanics with Professor Seemann. In January 2008 I received the doctor's degree with my dissertation on self-excited vibrations due to friction in systems of moving elastic bodies with application to brake squeal ("Zur Stabilität von Systemen bewegter Kontinua mit Reibkontakten am Beispiel des Bremsenquietschens").

After a short period as post-doc, I got a so called "shared KIT-Industry Fellowship", which means that I am holding a position that is co-financed by Robert Bosch GmbH and the KIT (Karlsruhe Institute of Technology, i.e. the fusion of Karlsruhe University and the Research Center Karlsruhe). Within this cooperation, I'm partially working at the Central Research of Bosch as well as at the Institute of Engineering Mechanics. Furthermore, I'm supervising two PhD-students, one at each place.

The working field of the group is "Multibody Systems with Tribological Contacts", where the focus is set on modelling and simulation of multifield-problems arising from lubricated contacts in multi-body environments.

Daniel Hochlenert

Dynamics and Vibrations Group, Technische Universität Darmstadt

I was born on March 21st 1978 in Frankfurt am Main, Germany.

In 1997 I finished high-school (Abitur) and did civilian service for 13 months. In October 1998 I started the studies of industrial engineering / mechanical engineering at Darmstadt University of Technology.

After finishing my preliminary diploma in 2001 I switched to the studies of applied mechanics with the main focus on dynamics. I continued my studies in the fall semester 2001 and the spring semester 2002 at the University of California at Berkeley.

In Juli 2003 I started as a Ph.D. student at Darmstadt University of Technology in the group of Professor Hagedorn. In October 2006 I finished my dissertation with the title „Self-excited vibration in disk brakes: mathematical modeling and active suppression of disk brake squeal“.

My hobbies are cycling (road and mountain bike), skat and cooking.

Chiung-Shiann Huang
National Chiao Tung University

Chiung-Shiann Huang's current position is a Professor in the Department of Civil Engineering, National Chiao Tung University, Taiwan. He received his Ph. D in 1991 at the Department of Engineering Mechanics at the Ohio State University. After that, he spent nine months as a postdoctoral research associate in the Department of Civil Engineering at the Ohio State University. The doctoral and postdoctoral research dealt with the use of singular corner stress functions to permit accurate solutions for free vibration frequencies of thin plates having sharp corners.

In 1992, he went back Taiwan and joined the research staff at the National Center for Research on Earthquake Engineering (NCREE). In addition to continue his serious interests on computational mechanics, he began to study the system identification of structures from monitoring earthquake responses of structures and the responses from various tests in field, such as ambient vibration test and forced vibration test.

After having stayed in NCREE for nine years, he joined the faculty of the Civil Engineering Department at National Chiao Tung University in 2000. His current main interests are vibrations of plates with stress singularities and system identification for structures using time series, neural network, and wavelet transform.

James R. Hutchinson

Jim was born in San Francisco Ca. He graduated from Stanford University with a BS in Mechanical Engineering in 1954. Upon graduation he went to work for Westinghouse's Atomic Power Division in Pittsburgh Pa. While working at Westinghouse he earned his masters in Mathematics in 1958. He then went to work for Lockheed Missiles and Space Division in Palo Alto Ca. While working at Lockheed he went back to Stanford as a part time student, earning his Ph.D. in Engineering Mechanics in 1963. He stayed on at Lockheed for another year before taking an academic position at the University of California, Davis. He was at Davis until his retirement January 1 1993.

His interest in vibrations began while he was working at Lockheed. His primary responsibility at Lockheed was in missile vibrations. When he arrived at Davis he was asked to teach the graduate course in Mechanical Vibrations. Many of his students were from Agricultural Engineering. They were interested in shaking fruit and nuts from trees. Of course, the solution methods were the same whether the vibrating body was a missile or a tree, and a number of cooperative projects took place on the study of tree vibrations. His early interest in continuum vibration also had its roots in missile applications.

Jim loves to sing and was very active in the Davis Comic Opera Company that mainly produced the works of Gilbert and Sullivan. He is still singing with the University Chorus. Last Spring he had the privilege of singing Brahms' "Ein Deutsches Requiem" and this Spring Mendelssohn's "Elijah". Jim is also a home-brewer and has dabbled in photography, stained glass, auto mechanics, and lately web design.

He does volunteer work with Citizens Who Care (a local non-profit agency dedicated to helping the elderly), and is presently president of the board of directors of that organization He has become an avid golfer but still enjoys doing some research on topics of his own choosing.

Jim and his wife Pat moved into a retirement community last year. Jim enjoys the lack of yard work and Pat enjoys not having to cook dinner. So, it is working out great.

Sinniah Ilanko
The University of Waikato
Te Whare Wananga o Waikato

e-mail: <Ilanko@Waikato.ac.nz>
www URLs: <<http://sci.waikato.ac.nz/staff/engg/ilanko>>
<<http://www.geocities.com/ilanko/vibration.htm>>
<<http://www.geocities.com/ilanko/eng.html>>

Ilanko was born in the north of Sri Lanka (Jaffna) in 1957, and according to the common Tamil practice, he does not have/use a family name. Ilanko is his given name and Sinniah is his late father's given name.

He graduated from the University of Manchester (U.K) with a BSc in civil engineering and also obtained an MSc from the same university under the supervision of Dr S.C. Tillman. His move to England at an early age was the result of his late brother Senthinathan's foresight on the Sri Lankan political situation. After working as an assistant lecturer at the University of Peradeniya in Sri Lanka for about two years, he commenced doctoral studies at the University of Western Ontario under the supervision of Professor S.M. Dickinson. Soon after completing his PhD, he worked as a postdoctoral fellow at the UWO for about six months until he joined the University of Canterbury in 1986. He continued his academic career at Canterbury for nearly 20 years, in various positions, as lecturer, senior lecturer and associate professor until he joined the University of Waikato in 2006. He has also served as the Head of Mechanical Engineering Department at Canterbury for a year (2001-2002) and worked as a visiting professor at the Annamalai University (India) and Technical University of Hamburg-Harburg during his study leaves. In 1997, he was awarded the Erskine Fellowship and visited several universities in Australia, Canada, Singapore and the U.K.

His research areas include vibration and stability of continuous systems, numerical modelling and adaptive mechanisms. Since January 2009, he is serving as the Subject Editor for Journal of Sound and Vibration, for analytical methods for linear vibration.

He is also interested in computer-aided learning and has developed and used several interactive lectures and tutorials for teaching Mechanics of Materials and Vibration, as well as computer tutorials and games for learning/teaching Tamil language. He maintains a "vibration resources homepage" (see the second URL above), which at present contains some interactive simulation programs for calculating natural frequencies and modes of some structural elements.

He is married to Krshnanandi and they have two daughters, Kavitha and Tehnuka. Ilanko's birth family is scattered across the globe (Australia, Canada, New Zealand, the U.K. and the U.S.A.) because of the civil war in Sri Lanka.

David Kennedy
Reader in Structural Engineering
Cardiff School of Engineering, Cardiff University, United Kingdom

David Kennedy obtained a First Class Honours degree at the University of Cambridge in 1978 and a PhD in the area of efficient transcendental eigenvalue computation from the University of Wales, Cardiff in 1994.

From 1978 to 1983 he was employed as an Analyst/Programmer for the computer services company Scicon Ltd, where he worked on the development of the Mathematical Programming software SCICONIC/VM. In 1981 he was awarded a 2-year BP Venture Research Fellowship in Non-linear Optimization, supervised by the late Professor Martin Beale.

In 1983 he was appointed as a Research Associate in the University of Wales Institute of Science and Technology, which was merged into Cardiff University in 1988. Working under the supervision of Professor Fred Williams and funded under a collaborative agreement with NASA, he coordinated the development of the space frame analysis software BUNVIS-RG which was released by NASA to US users in 1986/87. Further collaboration with NASA and British Aerospace (now BAE Systems) led to the development and successive releases, starting in 1990/91, of VICONOPT, a buckling and vibration analysis and optimum design program for prismatic plate assemblies. Both of these programs use analysis methods based on the Wittrick-Williams algorithm.

He was appointed to a Lectureship in the Cardiff School of Engineering in 1991, promoted to Senior Lecturer in 2000 and to Reader in 2005. He has continued to manage the collaborative development of VICONOPT, successfully co-supervising 10 PhD students and holding Research Council grants on parallel computing, aerospace panel optimization, local postbuckling and mode finding. He has visited NASA Langley Research Center several times, most recently for 4 weeks in 2004. In 2007 he was awarded a Royal Society Industry Fellowship for a 6-month secondment to Airbus UK.

As Deputy Director of the Cardiff Advanced Chinese Engineering (ACE) Centre, Dr Kennedy has assisted in the development of research agreements with leading Chinese universities, including Tsinghua University, Dalian University of Technology and Shanghai Jiao Tong University.

Dr Kennedy is the author of 125 publications of which approximately 50% are in refereed journals of international standing.

He lives with his wife Helen and 3 cats, and enjoys choral singing, organ playing and hill walking. Having been a keen cross-country and road runner at student level, he has now trying to emulate this success as a veteran (50+) and has competed 3 times in the Cardiff Half Marathon.

Alexander Lacher

- Born 30th of December 1981 in Berlin, Germany
- 2002-2007 Studies of Physical Engineering Science at TU Berlin
- Scholarship of the “German National Academic Foundation”
- 2006-2007 academic year at University of Maryland (UMD), College Park, MD, USA with a FULBRIGHT scholarship
- Research Assistant at UMD, research on a bio-inspired directional microphone and a wireless fiber sensor system for pressure and strain measurements on rotor blades (NASA-project)
- 2007 Diploma thesis on anisotropic yield criteria (Diplom-Ingenieur)
- Since 2007 Research and Teaching Assistant at TU Berlin, Chair of Mechatronics and Machine Dynamics (Prof. Dr.-Ing. Utz von Wagner), Dissertation on response of continuous structures under transient excitation

Arthur W. Leissa

After earning two degrees in mechanical engineering, with a strong interest in machine design, I decided to seek better understanding of stress and deformation of bodies, so I got my Ph.D. in engineering mechanics (from Ohio State University in 1958). My dissertation research was in the theory of elasticity. I then stayed on there as a faculty member.

Working part-time for two aircraft companies (Boeing and North American Aviation) made me very interested in vibrations. In 1965 I approached NASA to support me with research funds to collect the literature of the world in plate and shell vibrations, and summarize it in two monographs. They did, and the two books were published in 1969 and 1973. Plate vibrations involved approximately 500 references while shell vibrations had about 1000. The two books were out of print for a long time. But in 1993 they were reprinted by The Acoustical Society of America and are currently available from them.

After gaining considerable knowledge in writing the two books, I continued to do extensive research on vibrations of continuous systems, including laminated composites, turbomachinery blades, and three-dimensional problems. Approximately 150 published papers, and most of the 40 dissertations I supervised, were in this field.

I always intended to update the "Vibration of Plates" monograph. Indeed, more than 20 years ago I had a graduate student collect the more recent literature. This consisted of 1500 additional references dealing with free vibrations. But I never could find the time needed to undertake the writing.

In June of 2001 I formally retired from Ohio State University after having been on its faculty for 45 years. In July, 2002 Trudi and I moved to Fort Collins, Colorado, approximately 60 miles north of Denver, and close to the mountains. I am now an Adjunct Professor in the Department of Mechanical Engineering of Colorado State University. Having no serious responsibilities there, I still collaborate somewhat with others on research.

My serious interest in the mountains began as a boy, reading books about Mallory and Irvine on Everest, and others. In 1961 when I could first afford it (with a family) I began climbing mountains, which I pursued strongly for decades. Now being 77, I can no longer climb them, but I still enjoy greatly being in the mountains --- hiking, skiing and snowshoeing. They restore one's vitality and one's peace.

In 1995 Mark Ewing, who was in Colorado then, agreed to help me organize the first International Symposium in Vibrations of Continuous Systems, held in 1997 in Estes Park, Colorado. It was well-received, and so it has continued every two years, in marvelous mountain locations worldwide. I look forward to being in Zakopane and the Tatra Mountains.

Wenlong Li
Wayne State University
Department of Mechanical Engineering
5050 Anthony Wayne Drive
Detroit, MI 48202, USA

(a) Professional Preparation

University of Kentucky, Lexington, Kentucky	Mechanical Engineering	Ph.D., 1991
Beijing Institute of Technology, Beijing, China	Engineering Mechanics	M.E., 1984
Liaoning Teachers University, Dalian, China	Physics	B.S., 1982

(b) Professional Appointments

2007-present	Associate Professor	Dept. of Mech. Eng., Wayne State University
2004-2007	Associate Professor	Dept. of Mech. Eng., Mississippi State University
2002-2004	Principal Engineer	United Technologies Research Center
1995-2001	Senior Staff Engineer	Corporate Research, Carrier Corporation
1992-1995	Technical Specialist	Engineering Center, Case Corporation
1984-1987	Research Engineer	North Vehicle Research Institute, Beijing, China

(c) A Selective List of Publications

1. W. L. Li, X.F. Zhang, J.T. Du and Z.G. Liu. (2009). An exact series solution for the transverse vibration of rectangular plates with general elastic boundary supports, *J. Sound & Vib.*, 321, 254-269.
2. W. L. Li (2001). An analytical solution for the self and mutual radiation resistances of a rectangular plate, *J. Sound & Vib.*, 245, 1-16.
3. W. L. Li (2006). Vibroacoustic analysis of rectangular plates with elastic rotational edge restraints, *J. Acoust Soc. Am.*, 120, 769-780.
4. W. L. Li (2004). Vibration analysis of rectangular plates with general elastic boundary supports, *J. Sound & Vib.*, 273, 619-635.
5. W. L. Li and H. J. Gibeling. (2000). Determination of the mutual radiation resistances of a rectangular plate and their impact on the radiated sound power, *J. Sound & Vib.*, 229, 1213-1233
6. W. L. Li (2000). Free vibrations of beams with general boundary conditions, *J. Sound & Vib.*, 237, 709-725.
7. W. L. Li, M. Daniels and W. Zhou. (2002). Mechanical power transmissions from a vibratory machine to its supporting cylindrical shell, *J. Sound & Vib.*, 257, 283-299.
8. W. L. Li (2002). A new method for structural model updating and joint stiffness identification, *Mechanical System and Signal Processing*, 16, 155-167.
9. W.L. Li, T.W. Wu and A.F. Seybert (1993). An accurate boundary element method for acoustic problems with a reflecting plane of arbitrary impedance, *J. Sound & Vib.*, 171, 173-184.
10. W. L. Li and H. J. Gibeling (1999). Acoustic radiation from a rectangular plate reinforced by springs at arbitrary locations, *J. Sound & Vib.*, 220, 117-133.

Biographical Sketch of Chee W. Lim

I graduated with a B.Eng. degree in Mechanical Engineering (Aeronautics) from University of Technology, Malaysia in 1989. I was conferred a M.Eng. degree in Mechanical Engineering from National University of Singapore in 1992 for the research in hydrodynamic stability of potential and boundary layer flows over periodically supported compliant surfaces. The research was an attempt to model and understand the mechanism and responses of flows over the skin of a dolphin and the ability of a flexible skin to stabilize boundary layer flows. Subsequently, I pursued research in vibration of isotropic and laminated plates and shells and was awarded a PhD degree in Mechanical Engineering from Nanyang Technological University, Singapore in 1995.

I continued research as a postdoctoral fellow at Department of Civil Engineering, The University of Queensland, Australia from 1995 to 1997, and as a research fellow at Department of Mechanical Engineering, The University of Hong Kong from 1998 to early 2000. I joined Department of Building and Construction, City University of Hong Kong as an assistant professor in 2000 and was promoted to associate professorship in 2003.

My main research interests are in developing new models and applications of plate and shell structures including flow-structures interaction in advanced engineering fields such as smart piezoelectric structures, micro-electro-mechanical systems (MEMS) and nanomechanics. Recently, I have much interest in a new subject symplectic elasticity which has been applied in multidisciplinary areas including quantum mechanics, electromagnetism, control theory and applied mechanics.

I am married to Moi P. Choo, have a daughter Qin Y. Lim, fourteen, and a son Ying H. Lim, now ten.

Ken-ichi Nagai
Gunma University

Ken is a professor of the Department of Mechanical System Engineering in Graduate School of Engineering, Gunma University.

He was born in Fukushima north-east of Japan. He graduated from the national college of technology in Fukushima. During the student, he received deep impression from the book "Mechanics" by Den Hartog. At the time, he wanted to devote himself to research and education. He received his B. Eng. in 1970 from Ibaraki University. He obtained M. Eng. and Dr. Eng. in 1972 and 1976 from Tohoku University, respectively.

Since 1976, he has been taking an academic position in Gunma University. From 1990 to 1991, he was a visiting fellow at Cornell University in U. S. A., Technische Hochschule Darmstadt in Germany and Polish Academy of Sciences in Poland.

He is a Fellow of the Japan Society of Mechanical Engineers and was the chairman of the Division of Dynamics, Measurement and Control in JSME in 2007. He organized JSME Dynamics and Design Conference 2008. More than 350 papers were presented. He organized the Technical Section on Nonlinear Vibration under the division. He has been a consultant to ministry, local government and automobile industry.

He is now devoted in the research filed of nonlinear vibration, dynamic stability and chaotic oscillations of structure such as beam, arch, plate and shell.

Recently, he published the book of "Dynamic system Analysis-Energy Approaches from Structural Vibration to Chaos-".

His personal interests include hiking and drinking a little. He feels spiritual happiness as walking in fields and facing to new phenomena of chaotic vibration.

Yoshi (Yoshihiro Narita)

Hokkaido University, Sapporo, Japan

I am Yoshi (Yoshihiro) Narita of Hokkaido University, Sapporo, Japan. I moved to HU five years ago from Hokkaido Institute of Technology, where I had spent twenty-four years. I enjoy the best surroundings of HU, and I can work with graduate students who are capable of doing excellent research. Our laboratory has only one professor (me), because my colleague was promoted this spring to a full professor in another laboratory, and I still have about twenty students including five senior undergraduate students for graduation theses and fifteen Japanese (eleven) and foreign (four) graduate students.

Right after I come back from this symposium, I will be the chairman of domestic annual conference D&D2009 for Division of Dynamics, Measurement and Control, JSME. The venue of conference is on HU campus and the conference continues six days (3rd-8th August). The number of presentations is about five hundreds, including the accompanying First Japan-Korea symposium.

I started my research on vibration of continuous systems when I was a graduate student under adviser Prof.Irie of HU in 1976, and had a chance to study one year in 1978-1979 under Prof.Leissa at the Ohio State University. I have kept the same topic more than thirty years. Somehow, I like the research in the area of dynamics of continuous systems. Recently, I combine the vibration and buckling of plates and shells with optimization.

On a personal note, I have a wife and three children (a male HU graduate student of 24 year old, a female second-year student of Keio University and a high-school freshman of 16 year old). They used to come with me in early ISVCS's, but my children are now busy with their own schedules. I am happy to bring my wife this time.

I am also happy that I could join all the ISVCS's, including ISVCS-I(Estes Park, USA), II(Grindelwald, Switzerland), III(Grand Teton, USA), IV(Keswick, UK), V(Berchtesgarden, Germany) and VI (Squaw Valley, USA). These visits are full of good memories. In the present ISVCS, I look forward to meeting old and new friends in the research community of applied mechanics.



Let's enjoy!

Biography of Francesco Pellicano

Francesco Pellicano was born in Rome, Italy on 1966. He received a M.S. degree in Aeronautical Engineering in 1992 and Ph.D. in Theoretical and Applied Mechanics in 1996, both at the University of Rome "La Sapienza", Dept. of Mechanics and Aeronautics.

He was Researcher at the University of Modena and Reggio Emilia, Faculty of Engineering, Dept. of Mechanical and Civil Engineering, 1996-2003.

He is currently Associate Professor at the same University since January 2004.

He was involved in investigations concerning: nonlinear vibrations of structures; nonlinear normal modes; axially moving systems; nonlinear vibration of shells with fluid structure interaction; gears modeling; non-smooth dynamics; Chaos; Nonlinear Time Series Analysis; Forecasting Methods in Oceanography.

He cooperated with Prof. Vestroni, Prof. Sestieri and Prof. Mastroddi of the University of Rome "La Sapienza" and with with: Prof. Païdoussis (Mc Gill Univ. Canada); Prof. Vakakis (Univ. of Illinois at Urbana Champaign; recently National Technical Univ. of Athens, Greece); Prof. Amabili (Univ. of Parma, Italy).

The teaching activity regards: Vibrations of Discrete and Continuous Systems; Signal Processing; Machine Theory and Machinery.

He was coordinator of an international NATO CLG-Grant project on Nonlinear Dynamics of Shells with Fluid Structure Interaction and was the local coordinator of an Italian project on Shells Vibrations.

His research activity regards also industrial problems, he cooperated for research and consultancies with several companies about: vehicle stability; experimental vibrations; clutch instabilities and failures.

He was reviewer for the following international journals: SIAM Journal of Applied Mathematics, Nonlinear Dynamics, ASME Journal of Vibration and Acoustics, J. of Solids and Structures; J. of Sound and Vibration, Computer Methods in applied Mechanics and Engineering, Int. J. of Systems Science; and reviewer for the foundations: FCAR (Fonds pour la Formation de Chercheurs et l' Aide à la Recherche) Québec, CANADA; Natural Science and Engineering Research Council of Canada.

He is Associate Editor of the journal: *Mathematical Problems in Engineering, Hindawi*, and takes part to the international advisory editorial board of the journal: *Communications in Nonlinear Science and Numerical Simulation, Elsevier*.

He published a Book, 35 Journal papers and more than 60 conference papers.

Professor ROMULAD RZADKOWSKI

Brief statement of scientific career including academic qualifications, post held, research activities, etc:

**Master of Sciences in Engineering 1978 Technical University of Gdańsk,
Master of Sciences in Mathematics 1983, University of Gdańsk
Phd in Engineering 1988 Polish Academy of Sciences, Institute of Fluid Flow
Machinery,
DSc in Engineering 1998 Polish Academy of Sciences, Institute of Fluid Flow
Machinery,
Associate Professor since 1998
Professor Since 2004**

Field of specialization in brief:

**Dynamics of Turbomachinery, Life Estimation of Turbine Blades, Unsteady
Aerodynamics, Flutter**

Books:

Rządkowski R.: Numerical Analysis of Free and Forced Vibration of Tuned and Mistuned Bladed Discs, *Zeszyty Naukowe IMP PAN* 483/1438/97, 1997

Rządkowski R.: *Dynamics of Steam Turbine Blading, Part Two –Bladed Disc* Maszyny Przepływowe, Tom 22, Ossolineum, Wrocław, 1998.

Rządkowski R.: *Flutter of Turbine Rotor Blades in Inviscid Flow*, Wydawnictwo Akademii Marynarki Wojennej, Gdynia 2004.

Rządkowski R., Sokołowski J.: *Free Vibrations of the Bladed Discs on the Shaft*, Wydawnictwo Akademii Marynarki Wojennej, Gdynia 2005 (in Polish).

Rządkowski R., Soliński M.: Niestacjonarne siły aerodynamiczne działające na wirnik turbiny parowej, *Maszyny Przepływowe*, Tom 29, IMP PAN Gdańsk, 2007.

Main Papers – Journal 79, Conferences 94, Report for Industry 13, Reports tech 131.

Wolfgang Seemann

Institut für Technische Mechanik, Universität Karlsruhe (TH), Karlsruhe, Germany
Karlsruhe Institute of Technology

I was born on 31 March, 1961 in Kelttern (Germany, Baden-Württemberg). After school I studied mechanical engineering at the University of Karlsruhe between 1980 and 1985. After civil service (1985-1987) I began as a PhD-student working at the Institute of Applied Mechanics at the University of Karlsruhe. The PhD was finished in 1991 with a thesis on 'Wave propagation in rotating or prestressed cylinders'. In 1992 I joined the group of Peter Hagedorn at Darmstadt University of Technology to work in a post-doc position until 1998 when I got a professorship on machine dynamics in Kaiserslautern. In 2003 I got an offer to go back to the University of Karlsruhe on the chair of Applied Mechanics.

My previous and current research interests lie in ultrasonic motors, nonlinear vibration, multibody dynamics, vibration of continuous systems, active materials, nonlinear phenomena in piezoelectric materials, humanoid robots, dynamics of human motion, mechatronic systems, road-vehicle interaction, rotor dynamics and wave propagation.

Besides I am responsible for the French-German cooperation of our university.

CURRICULUM VITAE

Alexander P. Seyranian

Institute of Mechanics, Moscow State Lomonosov University

Michuynski pr. 1, Moscow 119192, Russia

Phone: (7495) 939-2039 Fax: (7495) 939-0165

E-mail: seyran@imec.msu.ru Homepage: <http://seyranian.imec.msu.ru>

A.P.Seyranian was born in Moscow, and spent his childhood in Armenia. In 1971 he graduated from the Moscow Physical-Technical Institute. In 1971-1973 he worked in the Central Aero-Hydrodynamic Institute of USSR as a research engineer. In 1977 he got Ph.D. degree from the Academy of Sciences of the USSR with the thesis "Structural optimization under several constraints". In 1977-1991 A.P.Seyranian was a Member of Scientific Staff at the Institute of Problems in Mechanics of the Academy of Sciences in Moscow. In 1988 he got D.Sc. degree with the thesis "Sensitivity analysis and optimization for problems of stability and vibrations of elastic systems" from the Academy of Sciences of the USSR in Moscow. In 1991-1992 he visited Denmark as a Guest Professor and gave a lecture course "Vibrations and Stability of Systems Depending on Parameters" at the Technical University of Denmark (Lyngby) and Aalborg University. Since 1993 A.P.Seyranian is a Leading Researcher and Professor of the Institute of Mechanics, Moscow State Lomonosov University. In 1995 he was elected a Member of The New York Academy of Sciences. In 1998 he was elected a Member of Editorial Board of the International Journal "Theoretical and Applied Mechanics" published in Yugoslavia. In 2001 A.P.Seyranian was Coordinator and Lecturer of the course "Stability of Structures. Modern Problems and Unconventional Solutions", held in International Centre for Mechanical Sciences in Udine (Italy), and Editor of the book "Modern problems of Structural Stability", 2002, Springer Wien. In 2002 he got the prize of Elsevier Publishers for the best paper published in Journal of Applied Mathematics and Mechanics in 2001. In 2003 he wrote a fundamental monograph on multi-parameter stability problems (with A.A.Mailybaev) published by World Scientific, Singapore. In 2003 A.P.Seyranian became a member of Editorial Board of International Journal Structural and Multidisciplinary Optimization. In 2007 A.P.Seyranian as a leader of Moscow group with the partners from Italy, France and Siberia got approval of the INTAS project "Advances of Stability Theory with Mechanical Applications" supported by European Union. In 2007 A.P.Seyranian became a member of Editorial board of the International Journal "Mathematical Methods in Engineering". In 2008 he was elected a Correspondent Member of Russian Academy of Natural Sciences. In November 2008 he was elected a Member of Academy of Sciences of Armenia.

A.P.Seyranian is a reviewer of ASME Journal of Applied Mechanics, American Mathematical Society, Proc. Royal Society (UK), Journal of Sound and Vibration, International Journal of Non-Linear Mechanics, European Journal of Mechanics, International Journal of Solids and Structures, Structural and Multidisciplinary Optimization, Journal of Applied Mathematics and Mechanics (Russia), Doklady of Academy of Sciences (Russia), Mechanics of Solids (Russia). He gave lectures and presented seminars in many Conferences and prominent Universities in Russia, Armenia, USA, Canada, UK, Germany, France, Japan, Austria, Brazil, Italy, Spain, Serbia, Ukraine, Bulgaria, China, Denmark, Netherlands, Korea, Poland, Sweden, Hungary, Slovakia, Turkey. His biography is included in the reference books "Who is Who in the World", Marquis, 1999 and 2001, and "Who is Who in Science and Engineering", Marquis, 2007.

Anand V. Singh

I was born on July 05, 1948 in a village Rahimpur in the district of Monghyr, Bihar, India. I completed my elementary and secondary educations from Monghyr Zila School and was directly admitted to the Bihar Institute of Technology in Sindri. I graduated in 1968 with B.Sc. Engineering (first class with distinction in Mechanical Engineering). In September of 1969, I joined the school of graduate studies at the University of Ottawa; began my research work with the derivation of the constitutive equations from the first principles to study the free axisymmetric vibration of sandwich spherical shell structures under the noble supervision of Professor S. Mirza and subsequently received M. A. Sc. and Ph. D. degrees. These equations were developed in the spherical coordinate system and had solutions in Legendre functions of complex order for which I had to develop many new programs. During this study I also used energy methods to deduce the equations of motion for the free vibration of isotropic and sandwich plates and shells.

After graduation, I worked as a defence scientist at the Defence Research Establishment Suffield (DRES) near Medicine Hat Alberta from January 1978 to April 1981. Then, I accepted a design-engineer position in the Civil Design Department of Ontario Hydro in Toronto and worked there until December 1984, when I came to the University of Western Ontario to teach machine component design and the finite element methods. Professor Stuart Dickinson was the chair of the Mechanical Engineering at that time and he is the one who hired me. This year I shall be completing 25 years of service to the university. During these years I taught graphics and engineering drawings, dynamics, kinematics and dynamics of machines, and the theory of modern control systems in addition to the above mentioned two courses. I worked with some remarkable students in the field of computational solid mechanics dealing with the linear and nonlinear vibrations of plates and shells.

On the personal note, since March of 1968 I am married to Bimla with whom I have had more than forty great years and have two adult children, the son Bidhi and daughter Shikha. Both are graduates of the University of Western Ontario. Bimla and I attended all the ISVCs except the very first one. Also, we like to travel and have camped in the past while traveling with our children; enjoy walking in the park and on the beaches (whenever possible); and wish to live our lives to the fullest as long as there is the wellness.



TECHNISCHE
UNIVERSITÄT
DARMSTADT

Fachbereich Maschinenbau

Gottfried Spelsberg-Korspeter
Fachgebiet Dynamik

Hochschulstr. 1
64289 Darmstadt
Telefon + 49 6151 16-2685
Telefax + 49 6151 16-4125
speko@dyn.tu-darmstadt.de

Gottfried Spelsberg-Korspeter ***Technische Universität Darmstadt***

On August 13th 1978 I was born in Dortmund Germany.

I grew up in Dortmund, Düsseldorf and Ludwigsburg where I finished high-school (Abitur) in 1998. After completion of the compulsory military service I started studying at TU Darmstadt in 1999.

In 2001 I finished my preliminary diploma in industrial engineering and in mechanical engineering and decided to pursue my mechanical interests in the applied mechanics department with main focus on dynamics. Taking part in an exchange program of the industrial engineering department I spend the fall semester 2002 and the spring semester 2003 at the University of Illinois at Urbana Champaign where I mainly worked in the area of operations research.

In 2004 I finished my masters degree in applied mechanics with a thesis related to mechanical modelling of ultrasonic motors and went back to the University of Illinois to write my master thesis in industrial engineering in the area of operations research. After completion I joined the research group of Professor Hagedorn in January 2005. In 2007 I completed my Ph.D. work with a thesis on self excited vibrations in gyroscopic systems. Since then I have been teaching classes on nonlinear vibrations, multibody dynamics and vibrations of continuous systems for master students and engineering mechanics for bachelor students.

My hobbies are hiking, climbing and other sports.

Utz von Wagner Bio

- born 1968
- 1994 Diploma Mechanical Engineering Universitaet Karlsruhe
- 1998 Doctoral degree (Dr.-Ing.) Universitaet Karlsruhe
- 1999 Development engineer ADtranz Daimler Chrysler Rail Systems Nuremberg
- 1999 - 2004 Lecturer at Technische Universitaet Darmstadt
- 2003 Habilitation
- since October 2004: Professor at Technische Universitaet Berlin, chair of Mechatronics and Machine Dynamics
- 2007-2009 vice dean of School of Mechanical Engineering and Transport Systems at TU Berlin
- since April 2009 dean of School of Mechanical Engineering and Transport Systems at TU Berlin

Biographical sketch

Jörg Wauer

I am a Professor of Technical Mechanics at the University of Karlsruhe, Germany, in the Department of Mechanical Engineering, holding this position since 1977. I apprenticed as a mechanic and studied mechanical engineering at the Engineering College of Kaiserslautern and the University of Karlsruhe. I received my Ing.-Grad. and Dipl.-Ing degree in 1964 from the Engineering College of Kaiserslautern and in 1969 from the University of Karlsruhe, respectively. At the University of Karlsruhe, I was promoted to Dr.-Ing. in 1972 and Docent habil. in 1976. My industrial experience includes positions as a mechanic specialist and design engineer.

Structural dynamics and dynamics of machines are my principal research interests but during the last fifteen years, I extended this work to multi-field problems as dynamic fluid-structure interaction or vibrations of thermo-elastic and piezoelectric solids. I have authored or co-authored approximately 150 scientific papers concerning the mentioned topics, and I am a co-author of a book on mathematical methods in engineering mechanics. Together with my colleague W. Seemann, in 2005 we lectored the translation of the 3-volume book "Engineering Mechanics" by Hibbeler into German with significant adaptations and enlargements. In 2009 I published a German-written monograph on "Vibrations of Continuous Systems".

Teaching is the other part of my activities at the university. I gave courses in all undergraduate mechanics topics, and I taught and I am still teaching many advanced mechanics courses for graduate students as structural dynamics, dynamics of machines, measurement of mechanical vibrations, mathematical methods in engineering vibrations, stability of elastic structural members, and presently, dynamics of mechatronic systems.

As the principal adviser, I promoted sixteen students to their Dr.-Ing. degree and two of them also to his habilitation. I am a member of GAMM and EUROMECH, I am active in several committees and work as a reviewer for several mechanics journals. In 2004 I received an honorary doctor degree from the Technical University of Sofia, Bulgaria.

Besides all these scientific activities, from 1994 until 2002, I held an important position in administration of my faculty at the University of Karlsruhe: I was the so-called Studiendekan responsible for all our actual reform work in the curriculum of the study of Mechanical Engineering at the University of Karlsruhe. In addition, from 1999 until 2001, I chaired one of the University councils in Karlsruhe. From 2000 until 2008, I was a member of a nationwide committee for accrediting of Bachelor's and Master's studies in Engineering Sciences. Since October 2007 I am retired.

March 2009

A Short Biography

S. D. Yu

Shudong Yu received his Bachelor's degree in Mechanical Engineering from Jianxi University of Science and Technology (China) in 1982, Master's degree in Theoretical Mechanics from Northeastern University (China) in 1984, and PhD degree in Mechanical Engineering from the University of Toronto (Canada) in 1995.

He worked as a research associate under Professor D. J. Gorman at the University of Ottawa during 1988-89, and as a nuclear fuel design engineer/analyst at Atomic Energy of Canada Limited (AECL) during 1994-1997. He joined Ryerson University, Toronto, Canada, as an assistant professor in the Department of Mechanical and Industrial Engineering in 1997. He teaches courses in the area of solid mechanics and machine design. He is currently a professor of mechanical engineering at Ryerson University.

Dr. Yu's research interests include vibrations of continuous systems (beams, plates, shells and flexible multibody systems), thermal stresses in nuclear fuel, multiple body contacts and flow induced vibrations.

Dr. Yu has published papers and technical reports in several areas of his expertise.